UNIVERSIDADE DE LISBOA
INSTITUTO SUPERIOR TÉCNICO

Genetic engineering of Mesenchymal Stromal Cells to express anti-cancer proteins

Marília Maria Rodrigues da Silva

Supervisors: Doctor Cláudia Alexandra Martins Lobato da Silva
Doctor Nuno Filipe Santos Bernardes

Thesis approved in public session to obtain the PhD Degree in Bioengineering

Jury final classification: Pass with Distinction

2021

UNIVERSIDADE DE LISBOA
INSTITUTO SUPERIOR TÉCNICO

Genetic engineering of Mesenchymal Stromal Cells to express anti-cancer proteins

Marília Maria Rodrigues da Silva

Supervisors: Doctor Cláudia Alexandra Martins Lobato da Silva
Doctor Nuno Filipe Santos Bernardes

Thesis approved in public session to obtain the PhD Degree in Bioengineering
Jury final classification: Pass with Distinction

Jury:

Chairperson: Doctor Joaquim Manuel Sampaio Cabral, Instituto Superior Técnico, Universidade de Lisboa

Members of the Committee:

Doctor Arsénio do Carmo Sales Mendes Fialho, Instituto Superior Técnico, Universidade de Lisboa

Doctor Gabriel António Amaro Monteiro, Instituto Superior Técnico, Universidade de Lisboa

Doctor Nuno Filipe Santos Bernardes, Instituto Superior Técnico, Universidade de Lisboa

Doctor Joana Cancela de Amorim Falcão Paredes, Instituto de Investigação e Inovação em Saúde/ Instituto de Patologia e Imunologia Molecular, Universidade do Porto

Doctor Teresa Catarina Páscoa Madeira, Faculdade de Ciências Médicas, Nova Medical School da Universidade Nova de Lisboa

Doctor Vasco Temudo e Melo Cabral Barreto, individualidade reconhecida na área científica em que se insere a tese

Funding Institution – Fundação para a Ciência e Tecnologia

2021

Resumo

Atualmente, o sucesso dos tratamentos anti-cancerígenos convencionais é limitado pela falta de seletividade destes métodos, levando a efeitos secundários severos e falta de eficácia terapêutica. Como tal, o desenvolvimento de novas estratégias que atingem seletivamente o microambiente tumoral tem sido um dos pontos centrais da investigação na área do cancro. As abordagens recentes aplicam sistemas personalizados de entrega de fármacos e, recentemente, as terapias baseadas em células têm sido desenvolvidas para a entrega específica de novas fórmulas terapêuticas anti-tumorais. Nesta perspetiva, as células estromais do mesênquima (CEM) têm um elevado potencial terapêutico, devido ao seu potencial de migração específica para zonas tumorais. Nesta tese, foram desenvolvidos protocolos não virais e sem componentes de origem animal (*xeno-free*) para a engenharia de CEM para a expressão e secreção da proteína anti-tumoral azurina (hazu). Numa primeira linha de estudo, um método de expressão transiente de azurina foi desenvolvido como uma prova de conceito para a aplicação de CEM a expressar azurina no tratamento do cancro, através do efeito parácrino do seu meio condicionado (MC) enriquecido com azurina. Demonstrou-se que as CEM a expressar azurina preservam o seu tropismo tumoral nativo perante as linhas cancerígenas de mama e de pulmão, de forma equiparável com as suas versões não modificadas. Além disso, a azurina foi detetada no MC de *hazu*-CEM, e após a exposição das células cancerígenas a este MC, verificou-se uma diminuição da proliferação, migração e invasão celular, assim como um aumento da morte celular para ambas as linhas de células cancerígenas. Numa segunda linha de estudo, optimizou-se um protocolo para o estabelecimento de uma linha de CEM com expressão estável de transgenes aplicando o sistema CRISPR/Cas9. Direcionou-se a inserção do gene *hazu* para o locus *AAVS1* localizado no gene *PPP1R12C*, considerado um local seguro para inserção de material genético exógeno no genoma humano, alcançando 11.6% de eficiência de inserção através do processo de reparação por recombinação homóloga. Ao inserir o gene *hazu* de uma forma precisa no genoma das CEM, poder-se-á, por um lado, aplicar estas células como uma terapia celular, tirando partido do seu tropismo tumoral inato e potencial secretório; e poder-se-á também estabelecer uma linha celular que produz, de forma estável, um bioativo anti-tumoral adoptando o seu MC como uma estratégia de base celular, mas sem células (*cell-free*). Para além disso, prevê-se que outros transgenes terapêuticos poderão ser estudados aplicando o protocolo aqui desenvolvido, visando diferentes doenças ou contextos biológicos que não a terapia do cancro. Desta forma, prevê-se que este trabalho impulsionará estudos futuros para a edição precisa do genoma de CEM, com um elevado potencial de adequação a um cenário GMP com vista à sua aplicação clínica.

Palavras-chave: células estromais do mesênquima, edição genética não-viral, CRISPR/Cas9, azurina, terapia anti-cancerígena

Abstract

The success of conventional anti-cancer treatments if often constrained by their lack of specificity, which is accompanied by severe side effects and lack of therapeutic efficacy. As such, the development of new tumor-targeted strategies has been one of the focal points of cancer research. Novel approaches focus on selective tumor targeting by applying customized drug delivery systems and, recently, cell-based therapies have been explored as living tools for the delivery of anti-tumor therapeutics. In this perspective, mesenchymal stromal cells (MSC) hold a promising future, due to their unique tumor-specific migratory potential. Here, nonviral, serum/ xeno-free, strategies for the engineering of MSC towards the expression and secretion of the potent anti-tumoral protein azurin (hazu) were developed. In a first line of research, a transient gene delivery method was developed as a proof-of-concept to attest the biomedical potential of *hazu*-expressing MSC's conditioned media (CM) in anti-cancer treatment. Engineered *hazu*-MSC were shown to preserve tumor tropism toward breast and lung cancer cell lines, comparable to non-modified MSC. Moreover, hazu was detected in the CM of engineered cells and, upon treatment with *hazu*-MSC-CM, a decrease in cancer cell proliferation, migration, and invasion was observed, as well as an increase in cell death for both cancer cell lines. In a second line of research, a protocol for the establishment of a stable transgene-expressing MSC line was developed, through the clustered regularly interspaced short palindromic repeats (CRISPR)/Cas9 system. The *AAVS1* locus located on the *PPP1R12C* gene was targeted, a genomic safe harbor (GSH) in the human genome, achieving 11.6% homology directed repair knock-in efficiency. By stably inserting the *hazu* gene into MSC genome, MSC could be employed as a cellular therapy, taking advantage of their innate tumor tropism and secretory potential; in addition, it could be disclosed a streamline for the production of a bioactive anti-tumoral CM product, by employing *hazu*-MSC as a continuous living factory. Importantly, using the system established herein, other therapeutic transgenes could potentially be targeted, aiming at different disease or biological contexts other than cancer therapy. Thus, it is anticipated that the work here developed will boost precise MSC genome editing, under conditions amenable to GMP compliance, envisioning a clinical application scenario.

Keywords: mesenchymal stromal cells, non-viral gene editing, CRISPR/Cas9, azurin, anti-cancer therapy

Acknowledgements

First of all, I would like to express my gratitude towards my supervisors, Professor Cláudia Lobato da Silva and Doctor Nuno Bernardes, for accepting me in their research groups, giving me the opportunity to develop this work, for their unmeasurable support, prompted inspiration, great knowledge, and guidance in several questions, not exclusively related to science, since my master's degree. Also, I would like to thank Professor Arsénio Fialho, who primarily introduced me to this field and contributed for shaping my professional goals and research interests.

I acknowledge Professor Joaquim Sampaio Cabral, Director of the Stem Cell Engineering Research Group (SCERG) and to Professor Isabel Sá-Correia, Director of the Biological Sciences Research Group (BSRG), for the opportunity to develop my PhD work at the laboratories of Taguspark and Alameda (IST/IBB- Instituto Superior Técnico/iBB-Institute for Bioengineering and Biosciences). Also a big acknowledgement to Jaqueline Garcia and Mónica Rato, research technicians.

I also acknowledge all the co-authors of the publications presented in this dissertation, for their scientific contributions and inputs, with a special word to Doctor Evguenia Bekman for her continuous availability and assistance throughout this project. Your keen interest, above all your overwhelming enthusiasm to help was genuinely important to the completion of this work.

I would also like to acknowledge "Fundação para a Ciência e Tecnologia" for funding support of my PhD grant SFRH/BD/128372/2017.

To my colleagues and friends from iBB, but specially to Ana Carina Manjua, André Branco, Cristiana Ulpiano, Diogo Nogueira, Miguel Fuzeta, Sara Bucar, Sara Morini and Teresa Mendes. Your support has meant more to me than you could possibly realize. This journey would be a much more difficult feat without your friendship and knowledge. Thank you for your unwavering support and for reminding me to unwind, even when things got really hard and stressful. I must say that undoubtedly one of the biggest rewards of pursuing this PhD was the opportunity to meet you. A special acknowledgment goes also to Ana Fernandes-Platzgummer, Dalila Mil-Homens, Joana Feliciano, João Carreira.

To my older friends, Ana Rita Garizo, Lígia Coelho, Marcelo Ramires, Maria Silva, Marisa Matos, Rui Martins and Soraia Guerreiro, thank you for your constant friendship and your never-ending encouragement through all the matters of life. The extension of my gratitude towards your friendship goes beyond any words I could write in a finite text.

And lastly, to my family: to those I've never met, to the quatrain of the past and present, to the one who helped me grow flowers and to the one who taught me how to materialize them into reality; and to those who still don't add to the disturbance, but are there, in the space-time continuum.

For everything that is (un)divided between us.

Table of contents

List of figures

Figure II.4.2 - hazu-MSC CM inhibit cancer cell proliferation and induce cancer cell death *in vitro*. (A) Cytotoxicity and tumor cell viability were assessed by PrestoBlue in breast cancer (MCF-7) and lung cancer (A549) cell lines upon 24h of exposition to conditioned media (CM) from MSC microporated with pVAX-hazu (hazu-MSC) (grey bars), pVAX-GFP (gfp-MSC) (light grey bars), or without DNA (microporation control 2) (black bars). MSC-CM was collected 96h post-transfection. Due to differences in expansion media between cancer cells and MSC, MSC-CM concentration was variated (0–50%) while maintaining a level of cancer cells' culture media at 50%. Untreated cells were exposed to media without CM, and their proliferation rate was admitted as 100% (p-values compare % of proliferation between gfp-MSC or hazu-MSC with MSC control 2; n = 4). (B) Annexin V expression detection after treatment with hazu-MSC' CM, assessed by flow cytometry. Living cells are seen in the lower left quadrant, Annexin V (−)/ PI (−), [Q1]. The early apoptotic cells are shown in the lower right quadrant, Annexin V (+)/ PI (−), [Q2]. Advanced apoptotic or necrotic cells are seen in the upper right quadrant, Annexin V (+)/ PI (+), [Q3]. Annexin V (−)/ PI (+), [Q4] are cells in late necrosis or cellular debris. Panels 1 and 2 correspond to MCF-7 treated with control 2 MSC-CM and hazu-MSC-CM, respectively. Panels 3 and 4 correspond to A549 treated with control 2 MSC CM and hazu-MSC CM, respectively (n = 2). (C) Percentage of A549 live and dead cells based on flow cytometry results on annexin V expression, after treatment with MSC-CM and the ratio between dead cells treated with hazu-MSC' CM or control MSC' CM (n = 1). (D) Percentage of MCF-7 live and dead cells based on flow cytometry results on annexin V expression, after treatment with MSC-CM and the ratio between dead cells treated with hazu-MSC' CM or control MSC' CM (n = 1). Statistical differences are indicated with $*p \leq 0.05$ and $**p \leq 0.01$.

Figure II.4.3 - Inhibition of cancer cell invasion and migration by hazu-MSC' CM *in vitro*. (A) A549 lung cancer cell invasion toward a chemoattractant (culture media supplemented with FBS) was evaluated in Matrigel invasion assays. Cells were treated with CM from gfp-MSC, hazu-MSC, MSC control 2, and cancer cell media (culture media control) during 24h and migrated cells were quantified. Results are presented as the percentage of invasive cells compared to the control condition (p-values compare % of cancer cell invasiveness between hazu-MSC' CM treatment and the remaining treatment conditions; n = 4). (B) Cell migration was estimated by means of a scratch assay and monitored by time-lapse microscopy. A549 and MCF-7 were treated with control 2 MSC' CM or hazu-MSC' CM, and the distances of migrated cells were measured at several time points: 0, 14, 16, 18, 20, 22 and 40h (p-values compare % of unoccupied area between A549 and MCF-7 treated with hazu-MSC' CM or MSC control 2 CM, at the same time point; n = 4). Statistical differences are indicated with $*p \leq 0.05$, $**p \leq 0.01$ and $****p \leq 0.0001$.

Figure II.4.4 - Evaluation of MSC expression profile on cytokines relevant in cancer progression. The levels of inteuleukin-6 (IL6), vascular endothelial growth factor (VEGF), stromal derived factor 1 alpha (SDF1-α) and transforming growth factor beta (TGF-β) were analysed by ELISA in MSC-CM before and after microporation with pVAX-hazu and pVAX-GFP. The results are given in the relative fold change of cytokine expression relatively to MSC-CM in the control condition (control 2) (p-values compare fold change between gfp-MSC and hazu-MSC conditions with MSC control 2; n = 3). (A) Cytokine expression profile in BM MSC-CM. (B) Cytokine expression profile in UCM MSC-CM. Statistical differences are indicated with $*p \leq 0.05$ and $***p \leq 0.001$.

Figure III.4.1 - (A) Agarose gel electrophoresis of PCR products amplified with primers correspondent to each sgRNA. Guide 1: Cut1.Fw, Cut1.RV; Guide 2: Cut2.Fw, Cut2.RV; Guide 3: Cut3.Fw, Cut3.RV; Guide 4: Cut4.Fw, Cut4.RV (see Table 2 on section Material and Methods section). G1 - Guide 1; G2 - Guide 2; G3 - Guide 3; G4 - Guide 4; uPCR – uncleaved PCR; Mk – 1Kb Plus DNA Ladder (Invitrogen™). (B) Agarose gel electrophoresis of PCR products digested with Detection enzyme following the GeneArt™ Genomic Cleavage Detection Kit (Invitrogen™) to determine cleavage efficiency of the tested guides. Efficiency ratios were obtained by Image J software (ratio of [cleaved/noncleaved]): Guide 1: non-cutter; Guide 2: 51%; Guide 3: 55%; Guide 4: impossible to

List of tables

List of acronyms

5-FC - 5-fluorocytosine

AAV - Adeno-associated virus

AAVS1 - adeno-associated virus integration site 1

ACAN - Aggrecan

ADA - Adenosine deaminase

AGE - Advanced glycation end products

AKI - Acute kidney injury

AS - Antisense

AT – Adipose tissue

AuNP - Gold nanoparticles

B2M - Beta 2-microglobulin

Bcl-2 - B-cell lymphoma 2

BDNF - Brain-derived neurotrophic factor

BM – Bone marrow

BMP2 - Bone morphogenic protein 2

BMP-6 - Bone morphogenic protein-6

BSA - Bovine serum albumin

C/EBP-β - CCAAT/enhancer binding protein beta

CAF - Carcinoma-associated fibroblasts

CAR - chimeric antigen receptor

CCL2 - C-C Motif chemokine ligand 2

CCR - Chemokine receptor

CD - Cytosine deaminase

CFU-F - Colony forming units - fibroblasts

CM - Conditioned medium

CNP - C-type natriuretic peptide

CRISPR - clustered regularly interspaced short palindromic repeats

crRNA - Crispr RNA

CTL - Cytotoxic T lymphocyte

CTS - Clinical trial study

CXC3R - Chemokine receptor 3

CXCL12 - Chemokine (C-X-C motif) ligand 12

CXCL5 - Chemokine (C-X-C motif) ligand 5

CXCL6 - Chemokine (C-X-C motif) ligand 6

CXCL7 - Chemokine (C-X-C motif) ligand 7

CXCL8 - Chemokine (C-X-C motif) ligand 8

CXCR - C-X-C motif chemokine receptor

DMEM - Dulbecco's modified eagle medium

DNA - Deoxyribonucleic acid

DP – Dental pulp

DS - Double-stranded

DSB - Double-strand break

dsDNA – Double-stranded DNA

DTT - Dithiothreitol

ERK1/2 - Extracellular regulating kinases 1/2

FA - Fanconi Anemia

FACS - Fluorescence-activated cell sorting

FasL - Fas Ligand

FBS - Fetal bovine serum

FDA - Food and Drug Administration

FGF - Fibroblast growth factor

Foxa2 - Forkhead box A2

FW - Forward

G - Guanosine

G1 - sgRNA 1

G2 - sgRNA 2

G3 - sgRNA 3

G4 - sgRNA 4

GAG - glycosaminoglycans

Gdf11 - Growth/differentiation factor 11

GDNF - Glial cell line-derived neurotrophic factor

GFP - green fluorescence protein

GMP - Good Manufacturing Practice

GV - Gingiva

GvHD – Graft-versus-host-disease

HA - Homology arms

Hap - Hydroxyapatite

Hazu - Human azurin

HCT - Hematopoietic cell transplantation

HDR - Homologous directed repair

HDR - Homology directed repair

HGF - Hepatocyte growth factor

HO-1 - heme oxygenase-1

hPL - Human platelet lysate

HR - Homologous recombination

HSC - Hematopoietic stem cells

Hsp27 - Heat shock protein 27

HSPC - Hematopoietic stem/ progenitors cell

HSV - Herpes simplex virus

IFN - Interferon

IL - Interleukin

IMAC - Immobilized metal affinity chromatography

Indel - Insertion/deletion

IPC - Insulin-producing cell

iPSC - Induced pluripotent stem cell

IPTG - Isopropyl-β-D-thiogalactopyranoside

ISCT - International Society for Cellular Therapy

LPS - Lipopolysaccharide

MHC - Major histocompatibility complex

mIR - microRNA

mNP - Magnetic nanoparticle

ms - Millisecond

MSC - Mesenchymal stromal cell

mV - Millivolt

NBM - Natural bone mineral

ng - Nanogram

NHEJ - Nonhomologous end-joining

NK - Natural killer

NP - Nanoparticle

NT-3 - neurotrophins-3

OGD - Oxygen-glucose deprivation

OPG - Osteoprotegerin

PAI-1 - Plasminogen activator inhibitor-1

PAM - Protospacer adjacent motif

PBAE - Poly (β-amino ester)

PD - Parkinson's disease

PDGFB - Platelet derived growth factor B

PDX-1 - pancreatic and duodenal homeobox 1

PEI - Polyethylenimine

PEX - Hemopexin-like domain fragment

PHD2 - Hydroxylase domain-containing protein 2

PI - Propidium iodide

PL - Placenta

PLGA - PEI-modified poly lactic-co-glycolic acid

PLL - Polylysine

PPP1R12C - protein phosphatase 1 regulatory subunit 12C

RNA - Ribonucleic acid

RNAi - RNA inference

RNP - Ribonucleoprotein

Runx2 - Runt related transcription factor 2

SCID - Severe combined immunodeficiency

SDC4 - Syndecan-4

SDF1α - stromal cell-derived factor 1

SEC - Size exclusion chromatography

SF – Serum-free

SG - Sweat gland

sgRNA - Single guide RNA

siRNA - small interfering RNA

SOX - SRY-box

SP - Spermine-pullulan

sRAGE - Soluble Receptor for AGE

SS - Sense strand

ssDNA - single-stranded DNA

ssODN - Single-stranded oligodeoxynucleotide

SV40T - Simian virus 40 large T antigen

TAF - Tumor associated fibroblast

TALEN - Transcription activator-like effector nucleases

TCR - T-cell receptor

TGF-β - Transforming growth factor beta

TGF-β3 - Transforming growth factor beta 3

TIDE - Tracking of Indels by Decomposition

TIL - Tumor-infiltrating lymphocyte

TK - Thymidine kinase

TNF - Tumor necrosis factor

t-PA - Tissue plasminogen activator

TRAIL - Tumor necrosis factor-related apoptosis-inducing ligand

UC - Umbilical cord

UCB - Umbilical cord blood

UCM - Umbilical cord matrix

US - United States

V - Voltage

v/v - volume/volume

VEGF - Vascular endothelial growth factor

WJ - Wharton' Jelly

WT - Wild-type

XF - Xeno-free

yCD::UPRT - Yeast cytosine deaminase::uracil phosphoribosyl transferase

ZF - Zinc finger nuclease

I. INTRODUCTION

The contents of this chapter are partially published as:

Silva, M., Ulpiano, C., Bernardes, N., Monteiro, G.A., da Silva, C.L. Gene delivery as a tool to improve the therapeutic features of mesenchymal stromal cells: methods and applications in Gene Delivery: Methods and Applications, Zimmer, V. (ed.), Nova Science Publishers, ISBN 9781536162684 (2019).

I.1. Mesenchymal Stromal Cells (MSC) for cell-based therapies

I.1.1. Mesenchymal Stromal Cells: an introduction

Mesenchymal stromal cells (MSC) are multipotent cells that can differentiate into a variety of lineages, including osteocytes, adipocytes and chondrocytes[1]. This differentiation capability, along with the release of trophic factors[2], immunomodulatory properties[3], anti-fibrotic[4] and anti-apoptotic[5] features, sparked the interest of the scientific community in the last decades. Cells with these features could potentially hold a great promise for cell therapies and tissue engineering, by replacing damaged tissues of mesodermal origin, to promote regeneration, and to treat immune-mediated diseases. As such, the number of clinical trials using MSC has been rising almost exponentially since 2004[6], achieving a total of 1194 studies in 2019, of which 361 have been completed to date (obtained at "clinicaltrials.gov" on July 6th 2021, using the terms "mesenchymal stem cells"; "mesenchymal stromal cells"). MSC were described for the first time in 1970 by Friedenstein and co-workers, as colony forming fibroblasts (CFU-F), a rare population of cells residing in the bone marrow (BM) of guinea-pigs and mice[7,8]. Although the term "mesenchymal stem cell" was suggested in 1991 by Arnold Caplan[9], the knowledge of the existence of MSC was not new, pointing at the 19th century when the Germain biologist Cohnheim hypothesized that fibroblastic cells derived from BM were involved in wound healing throughout the body[10,11]. Due to the increasing interest of researchers to study the therapeutic potential of MSC, different methods of isolation and expansion, and different approaches to characterize the cells, led to difficulties in comparing the outcomes of different studies. To address this issue, in 2006, the Mesenchymal and Tissue Stem Cell Committee of the International Society for Cellular Therapy (ISCT) defined the minimal criteria to characterize human MSC. These criteria include: MSC must be plastic-adherent when maintained under standard culture conditions; MSC must express CD105, CD73 and CD90, and lack expression of CD45, CD34, CD14 or CD11b, CD79a or CD19 and HLA-DR surface molecules; and MSC must differentiate into osteoblasts, adipocytes and chondroblasts *in vitro*[12]. Despite the first demonstration of the existence of MSC in the adult BM, cells with similar characteristics have been found from cultures of virtually all adult and fetal organs tested[13]. In fact, MSC can be found in nearly all tissues and are mostly located in perivascular niches. Some of the reported tissue sources include the BM[14], umbilical cord (UC)[15], Wharton' Jelly (WJ)[16], placenta (PL)[17], menstrual blood (MB)[18], AT (AT)[19], gingiva (GV)[20] and Dental pulp (DP)[21]. Since the pioneer studies by Friedenstein and colleagues[7], BM remains the gold standard as tissue source to obtain MSC, although cells isolated from adipose tissue (AT-MSC) and umbilical cord matrix (UCM-MSC) have also been tested in cell therapy studies. At a first look, MSC from different tissues share key characteristics such as fibroblast-like appearance *in vitro*, trilineage differentiation capacity (osteo-, adipo- and

chondrocytic lineages), and expression of certain cell surface antigens[12]. However, some studies have stated that MSC isolated from different sources in fact express different surface markers[22,23] and may differ in what concerns differentiation potential. For instances, cells from these three sources present a similar capacity for chondrogenic and osteogenic differentiation, with the exception of UCM-MSC that show reduced adipogenic potential[24,25]. Although BM has been the main source for the isolation of multipotent MSC, the harvest of BM is a highly invasive procedure and the number, differentiation potential, and maximal life span of BM-MSC decline with increasing age[25]. A significant advantage of the neonatal tissues, such as the UCM, as sources of MSC is that they are readily available, thus avoiding invasive procedures and ethical problems associated to adult tissues. It is also suggested that MSC from these neonatal tissues may have advantages in comparison to MSC derived from adult sources as BM. Indeed, several studies have reported superior proliferative capacity, life span and differentiation potential of MSC from birth associated tissues over BM-MSC[24,25]. AT is another alternative source to retrieve MSC that can be obtained by a less invasive method and in larger quantities compared to BM. AT-MSC can be isolated from liposuctions in large numbers and grown easily under standard tissue culture conditions. Importantly, AT might be a robust cell source when envisaging an “off-the-shelf” product requiring mass cell production, due to the abundance, relatively easy harvest, and high MSC frequency in this tissue[25]. Nevertheless, depending on the applications and/ or therapeutic targets, MSC from different tissue sources could serve different purposes and should be selected accordingly.

I.1.2. Culture expansion strategies for MSC

Choosing the culture system and culture medium used to produce cells are key steps toward a safe, scalable, and cost-effective expansion bioprocess for cell therapy purposes. Special attention should be given to the choice of the culture medium used to produce the cells, which is a key compliance factor for Good Manufacturing Practice (GMP)-based expansion processes[26]. Traditionally, MSC have been cultured in a defined basal medium (Dulbecco's Modified Eagle Medium (DMEM) or α- Minimum Essential Medium (αMEM)) supplemented with fetal bovine serum (FBS). Although effective and widely used, the use of FBS or other animal-derived components in manufacturing processes is highly discouraged by regulatory agencies due to the risk of transmitting xenogeneic (xeno) infectious agents and immunization[27,28]. Additional drawbacks include bath-to-batch variability, ill-defined nature and ethical aspects[29]. Serum components in MSC cultures are crucial for effective cell expansion[30] and efforts to replace commercially available bovine or calf serum with GMP alternatives, such as autologous or allogeneic human sera or human platelet lysate (hPL), have encountered

technical difficulties in achieving large-scale expansion of MSC, and also in meeting the laboratory requirements of these supplements in large amounts[28]. Most recently, the development of GMP culture systems, free of any animal derivatives (*i.e.*, serum/ xeno-free – SF/ XF), has been achieved by leading life science companies aiming to provide culture media supporting expansion of homogeneous, well-defined MSC populations with unchanged "stemness" characteristics, minimized variability and closely controlled MSC functions, meeting the EU regulatory requirements[31]. Several groups have been adapting and optimizing MSC expansion protocols towards complete animal-free workflows under SF/ XF conditions, successfully demonstrating that their stem-cell characteristics are maintained, including the immunophenotype, multilineage differentiation potential, and proliferation capacity, and their predictable therapeutical function[28,30,32–36]

These novel SF/XF culture conditions have great potential for clinical use, though additional preclinical safety and efficacy studies must be undertaken and standardized before using in clinical treatments. Off-the-shelf cell products will require effective SF/XF conditions in which the basic stem-cell characteristics of MSC are maintained, the proliferation rate is high, and the cells retain their functionality. The development of efficient and safe SF/XF-culture conditions is one step closer to the normalization of an allogeneic MSC-based clinical product.

I.1.3. MSC as a delivery platform for cell and gene therapies

Beyond all the interesting features of MSC previously stated, several studies have demonstrated the ability of MSC to selectively migrate towards sites of injury[37]. This is one of the most unique and attractive features of MSC regarding cell therapies, commonly known as homing capacity or cell tropism. Stem cell homing is a phenomenon that was initially related to hematopoietic stem cells (HSC) since these cells are able to migrate through the bloodstream to different organs and return to their niches at the BM under the guidance of specific biochemical signalling[38]. Similarly to HSC, MSC also exhibit homing properties. This phenomenon allows BM stromal cells to migrate and engraft into damaged tissues throughout the body. When BM-MSC are systemically administered after a stroke, the cells migrate and home towards the brain, improving the functional outcome[39]. Several animal studies indicate that direct delivery of MSC to injured tissues can significantly promote their structural and functional recovery. These cells migrate and engraft into different tissues regardless of the causes of the injuries and the tissue type[40]. While there is much still to uncover concerning the mechanisms underlying this remarkable and complex feature of MSC, it is acknowledged that these cells are specifically attracted to the sites of pro-inflammation and tissue damage, which is typically associated with cytokine signalling, and in this process the C-XC chemokine

receptor type 4 (CXCR4) - stromal cell-derived factor 1 (SDF1α) axis has an important role[41]. *In vivo*, MSC are able to secrete a wide variety of different growth factors, cytokines, and adhesion molecules by which they will affect the microenvironment of the inflamed and degenerating target tissue and thus maintaining a positive paracrine effect on the tissue repair[41]. The capacity of homing towards inflammatory sites along with the ability to modulate the defence mechanisms of the host, makes MSC a promising therapeutic agent in maintaining transplantation tolerance, and exerting a therapeutic effect in multiple disease models, such as graft-versus-host-disease (GvHD)[42], diabetes mellitus type 1[43], experimental autoimmune encephalomyelitis (EAE)[44], contusive spinal cord injury and its subsequent inflammation-related damage[45], among others. Very importantly, MSC have been described as immune privileged, being able to escape, to a certain extent, of the recognition mechanisms by the immune system due to low expression of major histocompatibility complex (MHC) I and lack of expression of MHC class II along with other co-stimulatory molecules[46]. This reduced alloreactivity is a major benefit in terms of host compatibility issues, allowing MSC administration in an allogenic context[47]. In fact, to date, clinical trials have shown mild or no adverse effects from MSC treatment[48]. MSC may also act as primary matrices in processes of tissue repair caused by inflammation and injury, such as bone regeneration[49] and cardiac injury repair[50]. Considering their homing capacity to tumor sites, a pro-inflammatory microenvironment, MSC can also serve as targeted carriers of therapeutic agents, as part of the tumor stroma in anti-cancer therapy[37]. Altogether, these features suggest MSC as a valuable tool for targeted cell and gene therapies and regenerative medicine settings. However, one of the major limitations that remains to be overcome is the low survival and engraftment rate of MSC after infusion. The viability of MSC and their capacity to effectively home to lesions following administration into the recipient are limited, and the majority of the cells die within a few hours, even if the cells were delivered into the local lesion site[51]. Several studies have exploited genetic engineering approaches aiming at expanding the robustness and boosting the therapeutic profile of MSC, and the field has progressively gained more significance over the last years (Figure I.1.1). Essentially, by improving their innate secretory functions through cell modification, tissue repair/ cell therapy can be accomplished in a more targeted manner, in the most diverse range of pathologies. This improvement can be achieved by overexpression or suppression of factors naturally secreted by MSC, using expression vectors or RNA inference (RNAi) molecules, respectively. MSC have also been studied as a cellular vehicle for gene-transfer applications either designed to replace a missing protein or used to express non-native therapeutic proteins. Although in preliminary stages, molecular editing of MSC using clustered regularly interspaced short palindromic repeats (CRISPR) systems have also been exploited to improve or add to their innate therapeutic properties.

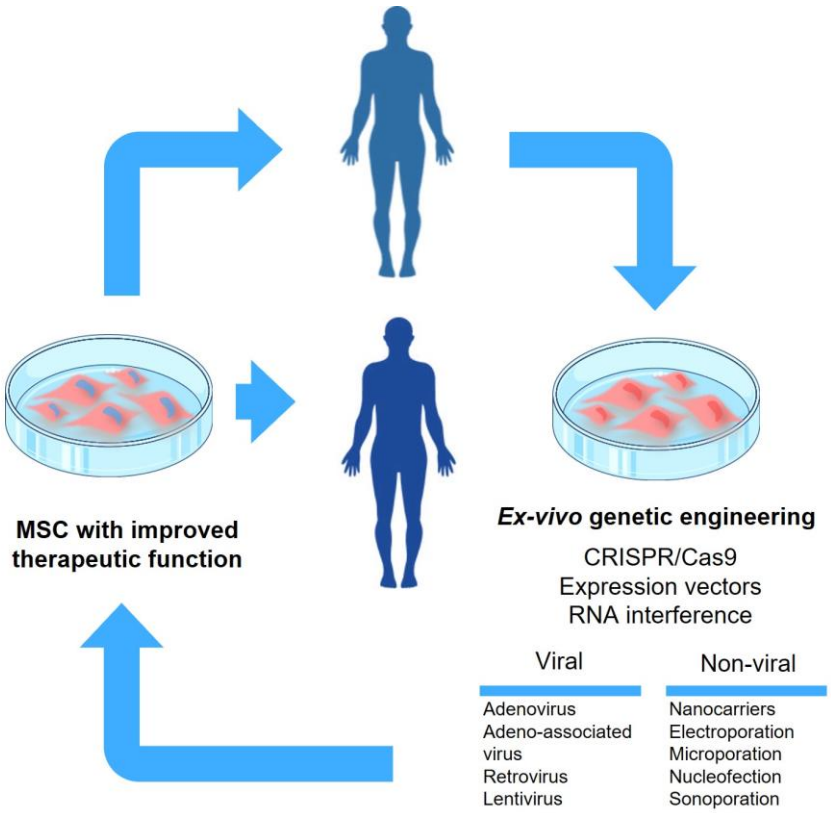

Figure I.1.1. - Improving the therapeutic profile of Mesenchymal Stromal Cells (MSC) through different genetic engineering approaches relying on viral and non-viral methods.

I.2. MSC secretome as a cell-free platform for therapy

The “secretome” of MSC includes a variety of secretory proteins such as growth factors, cytokines, chemokines and extracellular vesicles (EVs) such as microvesicles (MVs; 100–1,000nm diameter) and exosomes (40–150nm diameter)[52]. These molecules are involved in cell-to-cell interactions and play a key role in processes such as immunomodulation, tissue repair/ regeneration, and communication to exert their effects. Among EVs, exosomes have been extensively studied over the last years. These vesicles transport a variety of cellular components and mediators such as proteins, lipids, and many different species of RNAs to the neighbour or distant cells[53]. Interestingly, there are some studies suggesting that exosomes from MSC might retain some of their mother-cell features, such as tumor homing[54,55], potentially able to exert a therapeutic effect[56–58] in a cell-free approach, which can obviate some of the problems associated with living products in a clinical scenario. As such, in parallel with cellular therapy, cell-free therapy based on MSC secreted bioactive factors is being actively developed.

Cell-free preparations of MSC based products are generated by collecting culture media after MSC expansion. Conditioned medium (CM) preparations differ from other biologics because they represent a mixture of different factors secreted by the cells. These factors include growth factors and cytokines, enzymes, nucleic acids, and bioactive lipids (see[59] for recent review). Today, two types of CM products are being developed with the purpose of therapeutic/ cosmeceutical application, namely, CM concentrates and EVs isolates. Due to the fact that cell-free therapy has been evaluated only in a small number of early-stage clinical trials, literature reports remain scarce. As with cell therapy, cell-free therapy is being tested for several diverse applications. AT-MSC derived CM showed promise in enhancing wound healing after skin laser resurfacing[60] and limiting alopecia[61]. BM-MSC CM improved bone volume after maxillary sinus floor elevation[62]. Combination of BM-MSC with CM preparation demonstrated safety and possible efficacy in a phase 1/2 study of multiple sclerosis[63]. EVs from UCM-MSC showed promising result in the treatment of GvHD[64] and chronic kidney disease[65]. EVs from MSC are currently being tested for the treatment of type 1 diabetes, macular holes, and acute ischemic stroke[66]. The promising therapeutic effect of MSC derived CM and EVs is also extended to tumor inhibition in prostate[67], multiple myeloma[68], breast[69], ovarian[54], Hepatoma/Kaposi's sarcoma[54], and bladder[55] tumor cells lines. In these early proof-of-concept studies, testing several donors is required to prove the therapeutic effect. However, in the future, as for MCS-based therapies, the issue of donor heterogeneity can be avoided by immortalization of a secreting cell line[70] or alternatively, by identification and implementation of standardized criteria for comparing cell lines. Cell lines can also be genetically modified to allow enhanced production of certain factors[71] or modification of EVs membrane for targeting certain tissues[72]. In Table I.2.1 a list of various applications of CM in provided in different disease models with the observed effects.

Table I.2.1 - Examples of preclinical studies with non-engineered MSC derived conditioned media (CM). CM concentrates were delivered to mouse and rat models of vascular/ cardiovascular, bone and joints, brain/ nervous system, skin diseases, and malignant diseases. The MSC source and observed effects are provided.

CM MSC Source	Application	Effect	Reference
Human AT	Monocrotalin-induced pulmonary hypertension	Improved pulmonary blood flow; inhibited cardiac remodelling	73
	Bleomycin-induced pulmonary fibrosis	Reduced collagen deposition	73
	Critical limb ischemia	Improved blood vessel density, limb salvage, and blood perfusion	74
	Surgical bone lesions	Induced bone regeneration	75
	Amyotrophic lateral sclerosis in $SOD1^{G93A}$ mice	Increased post-onset survival and lifespan	76
	Prostate cancer	Inhibited tumor growth possibly by transferring miR-145 to reduce the activity of Bcl-xL and promote apoptosis through the caspase-3/7 pathway	67
Human: AT BM	Cisplatin-induced kidney injury	Improved renal pathology; promoted survival	77
Human BM	Lipopolysaccharide (LPS)-induced lung injury	Decreased lung inflammation and edema	78
	Ovalbumin-induced asthma	Decreased histopathologic changes; reduced leukocyte counts in lavage	79
	Fulminant hepatic failure	Reduced panlobular leukocytic infiltrates, hepatocellular death, and bile duct duplication	80
	Infarcted heart	Limited infarct size; improved ventricular function	71
	Antigen-induced arthritis	Reduced joint swelling, cartilage loss, and proinflammatory factors secretion.	81
	Experimental allergic encephalitis	Reduced functional deficits; promoted development of oligodendrocytes and neurons	82
	Spinocerebellar ataxia in SCA1 knock-in mice	Attenuated degeneration of axons and myelin in spinal motor neurons	83
	Hepatoma/Kaposi's sarcoma/ovarian tumor cell lines	Inhibited tumor growth	54

Table I.2.1 (continued)

CM MSC Source	Application	Effect	Reference
Human BM	Multiple myeloma	Inhibited tumor growth	[68]
	Mouse breast cancer cell line (4T1)	Suppressed angiogenesis via delivery of miR-16 and down-regulation of angiogenesis in the tumor	[69]
Human DP	Neonatal brain injury	Reduced tissue loss and pathologic score after hypoxia/ischemia	[84]
Human UCM	Radioactive dermatitis	Accelerated wound healing	[85]
Human: UCM WJ	Bladder carcinoma	Inhibited tumor growth by down-regulating phosphorylation of Akt protein kinase and up-regulating cleaved caspase-3	[55]

I.3. Gene delivery methods for MSC-based therapy

I.3.1. Viral methods

After the first ever approval in 2003 of an adenovirus-based gene product for head/neck carcinoma, Gendicine, in China[86] and with the first European marketing authorization in 2012 of an adeno-associated virus 1 (AAV1) vector for the treatment of a lipoprotein lipase deficiency (Glybera®)[87], the viral vector-based gene therapy has been evolving towards the first-line treatment of rare and acquired diseases for which different viral vectors systems are available. Being MSC readily suitable to viral transduction, with optimized protocols that can prompt up to 90% transduced cells with no impact on multilineage differentiation capacity or the intrinsic properties[88], there are several studies that have exploited viral vectors to improve gene delivery. The use of viral vectors for gene transfer takes advantage of their natural ability to infect the cells. Therefore, transgenes may be incorporated either in addition to the genome or by replacing one or more genes. Viral transduction can thus offer a long-term and stable production of the protein of interest. These genetic modifications can then be targeted to improve the survival of MSC, while mediating tissue repair and recovery in the *in vivo* environment, enhancing their therapeutic potential upon administration. Currently, the most common viral vectors being used include retrovirus, lentivirus, adenovirus, and adeno-associated virus.

Overall, currently viral modified MSC are playing a remarkable role in the treatment of a wide range of conditions such as bone regeneration, cardiovascular and autoimmune diseases,

central nervous system diseases, or cancer. A summary of some of the applications of genetically modified MSC using viral vectors is depicted in Table I.3.1.

Table I.3.1 - Genetically modified MSC tested for the treatment of different conditions employing viral gene delivery methods.

Therapeutic target	MSC source	Transduction Method	Therapeutic target	Reference	Observations
Apelin	Human WJ	Lentivirus	Type 2 diabetes mellitus	[89]	
BCL-2	Rat BM	AAV	Hepatic Cirrhosis	[90]	
Fibroblast growth factor (FGF)	Rabbit BM	Lentivirus	Bone regeneration	[91]	
FGF and Platelet derived growth factor (PDGF)-BB	Human PL	Adenovirus	Hindlimb ischemia	[92]	
Bone morphogenic protein (BMP)-2	Human UCM	Lentivirus	Bone regeneration	[93]	
	Mouse BM	AAV	Osteopenia	[94]	
BMP-6 and Vascular endothelial growth factor (VEGF)	Rat BM	AAV	Bone regeneration	[95]	MSC loaded onto a scaffold
BMP-7	Canine AT	Lentivirus	Bone regeneration	[96]	MSC transplanted into cell sheets
C-type natriuretic peptide (CNP)	Rat BM	Adenovirus	Articular cartilage regeneration	[97]	MSC loaded onto a scaffold
CXCR4	(Not provided)	Retrovirus	Improve MSC homing towards infarcted myocardium	[98]	

Table I.3.1 (continued)

Therapeutic target	MSC source	Transduction Method	Therapeutic target	Reference	Observations
Decorin	Human Umbilical Cord	Adenovirus	Radiation-induced lung injuries	99	
Extracellular regulating kinases 1/2 (ERK1/2)	Rat BM	Lentivirus	Stroke	100	
Herpes simplex virus 1 -thymidine kinase (HSV1-TK)	Mouse BM	Retrovirus	Anaplastic thyroid cancer	101	Prodrug suicide gene therapy system
Interleukin (IL) -10	Human BM	Adenovirus	Osteoarthritis	102	
	Rat BM	Adenovirus	Rheumatoid arthritis	103	
	Human BM	AAV	Acute Ischemic Stroke	104	
Interferon (IFN)-α	Mice BM	AAV	Melanoma	105	
IFN-β	Human UCM	Lentivirus	Lung cancer	106	
	Canine AT	Lentivirus	Melanoma	107	Combination of cell-based therapy and chemotherapy
	BM	Lentivirus	Ovarian cancer	108	
IL-12	BM	Retrovirus	Melanoma	109	
IL-32	Mouse BM	Adenovirus	Lung cancer Gastric cancer	110	
Klotho	Mice BM	Adenovirus	Acute kidney injury	111	
Tumor necrosis factor (TNF)-14	Human UCM	Lentivirus	Gastric cancer	112	

Table I.3.1 (continued)

Therapeutic target	MSC source	Transduction Method	Therapeutic target	Reference	Observations
MicroRNA (miR)-124a	(Not provided)	Lentivirus	Glioma	[113]	Exosome delivery
miR-26a	Mouse BM	Lentivirus	Bone regeneration	[114]	
Netrin-1	Mouse AT	Adenovirus	Diabetic peripheral neurovascular disease	[115]	
OPG	Human UCM	Adenovirus	Osteosarcoma	[116]	
PEDF	Mouse BM	Adenovirus	Lewis lung carcinoma	[117]	
Hydroxylase domain-containing protein 2 (PHD2)	Rat BM	Lentivirus	Periodontitis	[118]	Tissue-engineered construct to deliver MSC
TNF	Human Umbilical Cord	Lentivirus	Gastric cancer	[119]	
	Rat BM	AAV	Acute myocardial infarction	[120]	
Tumor necrosis factor-related apoptosis-inducing ligand (TRAIL)	Human AT	Lentivirus	Pancreatic cancer	[121]	
	Rat WJ	Lentivirus	Hepatocellular cancer	[122,123]	
	Human BM	Lentivirus	Lung cancer	[124]	
	Human AT	Retrovirus	Cervical carcinoma Pancreatic cancer Colon cancer	[125]	

Table I.3.1 (continued)

Therapeutic target	MSC source	Transduction Method	Therapeutic target	Reference	Observations
TRAIL	Human AT	Lentivirus	Pancreatic cancer	126	Combination of cell-based therapy and chemotherapy
	Human Gingiva	Lentivirus	Tongue squamous cell carcinoma	127	
	Human BM	Lentivirus	Colorectal carcinoma	128	
	Human Umbilical Cord	Lentivirus	Non-Hodgkin's lymphoma	129	
	Human BM	Adenovirus	Pancreatic ductal adenocarcinoma	130	MSC deliver oncolytic viruses carrying the TRAIL transgene
	Human: AT BM DP Menstrual Blood Umbilical Cord	Retrovirus	Prostate cancer Breast adenocarcinoma Glioblastoma	131	Prodrug suicide gene therapy system Exosome delivery

I.3.2. Non-viral methods

Viral systems are still a conventional method to introduce a therapeutic gene into mammalian cells, owing to their higher gene transfer efficiency and long-term stable gene expression both *in vitro* and *in vivo*. However, the clinical application of viral-engineered cells is still debatable due to safety issues related to risks of carcinogenesis and immunogenicity, as well as due to limited DNA packaging capacity and difficulty of vector production[132]. These limitations have motivated the development of alternative non-viral gene delivery systems, which can be classified as chemical and physical methods. The non-viral methods, featuring low

immunogenicity, no risk of transmission of infectious diseases, flexibility in loaded DNA capacity and low production cost, represent a promising and effective approach currently used for gene delivery[132–135]. However, both physical and chemical methods present some drawbacks, namely lower transfection efficiencies compared to viral vectors, the possibility to disrupt cellular/nuclear membranes and the unsuitability for the transfection of a large population of cells and hard-to-transfect cells. Particularly, the physical methods are difficult to be applied in an *in vivo* situation and can lead to tissue damage. On the other hand, chemical agents can lead to toxicity at higher concentrations, cause adverse reactions with negatively charged molecules and raise safety concerns due to the non-degradable nature of certain materials[134,136]. Still, in the last decades, numerous non-viral gene delivery strategies have been developed and applied for the transfection of human cells, in particular for MSC. Examples of studies that used non-viral systems to genetically engineer human MSC to adjust their therapeutic potential will be presented in the following sections.

I.3.2.1. Chemical methods

Chemical methods imply the use of natural or synthetic materials, also referred to as nanocarriers, which electrostatically condense or encapsulate nucleic acids into nanoparticles (NPs) or aggregate complexes that subsequently transfer the genetic material into the cell. These delivery systems can be physicochemically tuned in order to overcome the barriers and engineered to target specific tissues for improved gene delivery and expression[137]. A wide variety of nanocarriers including polymers, lipids, polysaccharides, peptides, and inorganic materials, have been used to facilitate transfection of MSC[134,136]. Cationic lipid- and polymeric-based nanocarriers, such as lipofectamine and polyethylenimine (PEI), are considered the gold standard for non-viral gene transfection and often used as transfection control, including studies specifically employing MSC. For example, Cho and co-workers[138] tested the delivery of a vector encoding the human forkhead box A2 (*Foxa2*) gene to rat BM-MSC using Lipofectamine, aiming at stimulating tissue regeneration after cell administration, protecting the liver from hepatic diseases. In this study, Foxa2-engineered MSC showed to efficiently incorporate into liver grafts.

Also using the lipofection method, Tsubokawa and colleagues[139] transiently overexpressed the human heme oxygenase-1 (*HO-1*) gene, which encodes an anti-oxidant and anti-inflammatory protein with potential to attenuate ischemic myocardial injury, in rat BM-MSC. The results showed that the engineered MSC exhibited enhanced anti-apoptotic and anti-oxidative abilities, contributing to improved repair of ischemic myocardial injury in a rat

infarction model, through cell survival and VEGF production. Additionally, lipofectamine has also been used to engineer human BM-MSC to express bacterial cytosine deaminase (CD), which catalyses the hydrolytic deamination of the non-toxic 5-FC molecule into the anti-cancer drug 5-Fluorouracil (5-FU). CD-expressing MSC showed anti-cancer therapeutic potential while minimizing the side-effects of 5-FU. *In vivo* studies have demonstrated that by intravenous injection, followed by systemic administration of 5-FC, the engineered cells are able to inhibit the growth of human gastric tumors in mice[140]. Furthermore, RNAi molecules have also been successfully transfected into MSC using lipofectamine, for example in the study by Yu and collaborators[141], mouse BM-MSC were transfected with let-7a miRNA inhibitors. let-7a is a miRNA that targets the mRNA of Fas and Fas Ligand (FasL), which are crucial proteins in the context of MSC therapy for inflammatory diseases, as these enhance the migration of T cells and activate the apoptosis pathway in T cells, respectively. The results showed that knockdown of let-7a significantly promoted MSC-induced T cell migration and apoptosis *in vitro* and *in vivo,* while reducing mortality, suppressing the inflammation reaction, and alleviating the tissue lesion of experimental colitis and GvHD mouse models. Moreover, synthetic small interfering RNA (siRNA) molecules were also successfully delivered to human BM-MSC using lipofectamine, as described by Teoh and colleagues[142]. BM-MSC promote the growth of myeloma cells mainly through IL-6 secretion, thus targeting its overexpression should disrupt the favourable microenvironment provided by the BM for multiple myeloma cell growth. siRNA-IL-6-transfected MSC inhibited cell growth and IL-6 production by the human multiple myeloma cell line U266 *in vitro*. Importantly, the modified MSC led to tumors with significantly reduced volumes and mitotic indexes in a murine subcutaneous model of human multiple myeloma. On the other hand, Li and colleagues[143] used PEI to deliver a plasmid encoding the antiapoptotic gene *BCL-2* to rat BM-MSC, as an attempt to improve functional recovery after acute myocardial infarction with BCL-2-engineered MSC. *In vivo* studies showed an increased cellular survival and capillary density in the infarct border zone as well as a remarkable functional recovery upon administration of *BCL-2*-engineered MSC into rat models of myocardial infarction. In the study by Rejman and co-workers[144], the authors tested the cationic nanocarriers lipofectamine, DOTAP/DOPE, and PEI for their ability to mediate the delivery of mRNA encoding the CXCR4 receptor into mouse MSC, with the aim of increasing their homing to injured tissues. mRNA complexed with the cationic lipids transfected a larger number of cells than the polyplexes, obtaining 80% and 40% of *CXCR4*-positive cells, respectively. Overall, it was possible to demonstrate that mRNA could be a suitable alternative to plasmid DNA in MSC. More complex polymers have also been developed and used to transfected MSC. For example, Park and collaborators[145] used PEI-modified PLGA NPs to transfect human BM-MSC with plasmids encoding the exogenous SRY-box (SOX) trio (SOX 5, 6, and 9) genes, which successfully led to increased chondrogenesis of MSC in *in vitro*

culture systems. In the context of therapeutic angiogenesis, Yang and colleagues[146] developed a set of biodegradable poly (β-amino esters) (PBAE) nanocarriers capable of delivering a *VEGF*-expressing plasmid to human BM-MSC. The engineered cells led to 2- to 4-fold higher vessel densities in the subcutaneous model and also enhanced angiogenesis and limb salvage after intramuscular injection into mouse ischemic hindlimbs. As such, the engineered MSC might represent a promising therapeutic tool for vascularizing tissue constructs and treating ischemic disease. Considering the aforementioned potential of MSC as tumor-targeting gene delivery vehicles, Malik and colleagues[147], used a PEI polylysine (PLL) copolymer for the delivery of the exogenous suicide gene herpes simplex virus (*HSV*) - Thymidine kinase (*TK*) and also tumor necrosis factor-related apoptosis-inducing ligand (*TRAIL*) gene to rat BM-MSC, as a potential combinational suicidal gene therapy for glioblastoma. After intra-tumoral injection, the double-transfected MSC along with prodrug GCV administration induced a significant synergistic therapeutic response both *in vitro* and *in vivo* in a rat C6 glioma model. Likewise, Zhang and colleagues[148] used a spermine-pullulan (SP) copolymer to engineer rat BM-MSC to transiently express *HSV-TK*, in order to investigate their effect on pulmonary melanoma metastasis. The engineered cells combined with the prodrug GCV, showed significantly tumor growth inhibition both *in vitro* and *in vivo* in the metastasis tumor model used. In a different context, Huang and colleagues[149] also used SP for the transfection of peptide-modified rat BM-MSC with miR-133b that is known to promote functional recovery from cerebral ischemia. The miR-133b-transfected MSC were shown to be beneficial for the recovery of injured neural cells as the administration of engineered cells resulted in a significant increase of the number of surviving astrocytes after subjection to oxygen-glucose deprivation (OGD) *in vitro*, suggesting a therapeutic role of the modified cells to increase cell survival, thus enhancing the recovery of ischemic injured cells. Inorganic materials have also been used for gene delivery into MSC including gold NPs (AuNPs), magnetic NPs (mNPs) and silica. Aiming at the development of an effective gene delivery system for bone regeneration, Kim and colleagues[150] used mesoporous silica modified with amine groups as nanocarriers to deliver the *BMP2* gene, which encodes a bone morphogenic protein important in bone repair and regeneration, into primary rat BM-MSC. Also using silica, Zhu and colleagues[151] used hollow mesoporous organo-silica NPs conjugated with PEI to facilitate the delivery of the HGF gene into rat BM-MSC. The engineered cells were transplanted into rat models of myocardial infarction and shown to be efficient in cardiac repair by largely decreasing apoptotic cardiomyocytes, reducing infarct scar size, and increasing angiogenesis in myocardium. Aiming to improve the transfection efficiency of difficult-to-transfect MSC, Das and co-workers[152] used AuNPs, which currently have diverse biomedical applications, modified with PEI. PEI-entrapped gold NPs and covalently bound PEI-gold NPs were tested as potential vehicles for the delivery of the CCAAT/enhancer binding protein beta

(C/EBP-β) gene, which encodes a key transcriptional regulator of adipogenic differentiation into human WJ-MSC. Overexpression of exogenous *C/EBP-β* significantly enhanced adipogenesis in MSC, while the NPs/DNA complexes showed favourable cytocompatibility in cell viability assays. This study showed that theses NPs represent a promising vehicle for gene delivery to control MSC differentiation and potentially other therapeutic gene delivery applications. Also using AuNPs, Muroski and colleagues[153] developed a novel zwitterionic cell penetrating pentapeptide that upon conjugation with AuNP facilitated the delivery of a linearised plasmid encoding for a brain-derived neurotrophic factor (*BDNF*) to rat BM-MSC. In the context of neural repair, Wu and collaborators[154] produced mNPs using synthetic hydroxyapatite (Hap) and natural bone mineral (NBM) capable of delivering a plasmid encoding the glial cell line-derived neurotrophic factor (*GDNF*), a potent neurotrophic growth factor, into rat BM-MSC under the action of a magnetic field. The results showed that these mNPs could be used for safe and effective transfection *in vitro*, and that MSC transfected *ex vivo* with the exogenous *GDNF* might be a promising cell therapy for the treatment of neurodegenerative diseases. It is important to note that MSC response following non-viral gene transfection may strongly differ depending on the selected nanocarrier, as reported in the study by Gonzalez-Fernandez co-workers[155]. The authors tested three non-viral gene delivery systems: PEI, Hap and an amphipathic peptide RALA to transiently deliver TGFβ3 and/or BMP2 genes to porcine BM-MSC in order to promote their osteogenesis or chondrogenesis and evaluate the influence of different gene nanocarriers on the lineage commitment of MSC. Despite showing similar gene transfection efficiencies these nanocarriers had different effects on MSC viability, cytoskeletal morphology and differentiation, as transfection of MSC using PEI failed to induce robust osteogenesis or chondrogenesis, whereas Hap transfection promoted osteogenesis in 2D culture and RALA transfection showed to be less osteogenic and promote a more cartilage-like phenotype, confirmed through relative expression levels of chondrogenic markers Aggrecan (ACAN), SOX-9 and osteogenesis marker Runt related transcription factor 2 (Runx2), and biochemical and histological analysis of glycosaminoglycans (GAG), calcium and collagen. The results demonstrate that the differentiation of MSC through the application of non-viral gene delivery strategies also depends on the nanocarrier itself and not only on the gene delivered. A summary of several studies where MSC were genetically engineered using nanocarriers is shown in Table I.3.2.

Table I.3.2 - Genetically modified MSC tested for the treatment of different conditions employing non-viral gene delivery methods.

Nanocarrier	MSC source	Therapeutic Cargo	Application	Reference
Lipofectamine	Rat BM	*Foxa2* encoding plasmid	Regeneration of damaged liver tissues	138
	Rat BM	*HO-1* encoding plasmid	Treatment of myocardial ischemia	139
	Human BM	*CD* encoding plasmid	Target human gastric tumors	140
	Mouse BM	miRNA targeting miR-let-7a	Reduced immunogenicity of MSC transplants	141
	Human BM	siRNA targeting *IL-6*	Treatment of multiple myeloma	142
PEI	Rat BM	*Bcl-2* encoding plasmid	Functional recovery after acute myocardial infarction	156
Lipofectamine; DOTAP/DOPE; PEI	(Not provided)	*CXCR4* mRNA	Increased homing into target tissues	144
PEI-modified poly lactic-co-glycolic acid	Human BM	*SOX-5, -6,* and *-9* encoding plasmids	Increase chondrogenesis	157
Poly (β-amino esters)	Human BM	*VEGF* encoding plasmid	Treatment of ischemic diseases	158
PEI-modified PLL	Rat BM	*HSV-TK* and *TRAIL* encoding plasmid	Target glioblastoma	159
Spermine-Pullulan	Rat BM	*HSV-TK* encoding plasmid	Target pulmonary metastasis	160
	Rat BM	miRNA-133b	Treatment of cerebral ischemia	149
Silica modified with amine groups	Rat BM	*BMP2* encoding plasmid	Bone repair and regeneration	161
Hollow mesoporous organo-silica conjugated with PEI	Rat BM	*HGF* encoding plasmid	Cardiac repair	162

Table I.3.2 (continued)

Nanocarrier	MSC source	Therapeutic Cargo	Application	Reference
PEI-coated gold NPs	Human WJ	*C/EBP* encoding plasmid	Increase adipogenesis	[163]
Zwitterionic pentapeptide conjugated with the AuNP	Rat BM	*BDNF* encoding linearized plasmid	Treatment of Neurodegenerative diseases	[153]
Magnetic hydroxyapatite NPs; Natural bone mineral	Rat BM	*GDNF* encoding plasmid	Treatment of Neurodegenerative diseases	[154]
PEI; Hydroxyapatite; RALA peptide	Porcine BM	*TGF-β3* and *BMP2* encoding plasmids	Increase chondrogenesis; Increase osteogenesis	[164]

I.3.2.2. Physical methods

Physical methods often imply *ex vivo* transfection of cells by disruption of cellular/nuclear membranes and consequent transfer of nucleic acids. Among different methods, microinjection, particle bombardment, electroporation, sonoporation and laser irradiation have been used to facilitate gene transfer into mammalian cells[165]. Some of these methods have been used to genetically engineer MSC for enhanced therapy, including electroporation and sonoporation.

I.3.2.2.1. Electroporation

Electroporation is one of the most common non-viral gene delivery methods and relies on the exposure of the cell membrane to high-intensity electrical pulses. The transient and localized destabilization of the barrier allow the permeabilization of exogenous molecules, such as DNA, present in the surrounding medium[165]. Electroporation is cost-effective and an efficient method that is widely used for *ex vivo* transfection of MSC[136]. For example, Kim and colleagues used electroporation to facilitate the delivery of a plasmid encoding the SOX trio genes into human BM-MSC. The results showed that electroporation-mediated co-transfection of these transcription factors enhances chondrogenesis and suppresses hypertrophy of MSC[166]. On the other hand, Lee and co-workers reported that the electroporation-mediated transfection of

plasmid encoding the *Runx2* and *Osterix* transcription factors, which are essential for osteogenic differentiation from uncommitted progenitor cells, into human AT-MSC enhances their *in vitro* and *in vivo*osteogenesis[167]. Kojima and collaborators used electroporation to engineer human BM-MSC to increase exosome production, which are promising therapeutic agents, by facilitating the delivery of a plasmid encoding for *STEAP3*, *syndecan-4 (SDC4)* and *L-aspartate oxidase (NadB)* proteins that are involved in exosome biogenesis. The combined expression of these genes from the engineered MSC led to significantly increased exosome production, up to a 40-fold increase compared to non-modified MSC. This booster effect was detected by supernatant luminescence due to the expression of a construct encoding the vesicle-associated CD63 marker fused with nanoluc that was co-transfected into MSC[168]. Another study that used electroporation as delivery system was reported by Liu and colleagues, in which human UCM-MSC were transfected with a vector encoding the non-senescent *heat shock protein 27 (Hsp27)*. Cells undergoing replicative senescence have diminished heat shock response, thereby alterations in Hsp7 production can potentially increase the accumulation of damaged proteins promoting further aging. The results showed that the engineered MSC promoted neuroplasticity in a mouse stroke model and decreased cellular senescence, thus increasing MSC engraftment[169].

I.3.2.2.2 Nucleofection

In alternative to conventional electroporation, the commercial system Nucleofector (Lonza, Germany) has also been used to efficiently transfect MSC, by employing cell-type specific pulse parameters and buffer formulations that allows the direct electroporation of DNA into the nucleus – nucleofection[170]. Pham and colleagues used nucleofection to transfect human UCB-MSC with mRNA encoding pancreatic and duodenal homeobox 1 *(PDX-1*), a transcription factor also known as insulin promoter factor 1, whose expression has been known to facilitate MSC differentiation into insulin-producing cells (IPCs). The results showed that *PDX-1* mRNA transfection significantly improved the differentiation of MSC into IPCs and led to 2-fold increase in production of insulin and C-peptide in response to glucose. Therefore, this approach could be a promising system to produce safe IPCs as a potential therapy for diabetes mellitus treatment[171]. The nucleofection method was also used by Fakiruddin and collaborators to facilitate the delivery of *TRAIL*-encoding vectors into human AT-MSC, to evaluate the anti-tumorigenic potential of the engineered MSC *in vitro* using several cancer models. TRAIL-expressing MSC selectively inhibit proliferation of tumor lines and markedly induces apoptosis[172]. In another example of a potential anti-cancer therapy, Kim and colleagues engineered human AT-MSC to target medulloblastoma (MBL), a common

malignant childhood brain tumor, using nucleofection as transfection method. AT-MSC were transfected with plasmid encoding neurotrophins-3 (NT-3), found to induce tumor cell apoptosis in MBL. The transfected cells showed a growth inhibitory effect on a MBL cell line *in vitro*, by inducing apoptotic tumor cell death and neuronal differentiation of tumor cells, showing potential as a targeted gene therapy for MBL[173]. Also using nucleofection, but in the context of bone repair, Pelled and colleagues genetically modified porcine AT-MSC to transiently overexpress BMP-6 protein as a potential therapy for a variety of conditions involving bone loss, namely osteoporotic vertebral compression fractures. In this study, the engineered cells showed to induce vertebral defect regeneration in a clinically relevant, large animal pig model[174].

I.3.2.2.3. Microporation

Although effective at transfection, cuvette-based electroporation is limited by cytotoxicity attributed effects of the pulsed electric fields on biomolecules, pH variation, increasing in temperature, and metal ion generation. Microporation is a unique electroporation technology that uses a pipette tip as an electroporation space and a capillary type of electric chamber instead of a cuvette, counteracting the harmful effects of conventional cuvette-based methods[175]. This technique has also been used in studies specifically employing MSC, for instances, to facilitate the delivery of a minicircle vector encoding the *CXCR4* gene into human BMMSC using microporation[176]. In this study, the engineered cells greatly increased their *in vivo* homing ability towards injury sites in a mouse model, compared to non-modified cells[176]. Moreover, Serra *et al.* also used microporation to deliver a minicircle vector encoding the VEGF gene into human BM-, UCM- and AT-MSC. *VEGF*-overexpressing MSC showed an improved angiogenic potential *in vitro*, confirmed by endothelial cell tube formation and cell migration assays[36,177].

I.3.2.2.4. Sonoporation

Another method is sonoporation, which relies on the application of ultrasounds to transiently enhance cell permeability through formation of small pores in the membrane, allowing for the direct transfer of genetic material into cells. The mechanism involved in sonoporation appears to be acoustic cavitation that through mechanical perturbation, collapse of active bubbles and the associated energy release leads to the permeabilization of adjacent cell membranes[165]. Although very few MSC related studies have been reported, Nakashima and colleagues used

sonoporation for the transfection of a plasmid encoding the growth/differentiation factor 11 (*Gdf11*), a member of the BMP family expressed in terminally differentiated odontoblasts, into bovine DP -derived MSC. After *in vitro* transfection, increased expression of dentin sialoprotein, a differentiation marker for odontoblasts, was shown, suggesting differentiation of the pulp stromal MSC into odontoblasts. Additionally, after *in vivo* transfection, restoration of the amputated DP was observed in canine teeth[178]. In another study, sonoporation using a combination of ultrasound and microbubbles was used to deliver siRNAs into rat BM-MSC to silence the expression of *PTEN*, which is known to be a tumor suppressor gene that negatively regulates PKB/Akt dependent cell survival. The transfected cells showed reduced levels of *PTEN* mRNA and increased levels of Akt phosphorylated protein. Thus, *PTEN* inactivation could be considered a promising method to improve the viability and therapeutic efficacy of transplanted MSC[179]. More recently, in the context of anti-cancer therapies. Haber and co-workers used ultrasound-mediated transfection to engineer MSC to target cancer. To this end, rat BM-MSC were transfected with a plasmid encoding for the hemopexin-like domain fragment (*PEX*), an inhibitor of tumor angiogenesis. The results showed that PEX-secreting MSC could be a promising cell-based delivery approach in cancer settings, by inhibiting prostate tumor growth up to 70% following a single I.V. administration and up to 84% after repeated administration to mice bearing prostate tumors[180]. In the context of kidney repair and envisaging the therapeutic benefits of an enhanced homing capacity by MSC, Wang and colleagues used microbubble-mediated ultrasound combined with PEI to facilitate the delivery of a vector encoding *CXCR4* into rat BM-MSC to improve their homing towards acute kidney injury (AKI). After injected into rats' tail veins, the modified MSC showed enhanced homing and retention into AKI-induced tissues[181].

I.3.2.2.5. Microinjection

Finally, microinjection is also considered a promising gene delivery method that uses a glass needle to directly introduce the genetic material into the cell cytoplasm or nucleus, by hydrostatic pressure. The injection is carried out on a single cell under direct visual control, using a microscope. Although conceptually simple, microinjection is difficult to apply since it requires extreme precision, and it is impractical for transfecting large numbers of cells. Although this method is not commonly employed for MSC engineering, microinjection with nanoneedles has proven to be efficient in delivering plasmid DNA into MSC, showing 65–75% reporter transgene expression efficiency while retaining cell viability after injection[182,183].

A summary of different studies of genetic modification of MSC using physical methods is shown in Table I.3.3.

Table I.3.3 - Genetically modified MSC targeting different therapeutic settings, using different physical non-viral gene delivery methods.

Method	MSC source	Therapeutic Cargo	Application	Reference
Electroporation	Human BM	*SOX 5, 6, and 9* encoding plasmids	Increase chondrogenesis	[184]
	Human AT	*Runx2* and *Osterix* encoding plasmids	Increase osteogenesis	[167]
	Human BM	*STEAP3, SDC4 and NadB* encoding plasmid	Increase exosome production	[185]
	Human UCM	*Hsp27* encoding plasmid	Neurological recovery after stroke	[169]
	Human UCB	*PDX-1* mRNA	Treatment of diabetes mellitus	[186]
Nucleofection	Human AT	*TRAIL* encoding plasmid	Target cancer	[172]
	Human AT	*NT-3* encoding plasmid	Target medulloblastoma	[187]
	Porcine AT	*BMP-6* encoding plasmid	Vertebral bone repair	[174]
	Human BM	*CXCR4* encoding minicircle	Increase homing	[176]
	Human BM	*VEGF* encoding mnicircle	Treatment of peripheral artery disease	[188]
Microporation	Bovine DP	*Gdf11* encoding plasmid	Dental tissue repair	[178]
	Rat BM	*PTEN*	Increased viability after transplantation	[179]
	Human BM, UCM and AT	*VEGF* encoding minicircle	Improved angiogenesis	[36,177]
Sonoporation	Rat BM	*PEX* encoding plasmid	Target cancer	[180]
	Rat BM	*CXCR4* encoding plasmid	Engraftment to acute kidney injury (AKI) tissues	[189]

I.4. Enhancing the therapeutic potential of MSC with the CRISPR/Cas9 system

I.4.1. CRISPR/CAS9 methodology

With genome editing, precisely modifying the nucleotide sequence of a genome of choice has become a realistic objective. Disrupting, inserting, or replacing a given gene, controlling its

expression, and inducing chromosomal rearrangements are some of the endeavours many groups are now undertaking[190]. Whatever the approach, genome editing requires the generation of nuclease-induced double-strand breaks (DSBs) or nicks in the target DNA, whose subsequent repair is expected to produce the desired modification through nonhomologous end-joining (NHEJ) in the absence of a homologous repair template, leaving "scars" in the form of insertion/deletion (indel) mutations; or homologous recombination (HR) in the presence of a homologous repair template[191]. The latter provides an effective method for making insertions or corrections in the genome, by supplying an exogenous repair template cassette, in a process called homology directed repair (HDR) (Figure I.4.1). Unlike NHEJ, HDR is generally active only in dividing cells, and its efficiency can vary widely depending on the cell type and state, as well as the genomic locus and repair template [192].

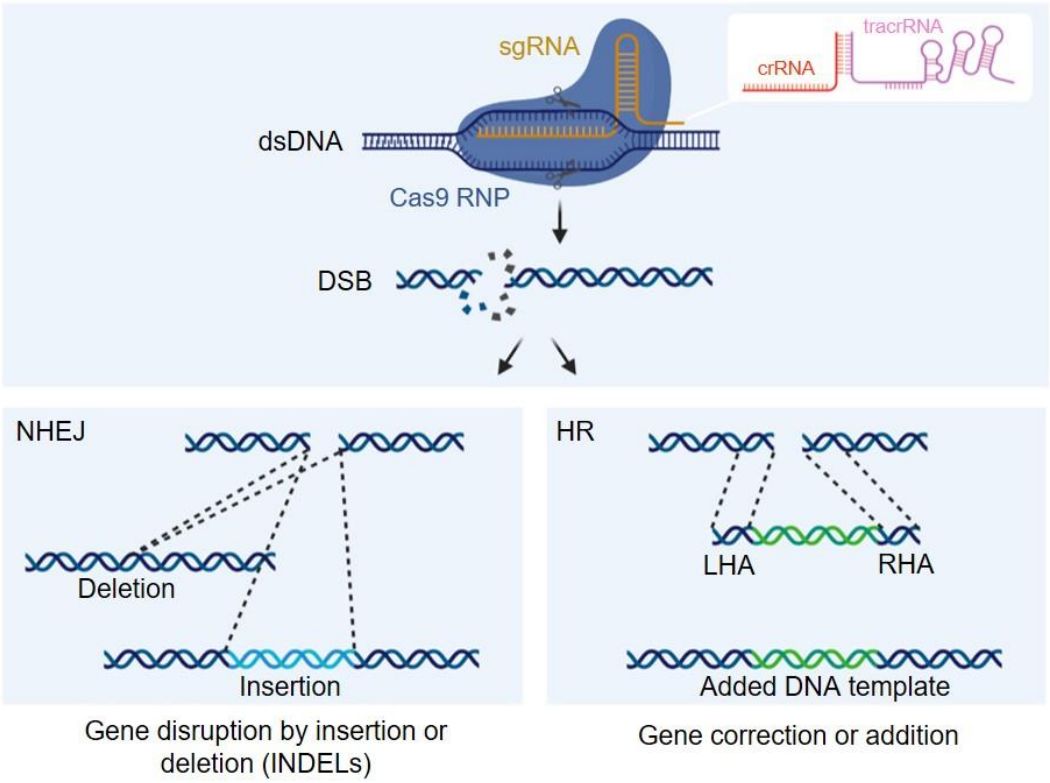

Figure I.4.1 - Genomic repair and recombination events are initiated by double-strand breaks (DSBs) induced by targeted cleavage of the genome with programmable nucleases (e.g., Cas9). When template DNA is absent from directing the repair process, the nonhomologous end-joining (NHEJ) pathway heals broken ends of chromosomes in a process that often generates small deletions and/or insertions at the site of the lesion. When a donor template with close homology to the site of the DSB is present, an event of homologous recombination (HR) may occur, and the donor sequence may guide homology-directed repair (HDR), resulting in a less error prone modification of host sequences. Created with *BioRender.com*.

The first engineered nuclease was the zinc finger nuclease (ZFs), introduced in 1991[193] when a zinc finger DNA-binding protein was fused to the catalytic domain of FokI, a bacterial restriction endonuclease[194]. Those remained the editing tools of choice until transcription activator-like effector nucleases (TALENs), which were generated by fusion of FokI to a class of specific-DNA biding transcription activator-like effectors, were discovered in pathogenic plant bacteria[195,196]. In practice, however, both ZFs and TALENs are difficult to reprogram, requiring extensive process engineering for each new target. In 2013, genome engineering took a huge step forward with the report that the microbial clustered regularly interspaced palindromic repeat (CRISPR)-associated protein 9 (CRISPR/Cas9) bacterial adaptive immune system could be repurposed for genome editing in mammalian cells[197,198]. Unlike ZFs and TALENs, which use a strategy of tethering endonuclease catalytic domains to modular DNA-binding proteins for inducing targeted DNA DSBs at a specific genomic loci, CRISPR/Cas9 uses small RNAs (known as single guide RNA - sgRNA) that complementarily bind to a target DNA through Watson-Crick base pairing achieving sequence specificity[199], and Cas9 is a nuclease, obviating the need to fuse it to an additional protein. The sgRNA is made up of two parts: a crispr RNA (crRNA), a 17-20 nucleotide sequence complementary to the target DNA, and a tracr RNA, which serves as a binding scaffold for the Cas nuclease. The success of the CRISPR/Cas9 system is mainly attributed to the easy design of sgRNA to target specific DNA locus and the high effectiveness and efficiency of Cas9 nuclease to generate DNA breaks[200]. Though, in order for Cas9 to function, it also requires a specific protospacer adjacent motif (PAM) that varies depending on the bacterial species of the Cas nuclease protein being used. PAM sequences are DNA sequences containing on average 3 base pairs located at the 5 ‘end of the CRISPR/Cas9 system target sequence. Since almost all *loci* adjacent to PAM sequences can be edited by this system, virtually all genes are editable by CRISPR/Cas9, given the frequency of PAMs in the genomes of several species – including the human species[200].

The simplicity and versatility brought into the system by entirely programmable sgRNAs have paved the way for the expansion in the number of new projects of either basic or clinical nature[199], and particularly the scope of stem cell research and its therapeutic applications, was vastly extended. There are several methods available to deliver CRISPR/Cas9 and its components to the target cells. It can be delivered in the format of DNA (“all-in-one” plasmid - Cas9 and sgRNA coding sequence), mRNA (Cas9 and sgRNA), or as a ribonucleoprotein complex (RNP – Cas9 protein complexed to sgRNA)[191] (Figure I.4.2).

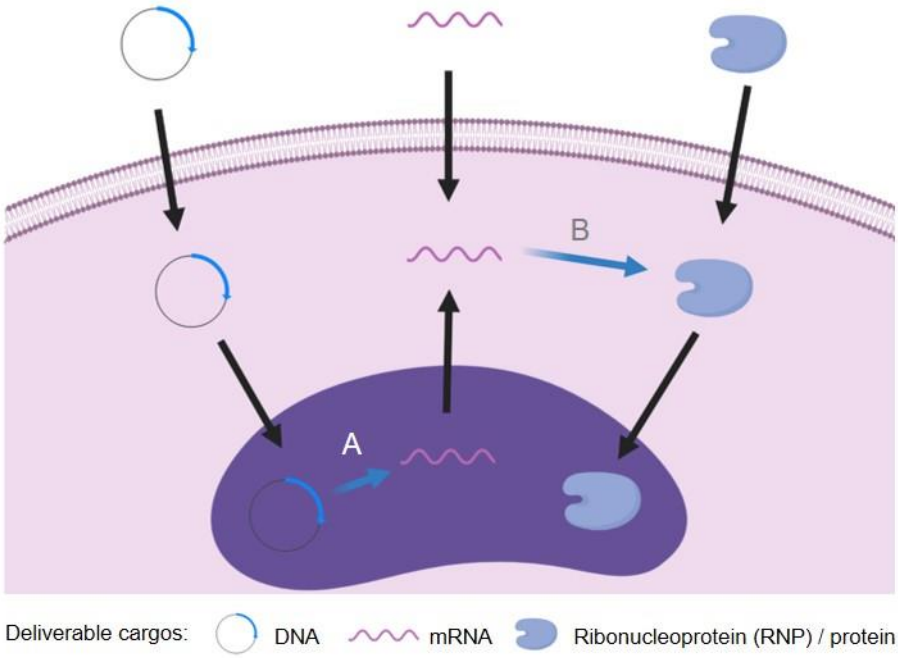

Figure I.4.2 - Cas9 may be successfully delivered in either a DNA, mRNA or protein format to achieve gene editing. While Cas9 ribonucleoprotein (RNP) results in the most immediate onset of gene editing, it can also be extremely transient, and difficult to cross the cellular and nuclear membrane. Delivery of Cas9 into a plasmid DNA may offer the most stable expression of Cas9, however the gene must undergo the biological processes of transcription (A) and translation (B) before the therapeutic effect can be realized, leading to a delay in the onset of gene editing and potentially leading to higher off-target probability. mRNA doesn't need to be delivered to the nucleus, as the cellular translation machinery is present in the cytoplasm. However, mRNA is extremely susceptible to enzymatic degradation. Cas9, CRISPR-associated protein 9. Created with *BioRender.com*.

The CRISPR/Cas9 insertion/expression is then mediated through electroporation, nucleofection, lentiviral vectors or by lipofectamine transfection (Figure I.4.3).

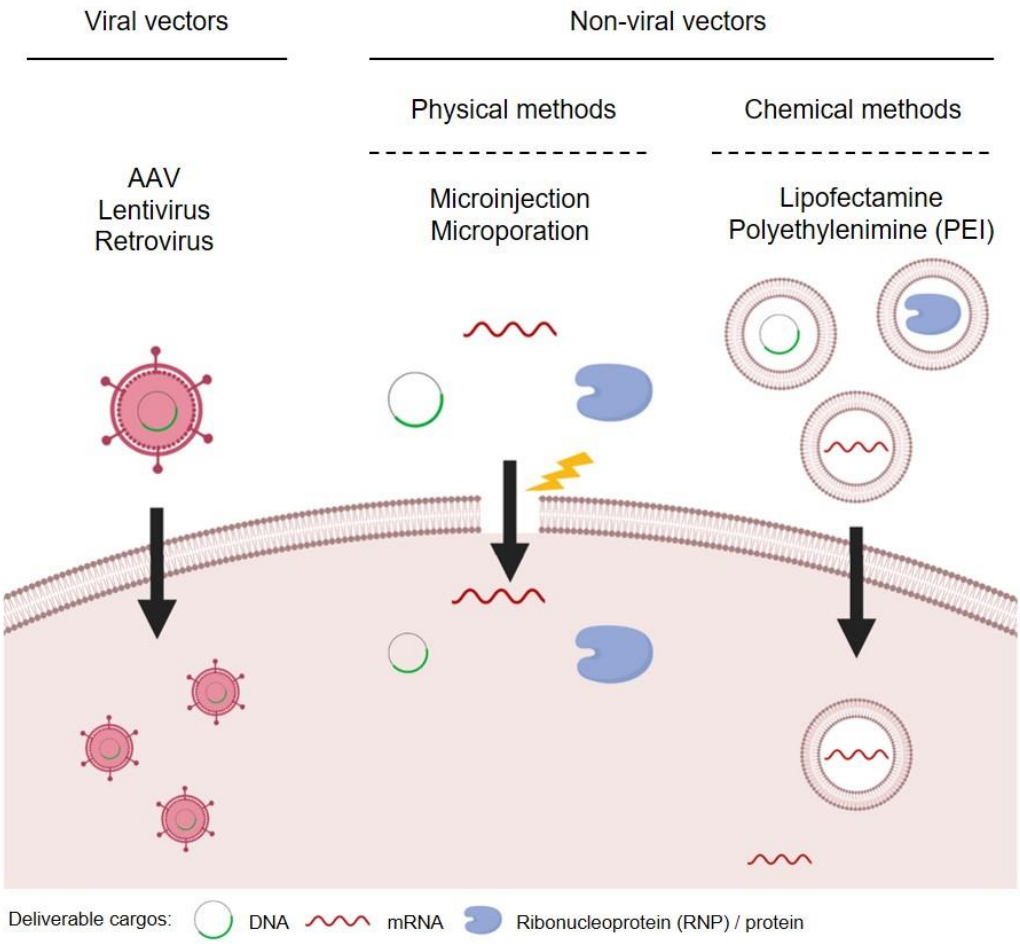

Figure I.4.3 - Delivery routes for Cas9. As a DNA or mRNA molecule encoding for the Cas9 gene, or as a functional ribonucleoprotein (RNP). A variety of viral and non-viral methods have been developed to successfully deliver the molecular cargo across the cell membrane. Created with *BioRender.com*.

I.4.2. CRISPR/CAS9 to engineer MSC

The CRISPR/Cas9 system can be applied to MSC research, for instance, by interfering with the expression of specific genes involved in the self-renewal and commitment of these cells with certain lineage, gene knock-in to acquire new functions or gene knockout, and other chromosome related usages, which would contribute to increase their engraftment and to develop elevated therapeutic MSC lines[201]. In addition, although the CRISPR/Cas9 system is still in preliminary stages, molecular editing of MSC have been exploited mainly aiming at the improvement of their innate therapeutic properties.

One such example of an MSC-based therapeutic strategy exploiting the CRISPR/Cas9 potentialities regards a study concerning an essential process for embryo implantation, placenta (PL) forming, and maintenance of pregnancy, known as decidualization of endometrium (ED). In this context, a tightly controlled plasminogen activator inhibitor-1 (*PAI-*

1) expression level by decidual cells has been reported to play a crucial role in this process. In the study of Deryabin and colleagues, the authors selected *PAI-1* as an engineering target, by developing a *PAI-1* overexpressing human MSC line and a *PAI-1* knockout MSC line, since a rhythmicity of *PAI-1* expression and secretion levels occurs in intervals throughout the pregnancy. This strategy could potentially improve the outcome of patients with infertility. In this study, the authors used lentiviral transduction to deliver the CRISPR/Cas9 components being able to obtain both cell lines successfully, representing the first evidence of the effective MSC secretome engineering via CRISPR/Cas9 genome editing technology[202]. Other study taking advantage of the CRISPR/Cas9 technology focus on ameliorating the quality-of-life of patients with a deep burn injury. These injuries are associated to a loss of function of perspiration and the sweat glands (SG) are unable to regenerate. Among several factors, ectodysplasin (EDA) is considered the most important for the development of the sweat gland. Therefore, Sun and colleagues hypothesized that EDA is a potential factor in BM-MSC differentiation into sweat gland-like cells and elaborated a strategy to overexpress this gene in MSC[203]. In this study, activation of EDA transcription in BM-MSC was also attained by lentiviral transduction with sgRNA-guided Cas9. BM-MSC acquired significantly higher transcription and expression of *EDA* by doxycycline (Dox) induction. Moreover, *in vivo* studies in a SG-injured mouse model showed that the therapeutic effect of the engineered cells on sweat gland injuries was enhanced[203]. Adeno-associated virus (AAV) were also employed as vectors for CRISPR/Cas9 components delivery in the study of Kosaric and colleagues. Aiming at the establishment of a MSC line that actively promotes wound healing, in this study the authors inserted a bi-cistronic soluble platelet derived growth factor B (*PDGFB*) -2A- green fluorescence protein (*GFP*) expression cassette at the Chemokine receptor (CCR) 5 locus, by CRISPR/Cas9. *PDGF-B* is known to contribute to tissue regeneration and favouring wound healing. The authors observed that single local injection of engineered cells under excisional wounds of diabetic mice at the time of wounding accelerated wound healing rates and reduced time to complete wound closure significantly when compared to injections of unmodified MSC[204]. Employing a similar strategy, Srifa and colleagues, developed an AAV-based genome editing tool in MSC isolated from the BM, the umbilical cord blood (UCB) and the AT to stably insert the *PDGFB* and *VEGF* genes stably into MSC genome, demonstrating superior wound healing properties when comparing with naïve-MSC from the same sources [205].

Viral vectors are popular among molecular delivery due to their high efficiency[179]. However, the high molecular weight of the Cas9 protein restricts the usage of this delivery method. This becomes particularly important as more intricate CRISPR applications such as HDR are employed, as these approaches require co-delivery of different molecular entities simultaneously. In addition, viral-mediated Cas9 delivery may result in permanent expression

of nuclease proteins and produce undesired DNA cleavage within the genome. Therefore, alternative non-viral delivery methods have gained significant importance. Moreover, studies report that the therapeutic capacity of non-viral modification methods such as electroporation as a transfection method for CRISPR/Cas9-engineered MSC is equivalent to that of therapeutic MSC generated by introduction of the same therapeutic gene by transduction with a lentivirus vector [206]. In the study from Xu and colleagues[207], electroporation has been used for the delivery of CRISPR/Cas9-mediated genome editing systems, where tube electroporation was used to deliver a CRISPR/Cas9 system that generates gene knock-out via precise homology-directed repair (HDR) to MSC from different human sources. The authors co-delivered a Cas9/gRNA RNP with a sequence targeting the β 2-microglobulin (*B2M*) gene, which is a well-established MHC class I molecule association protein, and a small DNA repair template that introduces a single base insertion in the PAM site creating a frameshift mutation that disrupts gene function. The delivery of such system resulted in *B2M* gene disruption, showing a maximum reduction in the cell surface B2M-expressing cells of 80%[207]. More recently, nucleofection was used to transfect a CRISPR/Cas9 RNP system to insert an expression cassette into UCB-MSC[208]. The insert consisted of the human elongation factor 1-alpha (*EF1-α*) promoter, soluble Receptor for AGEs (sRAGE) coding sequence and poly A tail. sRAGE is an inhibition factor of advanced glycation end products- albumin (AGE-albumin) from activated microglial cells, which is one of the main causes of Parkinson's disease (PD). After transplantation into a PD mouse model, MSC-expressing *sRAGE* showed to extensively reduce neuronal cell death in Corpus Striatum and Substantia Nigra and improved movement recovery[208]. CRISPR/Cas9 technology was also targeted to overcome the technical challenge of maintaining primary BM-MSC in long-term culture, in the study of Hu and colleagues, a reversibly immortalized mouse BM-MSC was established[208]. The strategy was to engineer MSC to express an immortalizing oncogene, such as the simian virus SV40 large T antigen (*SV40T*). CRISPR/Cas9-based HDR components were transfected into MSC with PEI, targeting SV40T to mouse genomic safe harbor *Rosa26* locus, leading to efficiently immortalized mouse BM-MSC. Cells retained MSC features both *in vitro* and *in vivo* and were non-tumorigenic *in vivo.* To compare the biological features and mediated reversibility, the authors also immortalized primary MSC with a retroviral immortalization system. Though SV40T mRNA expression is 130% higher in retroviral immortalized BM-MSC, CRISPR/Cas9 HDR-mediated immortalization of BM-MSC demonstrated to be more effectively reversed than that of retrovirus-mediated random integrations[209]*.* Also employing non-viral delivery methods, in the study of Meng and colleagues, lipofectamine was employed in BM-MSC transfection for overexpression of *IL-10* using CRISPR activation. *IL-10* has been shown to attenuate myocardial infarction (MI) by suppressing inflammation. The authors observed that after transplant into a diabetic mouse model, MSC overexpressing *IL-10*

inhibited inflammatory cell infiltration and pro-inflammatory cytokines production, improved cardiac functional recovery, alleviated cardiac injury, decreased apoptosis of cardiac cells and increased angiogenesis[210].

In what concerns advancing MSC therapy towards clinical studies, and despite the specificity of CRISPR/Cas9 technology in gene delivery[145], only one clinical trial in the recruitment stage of MSC modified with CRISPR/Cas9 has been registered (NCT03855631)[211], aiming to develop a therapeutic strategy that could ameliorate some of the abnormalities associated with Kabuki Syndrome.

A summary of the CRISPR gene engineered MSC studies is illustrated in Table I.4.1.

Table I.4.1 - Studies employing modified MSC using CRISPR-Cas9 technology.

MSC source	Gene	Outcome	Reference
Human AT, UCB and BM	*B2M*	Gene knock-out resulted in reduced immunogenicity of allogeneic transplants	207
Human BM	*EDA*	After transfection with sgRNA-guided dCas9-E, the BM-MSC acquired significantly higher transcription and expression of *EDA* by doxycycline (Dox) induction	203
Mouse BM	*IL-10*	Transplantation of CRISPR system engineered *IL10*-overexpressing BM-derived MSC for the treatment of myocardial infarction in diabetic mice	210
Human ED	*PAI-1*	Gene overexpression and gene knockout to improve decidualization insufficiency	202
Human BM	*PDGF-B*	Exogenous *PDGF-B* was inserted on *CCR5* locus. Accelerated wound healing kinetics was observed in wounds treated with *PDGFB*-MSC	204
Human AT, UCB and BM	*PDGF-B VEGF*	Exogenous *PDGF* and *VEGF* were inserted on *HBB*, *CCR5*, and *RANKL* gene loci. Enhanced wound healing capacity in mouse xeno-transplanted mice	205
UCB	*sRAGE*	After transplantation, MSC-expressing *sRAGE* showed to extensively reduce neuronal cell death in Corpus Striatum and Substantia Nigra and improved movement recovery in a mouse model of Parkinson's Disease	208
Mouse BM	*SV40T*	CRISPR/Cas9 HDR-mediated immortalization of BM-MSC can be more effectively reversed than that of retrovirus-mediated random integrations	209

I.5. MSC as candidates for cancer cell therapy

Conventional therapies for cancer include radiotherapy, chemotherapy, and surgery – individually or in combination. Surgical attempts at complete excision are rarely successful and local recurrence is common. Radiotherapy damages normal tissues and metastasis can recur due to radio-resistance. Chemotherapy drugs tend to act on fast-growing cells, including healthy cells such as hair follicles, blood cells, and cells of the intestinal tract. This leads to severe toxicity to healthy tissues, and once the disease becomes metastatic, standard chemotherapy has little effect[212]. Moreover, until recently, patients who have the same type and stage of cancer typically receive the same treatment. It has been established, however, that individuals with the same disease respond differently to the same therapy. Further, each tumor undergoes genetic changes that cause cancer to grow and metastasize. The changes that occur in one person's cancer may not occur in others with the same cancer type[213]. As expected, these differences also lead to different responses to treatment.

For these reasons, targeted cancer strategies aim to minimize or overcome such side effects and lack of efficacy by better targeting the tumor and avoiding healthy tissues, and therefore to treat cancer with more specificity and robustness. Novel approaches have recently focused on selectively target tumors by applying various drug delivery systems such as stealth liposome, carbon nanotubes, dendrimers, polymeric micelles, polymeric conjugates, polymeric NPs and also, tumor targeting cells[214]. These drug carriers not only transport the chemotherapeutic agents to tumors, avoiding normal tissues and reducing toxicity in the rest of the body, but also protect cytotoxic drugs from degradation, increase the half-life, payload and solubility of cytotoxic agents and reduce renal clearance[214].

The field of targeted cell therapy is evolving rapidly with novel therapeutic modalities that include tumor-infiltrating lymphocytes (TILs)[215], engineered T-cell receptor (TCR)[216], chimeric antigen receptor (CAR)-T cells[217], cytotoxic T lymphocytes (CTLs)[218], natural killer (NK) cells[219], mesenchymal stromal cells (MSC)[220], and others. The cell therapy category now has the largest number of active agents and the second largest number of active trials (after checkpoint inhibitors) in the immuno-oncology space. And as enlightened above, the integration of new technologies, such as CRISPR-edited cell therapies into next-generation cell therapies, could lead to greater progress and an open foundation for clinical breakthrough to benefit more patients with cancer in the near future.

I.5.1. Engineered anti-cancer MSC

As above mentioned, one of the most unique features of MSC is their homing capacity towards pro-inflammatory microenvironments regardless of the causes of the injuries and the tissue type[40]. And being tumors highly inflammatory microenvironments (also known as "wounds that do not heal"), MSC can be engineered as biological Trojan horses to deliver anti-tumoral therapeutics directly into the tumor stroma.

MSC homing is thought to occur in a chemokine directed manner within the context of ongoing inflammation. The diverse factors known to be present within tumors include: epithelial growth factor (EGF), VEGF-A, PDGF, FGF, TGF-β1, CXCL7, CXCL6, CXCL5, CXCL8, CXCL12, CCL2, IL-6, and urokinase-type plasminogen activator[221–224]. It is thought that combinations of these factors may help promote directed MSC recruitment. To help facilitate their directed migration, MSC are known to be able to express virtually all chemokine receptors (CCR, CXCR, Chemokine receptor 3 (CXC3R) and chemokine XC receptor (XCR)), but the level of expression may vary as a result of cell culture conditions, or with the tissue source of MSC[225,226]. Therefore this phenomenon occurs through an intricate crosstalk of biochemical cues, and even though the underlying mechanisms are still not fully elucidated in this process, it has been recognized that the CXCR4 - SDF1α axis plays an important role[227–229].

I.5.2. The duality of MSC in tumor progression

In the literature there is a strong discrepancy in what concerns the role of MSC in tumor progression[230]. Several studies have demonstrated MSC as stimulators of tumor growth and metastasis. In general, solid tumors are composed of two cell types: tumor cells and supportive non-tumor components, which is known as tumor stroma. Tumor stroma, includes tumor vasculature, cells of the immune system, extracellular matrix (ECM), fibroblastic stromal cells as tumor associated fibroblasts (TAF), and carcinoma-associated fibroblasts (CAF). In addition to the differentiation capacity to TAFs and CAFs, MSC are capable of forming the fibrovascular network of tumor and vascular pericytes. Therefore, MSC when reaching the tumor site may unintentionally contribute to the inflammatory process and tumor structure, adding to its complexity and strength. MSC have been shown to act in a multi-modal fashion and to contribute to tumor survival and progression directly or indirectly, although evolving data also argue for a role in tumor regression. This ambiguity is extended to MSC secretome. For example, UCM-MSC[231–234] and their CM[231,232,235] have been shown to inhibit *in vitro* the proliferation of breast cancer cells such as MDA-MB-231 and MCF-7, while others reported that CM[236] and EVs from UCM-MSC[237] promote the proliferation and migration of the same

cells. In summary, although the main reason for the duality of MSC function against tumors is not clear, there are many technical and biological aspects to be considered when comparing independent studies as it may be dependent upon several factors, including the type and source of MSC, large variety of cytokines, and growth factors produced by MSC, type of cancer cell line tested, *in vivo* or *in vitro* conditions and interactions between MSC, host's immune cells and cancer cells, differences in isolation/culture protocols, presence of xenogeneic, possibly immunogenic, factors (such as BSA), in culture media and in the experimental methods of both primary cells and commercial cell lines, as well as variation in oncogenic and mutational pattern, and in the expression of specific receptors by cancer cell lines. In addition, different ratios of MSC: tumor cells[238] and timing of MSC delivery into tumors[239] constitute an important argument in the comparison of different studies. Hence, all these details play a major role in defining MSC properties and impact the final outcome.

I.5.3. Engineered MSC versions for cancer therapy

As stated, the unclear role of naïve MSC in tumor progression could be a shot in the dark as a cell therapy for cancer. However, their innate tumor tropism combined with immunomodulatory properties and lack of immunogenicity propose these cells as potential living vehicles for anti-cancer drug therapies allowing for a more precise and less invasive administration. Hence, genetically engineered versions of MSC have been under pre-clinical and clinical development as cell delivery systems of several anti-cancer agents, aiming to develop the anti-tumorigenic potential of these cells. One of the most commonly adopted approach is the enhancement of endogenous anti-tumor immunity by engineering MSC to produce anti-tumor cytokines or soluble factors such as β-IFN[106–108], IL-2[40,240], IL-12[109,212], IL-15[241], IFN-alpha[242], or CX3CL1[243]. Another approach is the use of MSC to deliver tumor cytotoxic agents such as TRAIL[121–123,125–127,244], osteoprotegerin (OPG)[116], NK4[110], hepatocyte growth factor (HGF)[245]. The employment of MSC as gene-directed enzyme-producing vehicles, such as MSC expressing HSV-TK with ganciclovir as a prodrug (HSV-TK-MSC/GCV system)[246] and MSC engineered to express fused yeast cytosine deaminase::uracil phosphoribosyl transferase (*yCD::UPRT*) with 5-FC as a prodrug (*yCD::UPRT*-MSC/5FC system)[131] have also demonstrated very promising results (Figure I.5.1). Three first-in-human clinical trials assessing gastrointestinal cancer, lung cancer and ovarian cancer are being conducted to investigate the efficacy of genetically modified MSC in cancer patients with results demonstrating safety and tolerability, and some preliminary signs of efficacy[247]. These will be described in the following section.

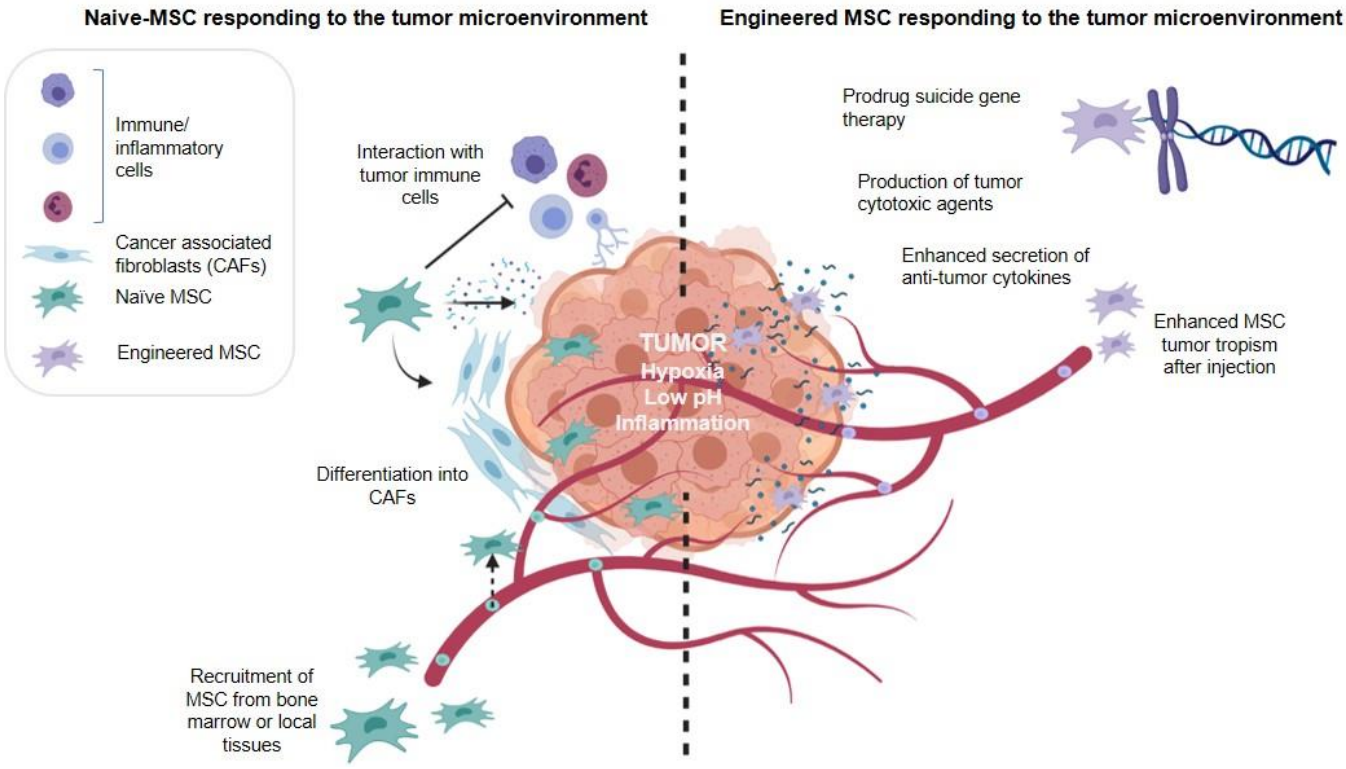

Figure I.5.1 - Naïve and therapeutic-MSC within the tumor microenvironment components. Established cancers are usually surrounded by a wide array of stromal cells and infiltrating immune cells of both innate and acquired immunity. They form a complex regulatory network that supports tumor growth by creating a tolerogenic environment that enables cancers to evade immune surveillance and destruction. Naturally, MSC may participate in tumor progression by incorporating the tumor stroma and interacting with immune cells. Engineered versions of MSC, possess tailored functions favouring their anti-tumoral properties. Created with *BioRender.com*.

I.6. Clinical translation of genetically engineered MSC

Although naïve and engineered MSC-based therapy has showed to be safe and effective in various clinical trials, there are still several limitations that restrict their clinical implementation. The preclinical studies are developing rapidly, and more standardized clinical trials are widely carried out. It might be expected that standard MSC therapies will be a reality in a near future. In this section, a selection of clinical trials testing cell therapies with genetically engineered MSC are described and summarized in Table I.6.1 (information obtained at “clinicaltrials.gov” on July 7th 2021, using the terms “mesenchymal stem cells gene”; “mesenchymal stem cells cancer” and “mesenchymal stromal cells cancer”).

Taking advantage of their tumor tropism characteristics, MSC have been widely used in preclinical studies as a vehicle for the delivery of anti-cancer agents, supporting their investigation at the clinical level. For example, the completed phase I/II study, held in Germany until 2017 (NCT02008539, completed), used MSC genetically modified to express *HSV-TK*

(MSC_apceth_101), using a retroviral SIN-vector, for the treatment of advanced gastrointestinal adenocarcinoma. The study was conducted with 10 patients that received three cycles of infusion of MSC_apceth_101, followed by GCV administration. Despite some adverse events were reported, five patients achieved a stable disease state, and all patients showed a median time to treatment progression of 1.8 months and an overall survival of 15.6 months. Overall, MSC_apceth_101 in combination with GCV was safe and tolerated well by patients with advanced gastrointestinal adenocarcinoma and showed preliminary signs of efficacy in terms of clinical stabilization of disease[247]. As aforementioned, MSC have been engineered to express *IFN-β* using lentivirus as a gene delivery system in a variety of cancer studies, including ovarian cancer[108]. In this regard, a phase 1 study, conducted in the United States since 2015 (NCT02530047), has been determining the effects of the administration of MSC genetically modified by a plasmid vector to produce IFN-β (INFβ-MSC), in patients with advanced ovarian cancer. In this trial, allogenic MSC isolated from the BM of healthy male donors are being used. The main objective of this study is to determine the highest tolerable dose of *INFβ*-MSC that can be administered to patients with ovarian cancer and test the safety of the *INFβ*-MSC infused intraperitoneally through a catheter placed in the abdomen of 21 female patients, with histologically documented diagnosis of epithelial ovarian cancer. After a specific period of time, the status of the disease will be checked in patients through tumor biopsies. Similarly, *TRAIL*-expressing MSC appear as a promising anti-cancer strategy with pre-clinical relevance against several types of cancer models. In particular, lentivirus have been used as a gene delivery method to engineer MSC to express *TRAIL*, targeting lung metastatic cancer[124]. In this context, a phase I/II study conducted in the United Kingdom since 2017 (NCT03298763 (recruiting)), known as TACTICAL, has been using allogeneic UCM-MSC engineered to express the *TRAIL* gene (*TRAIL*-MSC) using a lentiviral vector, for the treatment of lung cancer. *TRAIL*-MSC will be intravenously administered to 46 patients with lung adenocarcinoma, in combination with pemetrexed/cisplatin chemotherapy. The aim of the first part of study is to assess the recommended dose of *TRAIL*-MSC for the subsequent phase II. The second part of the research will compare the effect of *TRAIL*-MSC when given with chemotherapy compared to chemotherapy alone, aiming at assessing tolerability and preliminary efficacy of *TRAIL*-MSC. In a different context, another phase I/II study, which has been initiated in 2017 (NCT03351868 (recruiting)), will test the co-administration of genetically modified hematopoietic stem/progenitors cells (HSPC) and MSC for the treatment of Fanconi Anemia (FA), a rare, inherited disease that is caused by a defect of the *FANCA* gene, and is associated with a higher predisposition to cancer development[248]. Hematopoietic cell transplantation (HCT) is a common therapy for this condition, however, risks associated with HCT include rejection of the transplanted cells and GvHD. In this clinical study, autologous HSPCs and MSC will be transduced with the *FANCA* gene *ex vivo* with a self-inactivating

lentiviral vector by correcting the defective gene in HSPCs. The primary aim of this study is to evaluate the safety and efficacy of the *ex vivo* gene transfer clinical protocol. Gene-modified autologous cells will be infused into 30 FA patients. Also, in the context of HCT two phase I/II trials will be using genetically modified HSPCs and MSC to express human clotting factor VIII (YUVA-GT-F801) (NCT03217032 (not yet recruiting, 10 patients estimated)) or factor IX (YUVA-GT-F901) (NCT03961243 (not yet recruiting, 10 patients estimated)), using an advanced lentiviral vector, for the treatment of haemophilia A or haemophilia B, respectively. The primary aim of both studies is to assess the safety and preliminary efficacy of the genetically modified autologous cells. Finally, a clinical study testing the administration of autologous HSPCs and/or MSC transduced with a self-inactivating lentiviral vector carrying the adenosine deaminase (*ADA*) gene (TYF-ADA), will be held in China for the treatment of patients with severe combined immunodeficiency (SCID) due to a defective *ADA* gene. The study will be conducted in 10 patients diagnosed with ADA-SCID and severe infections. The primary objectives are to assess the safety TYF-ADA and preliminary efficacy of the *ex vivo* gene transfer clinical protocol towards immune reconstitution in patients overcoming frequent infections present at the time of treatment (NCT03645460 (not yet recruiting)).

Table I.6.1 - Representative clinical trials testing the safety and preliminary efficacy of genetically modified MSC in different therapeutic contexts.

Study Title	Phase	State	Country	Reference	Last Update Date
Treatment of Advanced Gastrointestinal Cancer in a Phase I/II Trial With Modified Autologous MSC_apceth_101	Phase I/II	Completed	Germany	NCT02008539	March 27, 2017
Phase 1 Study to Determine the Effects of Mesenchymal Stem Cells Secreting Interferon Beta in Patients With Advanced Ovarian Cancer	Phase I	Active	United States	NCT02530047	July 18, 2019

Table I.6.1 (continued)

Study Title	Phase	State	Country	Reference	Last Update Date
Targeted Stem Cells Expressing TRAIL as a Therapy for Lung Cancer	Phase I/II	Recruiting	United Kingdom	NCT03298763	April 28, 2021
Gene Transfer for Fanconi Anemia Using a Self-inactivating Lentiviral Vector	Phase I/II	Recruiting	China	NCT03351868	September 19, 2019
Gene Modified Hematopoietic and Mesenchymal Stem Cells for Haemophilia A and B	Phase I/II	Not yet recruiting	China	NCT03217032 NCT03961243	May 23, 2019
Gene Transfer for Adenosine Deaminase-severe Combined Immunodeficiency (ADA-SCID) Using an Improved Self-inactivating Lentiviral Vector (TYF-ADA)	(Not provided)	Recruiting	China	NCT03645460	September 20, 2019

I.7. Azurin, a potential anti-cancer protein

Azurin is a 128-aminoacid residue bacterial protein produced by *Pseudomonas aeruginosa* which has been studied in different *in vitro* and *in vivo* models, demonstrating its ability to interfere in different steps of tumor development[249,250]. Azurin is able to enter mammalian cells, preferentially cancer cells[251,252], acting at the membrane level by increasing its fluidity and attenuating proliferative signalling pathways. Azurin enters cancer cells co-localized with caveolin-1, present in lipid rafts. These plasma membrane microdomains are rich in proteins as well as lipids such as cholesterol and sphingolipids and have several functions in signal transduction[253]. A wide number of signal transduction processes that play a major role in the progression of many types of tumors are dependent on lipid rafts, including cell adhesion, migration, cell survival and proliferation[254]. Membrane rafts reorganization leads to an abnormal signalling route, which might be an effective target for anti-cancer therapy [255]. Azurin exerts an anti-cancer effect by entering the cell through endocytosis, a process that disturb caveolae and removes from the cell membrane selective receptors that may be over-activated

and are crucial for cancer progression. This impact on cancer cells is an important mechanism by which tumorigenesis is abrogated[256].

A preferential entry of azurin into a variety of human cancer cells[257] is mediated by the amino acid segment 50–77, termed p28. Furthermore, p28 also retains the antitumor activity of the whole protein [258] and has already completed two phase I clinical trials in the United States. In the first one it not only demonstrated no toxicity, but also showed tumor regression in 15 stage IV cancer patients with resistant solid tumors, substantially extending the lives of some patients without significant adverse effects[259,260]. In the second phase I trial against pediatric brain tumor patients in 11 Children's Hospitals in the United States. p28 was given intravenously to patients aged 3 to 21. Brain tumors are often highly invasive and difficult to treat because very few drugs can cross the blood-brain barrier to reach the brain tumors. The results of this second phase I trial suggest that p28 has shown acceptable toxicity and perhaps some tumor regressing effect in some of these pediatric brain tumor patients. Moreover, the US Food and Drug Administration (FDA) has approved on December 02, 2015 the designation of azurin-p28 as an orphan drug for the treatment of brain tumor glioma[261].

Azurin is a member of a family of copper-containing redox proteins named cupredoxins. These proteins exhibit remarkable typological similarity to a family of ligands called ephrins. Ephrin ligands bind to a family of extracellular receptor proteins known as Eph receptor tyrosine kinases. Eph and ephrin proteins have been shown to be up-regulated in many types of tumors. The Eph-ephrin complex formation leads to the trans-autophosphorylation of the tyrosine kinase domains of the receptor molecules, allowing cellular signalling that translates into a variety of pathological processes including tumor progression, angiogenesis, migration, and invasion related to many types of human cancers. Azurin selectively bind to EphB2 receptor leading to the blockage of the autophosphorylation step, interfering in vascular remodelling of the tumor tissue and consequently tumor growth and migration[262].

The tumor suppressor protein p53 is another target of azurin/p28. p53 is a major player in an intricate cellular network that is involved in multiple central cellular processes including transcription, DNA repair, genomic stability, cell cycle control and cell death through apoptosis. Azurin, upon entry into cancer cells, forms a complex with p53, stabilizes it to raise its intracellular level, generates enhanced levels of reactive oxygen species and induces apoptosis[263]. Many viral and mammalian proteins can modulate p53 function by physical interaction, although, azurin is the first bacterial protein reported to form a complex with p53. It has been demonstrated that four azurin molecules bind per p53 monomer, which may sterically shield p53 from degrading enzymes like Mdm2 oncoprotein that inhibits its transcriptional activity, favors its nuclear export, and acts as an E3 ubiquitin ligase, targeting

p53 for proteasomal degradation. This might explain the increased intracellular level of this protein in the presence of azurin[264]. It was also demonstrated that azurin/p28-stabilized p53 enters the nucleus and induces expression of proapoptotic genes like Bax and B-cell lymphoma protein 2 (Bcl-2)[265] and cell cycle inhibitors like p21 and p27[266].

Another important target of anti-cancer therapies is the aberrant angiogenic activity, mediated by VEGF and FGF, which are typically overexpressed in tumors. The interaction between VEGF-A and its receptor VEGFR-2 is a key regulator of angiogenesis in tumors[267]. The peptide p28 enters in endothelial cells and inhibits angiogenesis by reducing VEGFR-2 tyrosine kinase activity. Inhibition of kinase activity reduces the phosphorylation of the VEGFR-2 downstream targets focal adhesion kinase (FAK) and Akt, altering the intracellular architecture of endothelial cytoskeletal, focal adhesion, and cell contact proteins, leading to the inhibition of VEGF-induced migration, capillary tube formation, and neo-angiogenesis in multiple xenograft models[253]. The modulation of cell membrane properties by azurin may also be associated with the intracellular signalling responses of non-receptor tyrosine kinases, because the phosphorylation levels of FAK, Src, Akt, and PI3K are usually attenuated [249,261].

Moreover, a feature of malignant tumors is their ability to invade surrounding tissues in a process known as metastasis. To accomplish this, cells establish effective connections with the surrounding extracellular matrix (ECM). The physical connection between cancer cells and their surrounding tissues is achieved through cell-surface receptors including integrins. Increased expression of integrin might be associated with poor prognosis, thus this protein is a suitable target for anti-cancer therapy. Breast cancer cells and non-small cell lung cancer carcinoma, the most common form of lung cancer, when treated with azurin demonstrate a decrease in the protein levels of integrin receptor subunits with the subsequent decreased ability to invade and adhere to different ECM components and to grow in anchorage-independent conditions[261]. Azurin decreased adhesion of cells to proteins from the ECM and altered the expression profile of integrins[256].

Certain types of cancer are very resistant to anti-cancer drugs, leading to the need of high dosage administration, which is followed with marked side effects. Thus, finding a way to enhance the sensitivity of these cells to anti-cancer drugs is highly significant. Changes to the surface structure of cancer cells by azurin treatment render the cells more vulnerable to anti-cancer drugs. Azurin has a strong synergistic anti-cancer effect on certain types of cancer including oral squamous cell carcinoma, when combined with 5-fluorouracil or etoposide[268]. The synergistic effects of azurin were also observed in malignant mammary epithelial cells when co-administrated with tamoxifen[269] and in non-small cell lung carcinoma when co-administrated with gefitinib and erlotinib, tyrosine kinase inhibitors which target specifically the

epidermal growth factor receptor (EGFR), one of the main targets for clinical management of this disease[261]. Azurin is also described to be able to increase the effectiveness of anti-cancer chemotherapeutics such as doxorubicin and paclitaxel[251].

To conclude, azurin has a complex mechanism of action mediating specific high-affinity interactions with several independent signalling pathways relevant in tumor development, while inducing little side effects *in vivo*. This ability makes it distinct and promising relatively to other antitumor agents, which have a more limited range of action. Its broader mechanism of action could potentially prevent the acquirement of tumor resistance. Moreover, azurin is a small, water-soluble molecule with a hydrophobic patch, which might help in its tissue penetration and clearance from the blood stream. It is a protein with low immunogenicity since is a non-antibody recognized protein, preventing clearance from the host immune system[270]. Therefore, azurin could be a strong candidate as an anti-cancer agent alone or synergistically with other anti-cancer drugs. As such, the development of a delivery vehicle, like MSC, that specifically targets the tumor microenvironment, could constitute the elevation of the anti-cancer robustness of azurin.

I.8. Aim of the Study and Thesis Outline

Every year, cancer is responsible for millions of deaths worldwide and, even though much progress has been achieved in medicine, there are still many issues that must be addressed in order to improve cancer therapy[271]. For this reason, oncological research is putting a lot of effort towards finding new and effective therapies which can alleviate critical side effects caused by conventional treatments[271]. Particularly, the field of cellular therapy is evolving rapidly with novel therapeutic modalities that include a wide spectrum of products, including tumor-targeting cells, such as MSC[37]. These cells are among the most frequently used cell type for regenerative medicine, participating in a large number of studies and demonstrating beneficial effects in different pathologies, including cancer[272]. However, the role of MSC in cancer is still controversial. While some studies indicate that MSC may contribute to cancer pathogenesis, emerging data reported the suppressive effects of MSC on cancer cells[230]. In an attempt to unravel this ambiguity, genetic engineering represents a valuable tool for pinpointing and customize MSC characteristics towards an unequivocal therapeutic profile. In this context, in this thesis, nonviral, GMP compliant, strategies for the engineering of MSC towards the expression and secretion of the potent anti-tumoral protein azurin were developed, in order to i) contribute towards a better knowledge of the anti-tumoral effect of azurin, when coupled to a cell-based delivery platform; and ii) establish a reliable protocol to

safely edit the genome of human MSC elevating their potential therapeutic application in different biological contexts. The present document is organized into four main chapters:

Chapter I is a comprehensive literature review centered on engineered MSC and their derived products (*i.e.*, CM) as delivery platforms for therapeutic agents in diverse pathological contexts, with special focus on nonviral engineering methods, such as the CRISPR/Cas9 system. The applications of engineered MSC in cancer therapy are highlighted, along with the proposal of the anti-tumoral protein azurin as a research target for a new cell-based strategy.

Chapter II displays a transient gene delivery method, based on the microporation of a recombinant plasmid, developed as a proof-of-concept for the value of azurin-expressing MSC in anti-cancer treatment. Tumor inhibition was demonstrated in two cancer cell lines after treatment with azurin enriched CM, derived from engineered MSC.

Chapter III concerns the optimization of a CRISPR/Cas9-based methodology for the precise genome editing of MSC, specifically for the incorporation of transgenes in a GSH within MSC genome. A comparison of techniques to deliver the CRISPR elements to MSC is evaluated.

Chapter IV presents the development of a protocol for the establishment of a stable azurin/GFP-expressing MSC line mediated by the homology-directed-repair (HDR) system. By employing the knowledge gathered in *Chapter III*, a comparison of the HDR template formulations is evaluated towards the highest knock-in efficiency.

II. THE CONDITIONED MEDIUM OF TRANSIENT AZURIN-EXPRESSING HUMAN MESENCHYMAL STROMAL CELLS DEMONSTRATES ANTI-TUMOR ACTIVITY AGAINST BREAST AND LUNG CANCER CELL LINES

This chapter of the thesis is published as:

Silva, M., Monteiro, G.A., Fialho, A.M., Bernardes, N., da Silva, C.L. Conditioned Medium From Azurin-Expressing Human Mesenchymal Stromal Cells Demonstrates Antitumor Activity Against Breast and Lung Cancer Cell Lines. Front Cell Dev Biol 8:471 (2020)

II.1. Summary

Recently, cell-based therapies have been explored as a strategy to enhance the specificity of anti-cancer therapeutic agents. In this perspective, mesenchymal stromal cells (MSC) hold a promising future as cell delivery systems for anti-cancer proteins due to their unique biological features. In this study, we engineered human MSC to secrete a human codon-optimized version of azurin (hazu), a bacterial protein that has demonstrated anti-cancer activity toward different cancer models both *in vitro* and *in vivo*. To this end, microporation was used to deliver plasmid DNA encoding azurin into MSC derived from the BM and the UCM, leading to expression and secretion of hazu to the CM. Engineered hazu-MSC were shown to preserve tumor tropism toward breast (MCF-7) and lung (A549) cancer cell lines, comparable to non-modified MSC. Azurin was detected in the CM of transfected MSC and, upon treatment with hazu-MSC-CM, we observed a decrease in cancer cell proliferation, migration, and invasion, and an increase in cell death for both cancer cell lines. Moreover, expression of azurin caused no changes in MSC expression profile of cytokines relevant in the context of cancer progression, thus suggesting that the anti-tumoral effects induced by *hazu*-MSC secretome might be due to the presence of azurin independently. In conclusion, data shown herein indicate that MSC-produced azurin in a CM configuration elicits an anti-cancer effect.

II.2. Background

MSC are multipotent cells with the ability to modulate several biological mechanisms through paracrine activity[2], namely limiting apoptosis[3] and inducing angiogenesis[273–275], as well as to differentiate into a variety of cell lineages, including osteocytes, adipocytes and chondrocytes[1]. Cells with these features hold a promising future for cell therapies and tissue engineering, by potentially replacing damaged tissues of mesodermal origin, promoting tissue regeneration, and modulating immunological responses. In addition, MSC show an intrinsic ability to specifically migrate towards pro-inflammatory microenvironments, such as tumor sites[37,276,277]. This phenomenon occurs through an intricate crosstalk of biochemical cues, and although the underlying mechanisms are still not fully elucidated in this process, it has been recognized that the CXCR4 - SDF1α axis plays an important role[227–229]. Taking advantage of their innate tropism for tumors, genetically engineered versions of MSC have been under pre-clinical and clinical development as cell delivery systems of several anti-cancer agents. One of the most commonly adopted approach is the enhancement of endogenous anti-tumor immunity by engineering MSC to produce anti-tumor cytokines or soluble factors such as β-IFN[106–108], IL-2[40,240], IL-12[109,212], IL-15[241], IFN-alpha[242], or CX3CL1[243]. Another approach is the use of MSC to deliver tumor cytotoxic agents such as TRAIL[121–123,125–127,244], OPG[116], NK4[110], HGF[245]. The

employment of MSC as gene-directed enzyme-producing vehicles, such as MSC expressing thymidine kinase of the Herpes simplex virus with ganciclovir as a prodrug (tkHSV-MSC/GCV system)[246] and MSC engineered to express fused yeast cytosine deaminase::uracil phosphoribosyl transferase (yCD::UPRT) with 5-fluorocytosine (5-FC) as a prodrug (yCD::UPRT-MSC/5FC system)[131] have also demonstrated very promising results. Three first-in-human clinical trials assessing gastrointestinal cancer, lung cancer and ovarian cancer are being conducted to investigate the efficacy of genetically modified MSC in cancer patients with results demonstrating safety and tolerability, and some preliminary signs of efficacy[247].

Azurin, a small water-soluble (14kDa) protein from the bacteria *Pseudomonas aeruginosa*, has been explored in what concerns its anti-tumoral capacity. Azurin is able to enter mammalian cells, preferentially cancer cells[251,252], acting at the membrane level by increasing its permeability and attenuating proliferative signalling pathways[256,261]. After internalization, azurin forms a complex with the tumor suppressor protein p53, stabilizing it, and increasing its concentration at intracellular level, thereby inducing apoptosis [263]. Azurin is also described to be able to increase the effectiveness of conventional anti-cancer therapeutics such as doxorubicin and paclitaxel[251], and gefitinib or erlotinib[261]. In addition, a peptide derived from this protein (named p28) also enhances the activity of DNA damaging chemotherapeutic agents[278]. Azurin and p28 have a complex mechanism of action targeting several independent signalling pathways relevant in tumor proliferation, while inducing reduced side effects *in vitro* and *in vivo*[279]. These features turn azurin/p28 distinct and promising relatively to other antitumor agents, which have a more limited range of action.

In the present study, we couple azurin's anti-tumoral effect to the tumor tropism ability of MSC, in a cell-based approach, by genetically engineer human MSC to produce and secrete azurin through non-viral methods. Though viral systems have demonstrated the highest gene transfer efficiencies in preclinical and clinical trials, non-viral vectors and gene transfer approaches are emerging as safer and effective alternatives. In this context, we employ a non-viral method, previously developed by our group, of human MSC transfection through microporation aiming at a high gene delivery efficiency, without compromising cell viability and recovery[280].

When evaluating the role of naïve MSC in tumor progression/ suppression, the majority of studies employ MSC isolated from the BM, the UCM and from the AT (AT)[281–283]. Considering that MSC isolated from different tissue sources express different surface markers[22,284], and may differ in what concerns differentiation potential[24], the outcome from these studies may be dependent on the isolation source of MSC. Therefore, in the present study all experiments were validated with MSC from two tissue sources, BM and UCM. Moreover, envisaging the

translational potential of our approach, this study was performed under SF/XF culture conditions to avoid the batch-to-batch variations associated with the use of animal-derived products, allowing a better reproducibility, and preventing contagious health risks from animal-derived viral agents, mycoplasma and prions[399].

II.3. Materials and Methods

II.3.1. Cell lines and cell cultures

Cancer cell lines A549 (lung) and MCF-7 (breast) were obtained from ECACC (European Collection of Authenticated Cell Cultures) and cultured using high glucose Dulbecco's modified Eagles' medium (DMEM) supplemented with 10% of heat-inactivated fetal bovine serum (FBS) (Lonza), 100IU/ml penicillin, 100 mg/ml streptomycin (PenStrep, Invitrogen), and passaged between 2 and 3 times per week, by chemical detachment with trypsin 0.05%.

Human MSC used in this study are part of the cell bank available at the Stem Cell Engineering Research Group (SCERG), Institute for Bioengineering and Biosciences at Instituto Superior Técnico (iBB-IST). MSC were previously isolated/expanded according to protocols previously established at iBB-IST[286,287]. Originally, human tissue samples were obtained from local hospitals under collaboration agreements with iBB-IST (BM: Instituto Português de Oncologia Francisco Gentil, Lisbon; UCM: Hospital São Francisco Xavier, Lisbon, Centro Hospitalar Lisboa Ocidental, Lisbon). All human samples were obtained from healthy donors after written informed consent according to the Directive 2004/23/EC of the European Parliament and of the Council of 31 March 2004 on setting standards of quality and safety for the donation, procurement, testing, processing, preservation, storage, and distribution of human tissues and cells (Portuguese Law 22/2007, June 29), with the approval of the Ethics Committee of the respective clinical institution. Human MSC from the different tissue sources (BM and UCM) were kept cryopreserved in a liquid/vapor-phase nitrogen container. Upon thawing, cells were cultured in StemPro® Serum-free (SFM) medium and passaged two times per week, by chemical detachment with TrypLE^{TM} Select (Gibco).

All cell lines were grown in a humidified atmosphere at 37°C with 5% CO2 (Binder CO_2 incubator C150).

II.3.2. Construction of azurin recombinant plasmid and transfection into human MSC

Azurin coding sequence was obtained by gene synthesis following a codon optimization algorithm towards the human codon usage from the coding sequence from *Pseudomonas*

aeruginosa PAO1, to improve translation efficiency. Human codon optimized azurin (hazu) in fusion with the first 21 amino acids (aa) of the human tissue plasminogen activator (t-PA)[288] was subcloned into a pVAX1-GFP vector by replacing the *GFP* gene, producing the recombinant pVAX-hazu plasmid. pVAX-GFP was constructed and produced as described elsewhere[289]. The fidelity of the cloned sequence was evaluated by DNA sequencing. MSC were transfected with 10µg of pVAX-hazu plasmid through microporation (Microporator MP100 (Neon/ Invitrogen-Life Technologies) according to Madeira *et al*. 2011[38]. As a control, MSC were transfected with pVAX-GFP to assess the transfection efficiency. MSC conditioned media (CM) (MSC-CM) and cells were harvested at 72h and 96h post-transfection. The expression and secretion of azurin was evaluated through western blotting and the percentage of GFP-positive cells was detected by flow cytometry (FACSCalibur equipment, Becton Dickinson; FL1 filter (533/30nm)).

II.3.3. Western blotting

MSC-CM were collected at 96h, mixed with loading buffer (Tris–HCl 62.5mM, pH 6.8, 2.5% SDS, 10% glycerol, 0.002% bromophenol blue, and 5% β-mercaptoethanol), and boiled at 95°C for 5 min. Denatured samples were run on 15% polyacrylamide gel and transferred onto nitrocellulose membranes (Trans-Blot Turbo, BioRad). The membranes were incubated overnight with 1:2,000 dilution of specific custom-made primary anti-azurin antibody (SicGen)[249], 1:2,000 anti-GFP (Santa Cruz Biotechnology), or 1:1,000 anti-GAPDH (Santa Cruz Biotechnology). Following incubation, the membranes were washed with PBS–tween-20 (0.5%) and probed with 1:2,000 secondary antibody (Santa Cruz Biotechnology) during 1h by shaking at room temperature. Proteins were detected through the addition of enhanced luminol-based chemiluminescent substrate (ECL) reagent (Pierce) as a substrate and exposed and captured the chemiluminescence by Fusion Solo (Vilber Lourmat) equipment. For the cleavage of N-linked oligosaccharides, 10µg of total protein in MSC-derived conditioned medium (MSC-CM) was mixed with 1µl of Glycoprotein Denaturating Buffer (10x) and H_2O, before boiling the sample for 10min at 100°C. After briefly chilling on ice, 2µl of GlycoBuffer (10x), 2µl of 10% NP-40, and water were added to a final volume of 20µl. Finally, 1µl of PNGase F (New England Biolabs) was added and the mixture was incubated at 37°C for 1h before analysis by Western blotting.

II.3.4. Cancer cell proliferation assay

Presto Blue™ viability assay was used to determine proliferation of cancer cells upon treatment with MSC-CM. Cells were seeded on 96-well plates (Orange Scientific) at a density of 1×10^4 and 2×10^4 cells/well for MCF-7 and A549 cell lines, respectively. After 24h, medium was exchanged with 100µl of MSC-CM (keeping a baseline level of 50% cancer cells' culture media: 0%, 10%, 25%, and 50% MSC-CM). Afterward, Presto Blue Reagent (ThermoFisher) was added to each well and incubated at 37°C for 2h. Fluorescence was determined at the following wavelengths: 540nm excitation and 590nm emission. Untreated cells were used as control, in order to determine the relative cell proliferation of treated cells.

II.3.5. Assessment of cancer cell apoptosis

Cancer cell apoptosis was assessed using the Annexin V Apoptosis Detection kit (BD Sciences). Cells were plated on 6-well plates (Orange Scientific) at a density of 2×10^5 and 1.5×10^5 cells/well for MCF-7 and A549 cell lines, respectively. On the next day, medium was exchanged with MSC-CM (50% cancer cells' culture media/50% MSC-CM). After 24h incubation, cells were harvested and stained for Annexin V and propidium iodide (PI) by flow cytometry.

II.3.6. Cancer cell invasion assay

The ability of MSC to migrate toward tumor cells (tumor tropism) and cancer cell invasion was evaluated using CytoSelect™ 24-Well Cell Migration with 8µm pore size, coated with Matrigel. For tumor tropism experiments, 1.5×10^5 lung (A549) and breast cancer (MCF-7) cells were cultured on 24-well plates and left overnight at 37°C and 5% CO_2. MSC (4×10^4) were incubated in the upper compartment of the culture chamber, placed on the wells, and left for 24h at 37°C and 5% CO_2. For cancer cell invasiveness experiments, 1.5×10^5 A549 cells treated or untreated with MSC-CM were incubated in the upper compartment of the transwell, while culture medium (*i.e.*, DMEM supplemented with 10% FBS) was added to the 24-well plates. Incubation was held at 37°C and 5% CO_2 for 24h. Non migrated cells were removed from the upper side of the chamber's filter with a cotton swab dipped in PBS and chambers were washed with PBS. Migrated cells were fixed in cold methanol (4°C) for 10min. The membrane was removed with a scalpel and placed in a microscope glass, and cells were stained with DAPI and counted under a microscope (Zeiss). In each condition, 10 independent fields were counted, and the average of these fields was considered as the mean number of

migrated cells per condition. Results are presented as the fold change in the number of cells migrated in comparison with the control condition where no cancer cells were added.

II.3.7. Cancer cell migration Assay

A scratch assay was used to assess the migration of breast (MCF-7) and lung (A549) cancer cells *in vitro*, upon treatment with MSC-CM. Approximately 2×10^6 cells were seed in 2-well culture inserts (Ibidi), to ensure reproducibility within conditions, on 24-well dish and cultured in growth medium for 72h until approximately 70–80% confluence. Inserts were removed, and cells were treated with 250µl of MSC-CM (keeping the proportion 50% MSC-CM/50% cancer cells' culture medium). Cells were monitored over time by time-lapse recording and distance moved by the cells was determined by measuring the unoccupied scratch area (% of unoccupied area/h).

II.3.8. Cytokine quantification by ELISA

The levels of IL6, TGF-β, SDF1-α, and VEGF were measured in 100µl of MSC-CM collected at 96h with a sandwich ELISA kit, according to the manufacturer's instructions (RayBiotech).

II.3.8. Statistical Analysis

All data is presented as mean ± standard error of the mean (SEM). Statistical analysis was performed using GraphPad Prism 6 and significance was determined by Tukey's multiple comparison test and set at a p-value <0.05.

II.4. Results

II.4.1. Human MSC are able to express and secrete azurin without cell viability impairment

BM and UCM derived MSC cultured under SF/XF conditions, were transfected by microporation with plasmid DNA (pVAX-*hazu*) encoding for a human codon optimized version of azurin coding sequence containing on its N-terminal a secretory sequence leading to the secretion upon protein synthesis[288]. Codon optimization was used considering that azurin is from a bacterial source and its efficiency of translation in animal cells, such as MSC, could be reduced. Parallelly, MSC were transfected with a control vector, containing a *GFP* sequence (pVAX-GFP).

Notably, azurin production has not induced alterations on MSC themselves, as we monitored cell viability over a 96h period after cell microporation (Figure II.4.1-A). Non-transfected cells (control 1) displayed the highest cell number at day 2, 3 and 4, followed by cells microporated without DNA (control 2). Nevertheless, cells microporated with pVAX-GFP and pVAX-hazu entered the exponential growth phase with almost no differences between the groups. Flow cytometry demonstrated that 50 to 60% of the cell population was expressing GFP, 72h post-transfection (Figure II.4.1-B), with a cellular recovery of 46% and yield of transfection of 28% (comparable to 70%, 40%, 30%, respectively in Madeira et al, 2010[280]). As negative controls, non-transfected cells (control 1) and microporated cells without DNA (control 2) were also evaluated.

After microporation, MSC were cultured for 96h and the secreted azurin was detected in the conditioned medium (CM) by western blotting (Figure II.4.1-C) (Full membrane images are depicted in VIII Appendix section - Figure VII.1.1). Specific bands around the expected MW of 15kDa were observed only in the supernatants from MSC transfected with pVAX-hazu (hazu-MSC), which indicated that azurin was successfully expressed and released to the CM. However, it was possible to observe two bands corresponding to possible protein post-translational modifications. After treatment of MSC-derived CM (MSC-CM) with PNGase F (endoglycosidase that selectively removes N-glycans), only one band with more intensity was observed, which indicates that azurin is N-glycosylated in the CM of MSC-transfected cells (Figure II.4.1-D).

II.4.2. MSC preserve tumor tropism after microporation

Human MSC have been described to be intrinsically tropic to tumor sites[290], which is a central feature to their potential role as delivery vehicles for anti-cancer agents in cancer therapy. In this study, the *in vitro* tumor tropism properties of BM-derived MSC (BM-MSC) (3 donors) towards a breast cancer cell line (MCF-7) were evaluated by a transwell migration assay using CytoSelect chambers with 8µm pores. Aiming at a better mimicry of the *in vivo* microenvironment, we studied the effect of physiological barriers like collagen type I and Matrigel™ as coatings on transwell chambers. Tumor cell lines were seeded on 24-well plates and after 24h, the upper chambers containing seeded MSC were added to each well at a ratio of MSC / tumor cells = ¼. In the control condition, no tumor cells were added (the corresponding medium volume was added instead). Tumor cells triggered invasion of BM MSC as compared to the negative control, and the specificity of this process seems to be improved by the presence of Matrigel (Figure II.4.1-E).

Cell microporation and transgene expression could potentially induce changes in the physiological properties of MSC. Therefore, we compared the tumor tropism rate of un-modified MSC and hazu-MSC towards A549 cells (Figure II.4.1-F). As shown, the expression of azurin does not impact the homing ability of these cells, and these results are supported by the characterization of CXCR4 (VIII Appendix section - Figure VII.1.2.), a known chemokine receptor associated to the tumor tropism properties of MSC (21.2% expression in control MSC *versus* 23.2% expression in hazu-MSC, assessed by flow cytometry).

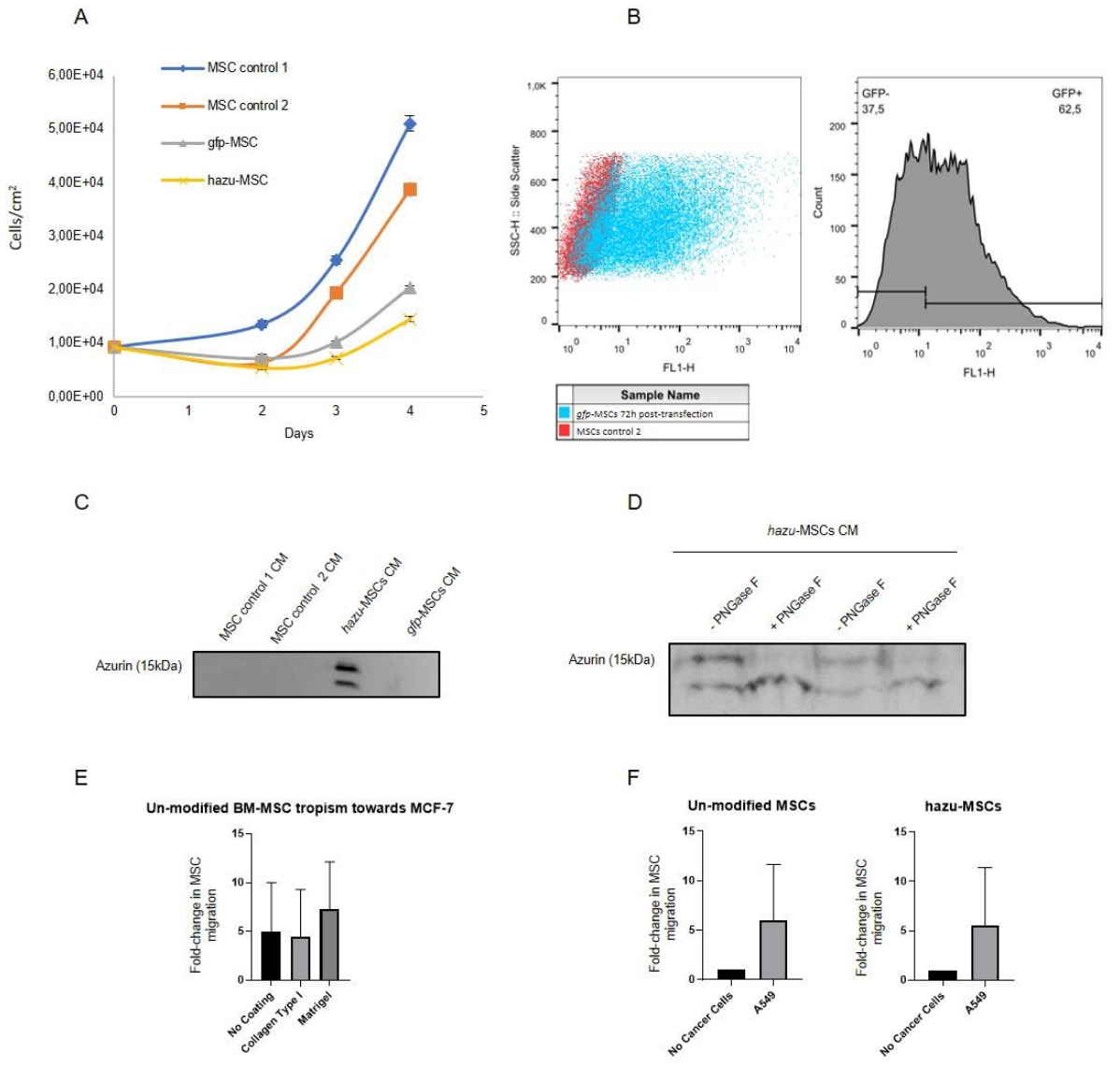

Figure II.4.1 - Engineering of mesenchymal stromal cells (MSC) to express azurin. (A) MSC number per square centimetres after microporation.

Figure II.4.1 - (continued) MSC non-microporated (control 1) (blue line), MSC microporation control were transfected without the plasmid DNA (control 2) (orange line), gfp-MSC were microporated with pVAX-GFP (grey line), and hazu-MSC were microporated with pVAX-hazu (yellow line). A total of 9.23 × 10^3 cells per condition were initially microporated and counted at days 2, 3 and 4. Values are mean ± SD (n = 3). (B) Flow cytometry demonstrated that 50 to 60% of cell population was expressing GFP 72h post-transfection. (C) Azurin is secreted by MSC to the conditioned media (CM) at 96h after microporation. A representative image of Western blotting for one donor is depicted. (D) Ten micrograms of total protein from CM were incubated with PNGase F to remove N-linked oligosaccharides from glycoproteins. Western blotting image of MSC-CM from two independent donors is depicted. (E) Tumor tropism of un-modified BM (BM)-derived MSC toward MCF-7 breast cancer cells. Results are presented as the fold change of migrated MSC toward tumor cells compared to negative control (migration toward culture media). (F) Comparison between tumor tropism rate of un-modified MSC and hazu-MSC toward A549. Results are presented as the fold change of migrated MSC toward tumor cells and the negative control (migration toward culture media).

II.4.3. Cancer cell proliferation decreases, and cell death increases upon treatment with hazu-MSC-CM

To investigate whether the secretome of azurin-producing MSC has an inhibitory effect on cancer cells' growth and proliferation, tumor cell lines A549 and MCF-7 were subjected to increasing concentrations of CM from hazu-MSC cultures, harvested 96h post-microporation. Since MSC and cancer cells were cultured in different culture media (MSC in StemPro® MSC SFM Xeno-free culture medium, whereas MCF-7 and A549 in DMEM high glucose supplemented with FBS), for this experiment, the concentration of MSC-CM was varied, while maintaining a baseline level of cancer cells' culture medium at 50%. Cytotoxicity and tumor cell proliferation were assessed by using PrestoBlue after 24h treatment with MSC-CM (Figure II.4.2-A). The results are presented in variation (%) of proliferation relatively to the control, where no MSC-CM was added (corresponding to 100% proliferation rate). The effect of hazu-MSC-CM seems to be inhibiting tumor cell proliferation and this effect is more pronounced by increasing concentrations. On the other hand, CM retrieved from control MSC cause no change in the proliferation of both A549 and MCF-7 cell lines. The effect of hazu-MSC-CM induced an inhibition of 38.1% in A549 and an inhibition of 17.3% in MCF-7 with the highest concentration of CM (50% vol/vol). Moreover, we observed an average of 1.6- and 3.9-fold increase in the apoptotic levels of A549, assessed by flow cytometry (Figure II.4.2-B; C) and MCF-7 cells (Figure II.4.2-B;D), respectively, after treatment with hazu-MSC-CM when compared with the control CM.

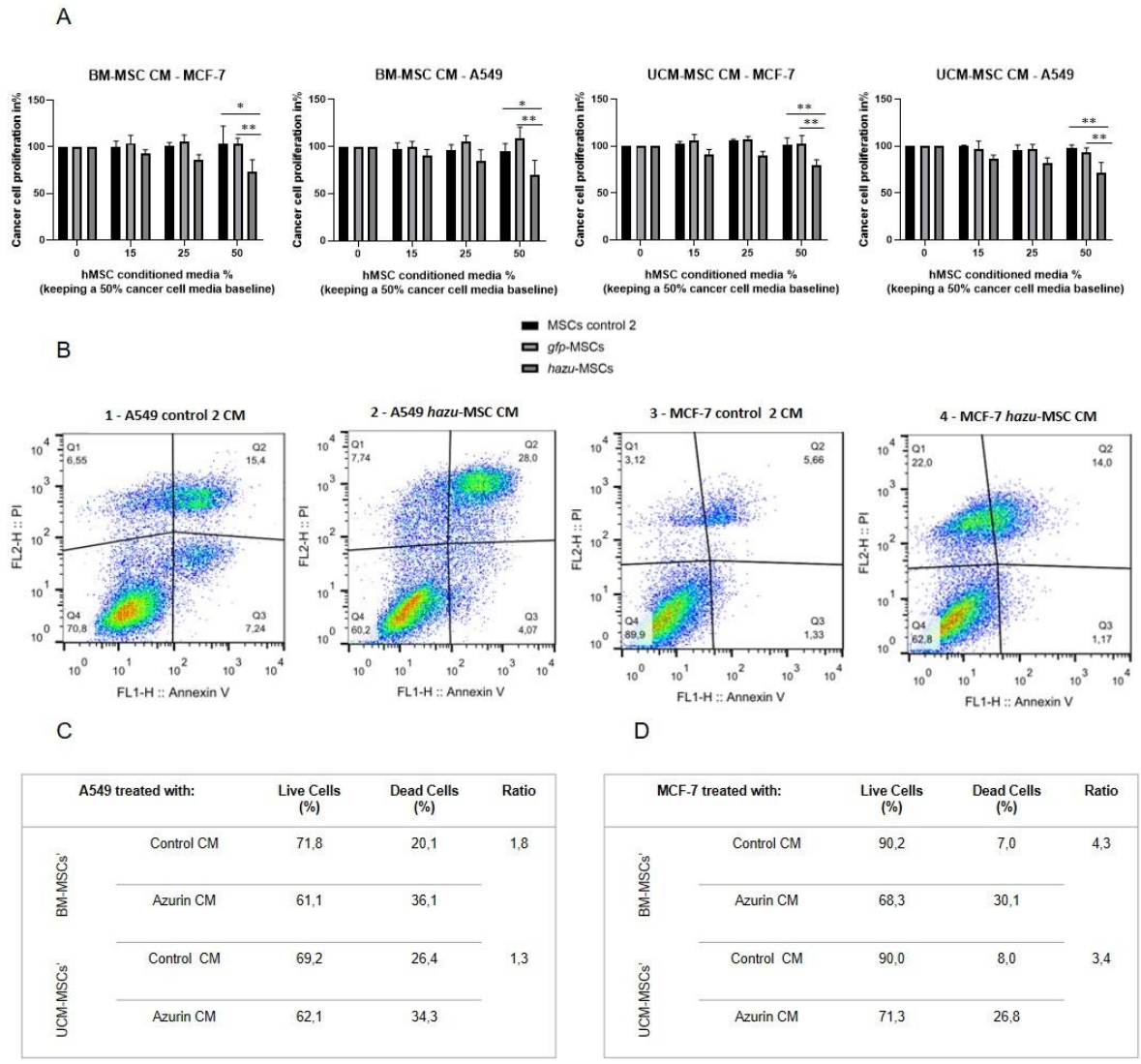

C

	A549 treated with:	Live Cells (%)	Dead Cells (%)	Ratio
BM-MSCs'	Control CM	71,8	20,1	1,8
	Azurin CM	61,1	36,1	
UCM-MSCs'	Control CM	69,2	26,4	1,3
	Azurin CM	62,1	34,3	

D

	MCF-7 treated with:	Live Cells (%)	Dead Cells (%)	Ratio
BM-MSCs'	Control CM	90,2	7,0	4,3
	Azurin CM	68,3	30,1	
UCM-MSCs'	Control CM	90,0	8,0	3,4
	Azurin CM	71,3	26,8	

Figure II.4.2 - hazu-MSC CM inhibit cancer cell proliferation and induce cancer cell death *in vitro*. (A) Cytotoxicity and tumor cell viability were assessed by PrestoBlue in breast cancer (MCF-7) and lung cancer (A549) cell lines upon 24h of exposition to conditioned media (CM) from MSC microporated with pVAX-hazu (hazu-MSC) (grey bars), pVAX-GFP (gfp-MSC) (light grey bars), or without DNA (microporation control 2) (black bars). MSC-CM was collected 96h post-transfection. Due to differences in expansion media between cancer cells and MSC, MSC-CM concentration was variated (0–50%) while maintaining a level of cancer cells' culture media at 50%. Untreated cells were exposed to media without CM, and their proliferation rate was admitted as 100% (p-values compare % of proliferation between gfp-MSC or hazu-MSC with MSC control 2; n = 4). (B) Annexin V expression detection after treatment with hazu-MSC' CM, assessed by flow cytometry. Living cells are seen in the lower left quadrant, Annexin V (−)/ PI (−), [Q1]. The early apoptotic cells are shown in the lower right quadrant, Annexin V (+)/ PI (−), [Q2]. Advanced apoptotic or necrotic cells are seen in the upper right quadrant, Annexin V (+)/ PI (+), [Q3]. Annexin V (−)/ PI (+), [Q4] are cells in late necrosis or cellular debris. Panels 1 and 2 correspond to MCF-7 treated with control 2 MSC-CM and hazu-MSC-CM, respectively. Panels 3 and 4 correspond to A549 treated with control 2 MSC CM and hazu-MSC CM, respectively (n = 2). (C) Percentage of A549 live and dead cells based on flow cytometry results on annexin V expression, after treatment with MSC-CM and the ratio between dead cells treated with hazu-MSC' CM or control MSC' CM (n = 1). (D) Percentage of MCF-7 live, and dead cells based on flow cytometry results on annexin V expression, after treatment with MSC-CM and the ratio between dead cells treated with hazu-MSC' CM or control MSC' CM (n = 1). Statistical differences are indicated with $*p \leq 0.05$ and $**p \leq 0.01$.

II.4.4. Cancer cell migration and invasion decreases upon treatment with hazu-MSC-CM

The anti-tumoral effects of hazu-MSC-CM are also extended to the impairment of cancer cell invasion. These experiments were performed with indirect co-cultures, in a transwell migration assay, by culturing cancer cells treated and un-treated with MSC-CM in invasion chambers coated with Matrigel. Results are given in the percentage of cancer cell invasion in comparison to the control condition where cancer cells were treated with culture medium only (*i.e.* without MSC-CM). By analysing the results, we can hypothesize that the naïve MSC' secretome by itself has an impact in reducing cancer cell invasion, and this effect is enhanced by the presence of azurin to a notorious extent (close to 20% invasive cells compared to control) (Figure II.4.3-A).

Cell migration in cancer cells is also affected by treatment with hazu-MSC-CM. Cell migration was estimated by means of a scratch assay and monitored by time-lapse microscopy. The distances of migrated cells were measured over several time points and the results show that treatment with conditioned medium from hazu-MSC induced a delay on cancer cell migration and repairment of the scratch area (Figure II.4.3-B). 20h after treatment, the percentage of unoccupied area for A549 treated with hazu-MSC-CM was 23.4%, compared to 1.4% unoccupied area for A549 treated with CM from control 2 MSC. Regarding MCF-7, a percentage of 32.8 was observed for cells treated with hazu-MSC-CM and 8.9 for cells treated with CM from control 2 MSC.

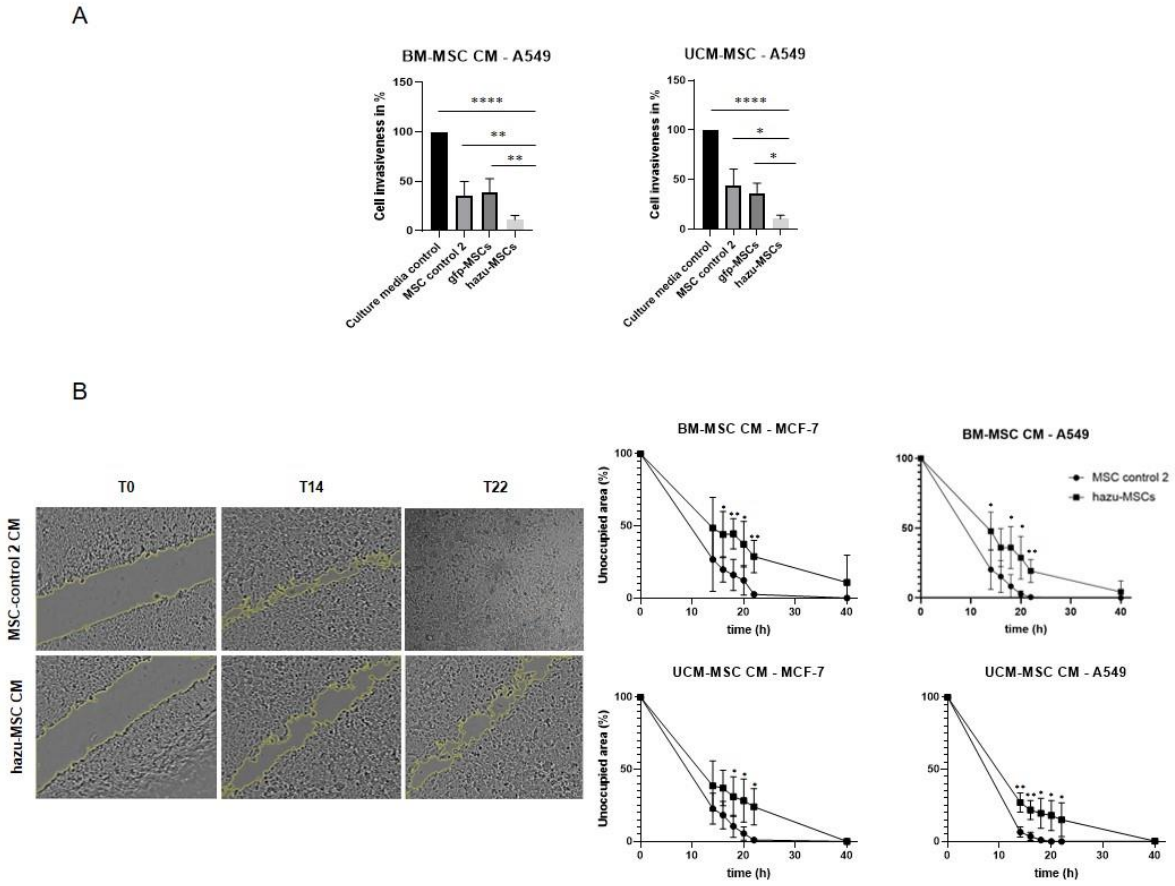

Figure II.4.3 - Inhibition of cancer cell invasion and migration by hazu-MSC' CM *in vitro*. (A) A549 lung cancer cell invasion toward a chemoattractant (culture media supplemented with FBS) was evaluated in Matrigel invasion assays. Cells were treated with CM from gfp-MSC, hazu-MSC, MSC control 2, and cancer cell media (culture media control) during 24h and migrated cells were quantified. Results are presented as the percentage of invasive cells compared to the control condition (p-values compare % of cancer cell invasiveness between hazu-MSC' CM treatment and the remaining treatment conditions; n = 4). (B) Cell migration was estimated by means of a scratch assay and monitored by time-lapse microscopy. A549 and MCF-7 were treated with control 2 MSC' CM or hazu-MSC' CM, and the distances of migrated cells were measured at several time points: 0, 14, 16, 18, 20, 22 and 40h (p-values compare % of unoccupied area between A549 and MCF-7 treated with hazu-MSC' CM or MSC control 2 CM, at the same time point; n = 4). Statistical differences are indicated with $*p \leq 0.05$, $**p \leq 0.01$ and $****p \leq 0.0001$.

II.4.5. Secretion of cytokines involved in tumor progression by engineered MSC quantified by ELISA

To get insights regarding the anti-tumoral effects induced by hazu-MSC-CM, namely if these are due to a crosstalk between the induced azurin expression and the native secretome of MSC, we evaluated the expression of 4 cytokines expressed by MSC that have been described to have a role in MSC interaction with cancer cells: IL6[290], vascular endothelial growth factor VEGF[291], SDF1-α[292] and TGF-β[293]. To this end, we analysed the concentration of these factors in MSC-CM by ELISA before and after microporation with pVAX-hazu and

pVAX-GFP (Figure II.4.4). The results are given in the relative fold change of cytokine expression relatively to MSC-CM in the control condition (control 2, *i.e.* MSC microporated without DNA). The microporation process seems to be inducing a general response in the expression of such cytokines, by decreasing their relative concentration. However, no significant differences were observed between the hazu-MSC-CM and gfp-MSC-CM, which might suggest that the effects observed in cancer regression can be due to the engineered expression of azurin independently.

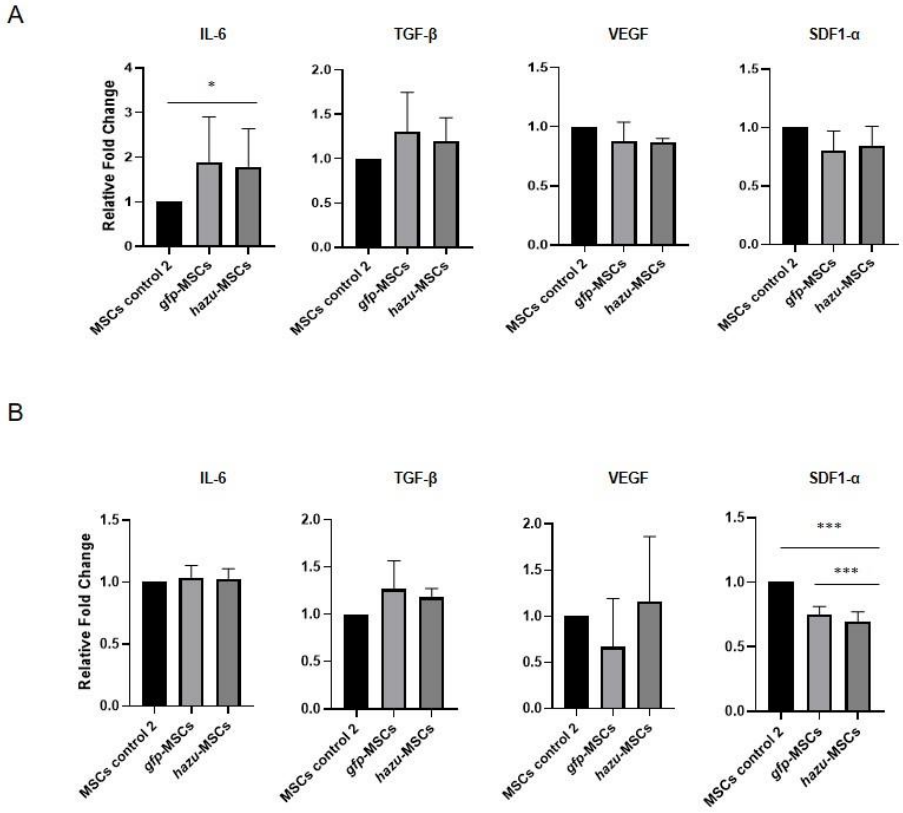

Figure II.4.4 - Evaluation of MSC expression profile on cytokines relevant in cancer progression. The levels of inteuleukin-6 (IL6), vascular endothelial growth factor (VEGF), stromal derived factor 1 alpha (SDF1-α) and transforming growth factor beta (TGF-β) were analysed by ELISA in MSC-CM before and after microporation with pVAX-hazu and pVAX-GFP. The results are given in the relative fold change of cytokine expression relatively to MSC-CM in the control condition (control 2) (p-values compare fold change between gfp-MSC and hazu-MSC conditions with MSC control 2; n = 3). (A) Cytokine expression profile in BM MSC-CM. (B) Cytokine expression profile in UCM MSC-CM. Statistical differences are indicated with $*p \leq 0.05$ and $***p \leq 0.001$.

II.5. Discussion

One of the major challenges of developing more effective cancer therapies concerns the specific delivery of anti-cancer drugs to the tumor site. In this context, human MSC have been recently considered for cell-based therapies for cancer, due to their ability to migrate specifically and to incorporate within tumors, their low immunogenicity and the fact that these cells are relatively easy to isolate, culture and manipulate[1–3,273–275]. Altogether, these features turn MSC exciting therapeutic candidates as drug delivery tools towards cancer. In the perspective of cell-based therapies, MSC do not only potentially solve the drug delivery specificity problem, but also allow for the heightening of the half-life of drug compounds in the organism, as well as a lower dosage and less repeated injections to potentially achieve meaningful responses[294].

Furthermore, MSC demonstrate a strong paracrine effect resulting from the high levels of bioactive molecules they secrete in response to their microenvironment. The panoply of factors produced by these cells is highly context dependent, being able to be modulated *in vitro*. For this reason, MSC's secretome, either in the format of CM or as purified EVs, has been explored as a cell-free approach in several applications in regenerative medicine[295,296]. Despite the potential benefits of using MSC as a cell delivery system, studies have reported the supportive role of MSC in the progression of tumor density and metastasis, while others have shown anti-tumor effects both *in vitro* and in different models of cancer[282,283,297]. The conflicting data in the literature may hamper the establishment of cell therapies for cancer based on non-modified MSC since the therapeutic safety of such approach might be jeopardized[281].

The availability of genetic engineering tools may potentiate MSC as living factories of anti-tumoral proteins for cancer therapy. In this study, we genetically engineered human MSC, through non-viral methods, towards the production and secretion of the anti-tumoral protein azurin. Azurin, originally produced by *Pseudomonas aeruginosa*, has a complex anti-cancer mechanism of action, targeting several independent pathways critical for tumor progression. These features allow a much broader action of azurin regarding the tumor types that it can target, while also supporting the prevention of tumor resistance[251,256,261]. We engineered a recombinant plasmid containing the azurin coding sequence and an engineered secretory sequence that provides a signal for translocation of recombinant proteins into the lumen of the endoplasmic reticulum (ER), for transport through the ER and Golgi apparatus to the extracellular environment[288]. To the best of our knowledge, this study is the first to combine a cell-based approach to deliver a protein originated in bacteria for anti-cancer therapies.

Over the last years, significant efforts have been made to address the limitations of MSC in early clinical trials, namely by using genetic engineering tools to improve the therapeutic potential of these cells[298]. Despite the advantages of employing non-viral gene delivery methods, to date, the majority of conducted clinical trials based on genetically engineered MSC are relying on the use of viral methods. Although transduction efficiency is higher, issues regarding vectors safety and manufacturing have encouraged the implementation and optimization of non-viral based techniques such as microporation. The method used in this study is based on previous studies from our group[280], aiming at a cell transfection with high efficiency without compromising cell viability and recovery. Regarding the percentage of GFP-positive cells, herein we obtained 60%, a cellular recovery of 46% and yield of transfection of 28% (70%, 40%, 30%, respectively in Madeira et al, 2010[280]). hazu-MSC supernatants were collected at 96 h and azurin was detected by western blotting. Besides the expected azurin, it was possible to observe a second band corresponding to a post-translationally modified protein, that was later identified as a glycosylated azurin after treatment with PNGase F. This brings us to hypothesize that the activity of this glycosylated form of azurin may differ from the native protein. Therefore, in future studies, it would be important to characterize this modified protein in terms of structure, functionality and anti-tumoral activity.

We tested the effect of hazu-MSC secretome in tumor progression by exposing MCF-7 and A549 cells to increasing concentrations of engineered MSC-derived CM. The plenitude of hazu-MSC produced factors inhibited 17.3% and 38.1% tumor proliferation in MCF-7 and A549, respectively, with the highest concentration of CM tested (50%, vol/vol) comparing to MSC microporated with pVAX-GFP and MSC microporated with no DNA (control 2), where no inhibition was observed. In this experiment, we varied the concentration of MSC-CM, while maintaining a baseline level of cancer cells' culture medium at 50%. Thus, the effects observed in cancer proliferation are not associated with the medium change or the lack of FBS components. Along with a decrease in cancer cell proliferation, an increase in cancer cell apoptosis was observed. These results are in agreement with the anti-cancer properties of azurin, as previously mentioned[263]. Moreover, upon treatment with hazu-MSC-CM, a decrease in invasion through Matrigel for the A459 invasive cell line[299] and a decrease in cell migration was observed for both cancer cell lines. In previous work from our group, we demonstrated that bacterial produced azurin interferes with pro-tumorigenic and proliferative signalling pathways FAK, Src and AKT, by attenuating the phosphorylation levels of these proteins in lung[261] and breast cancer cell lines[249], which associated to decreased invasion behaviour through Matrigel. In this context, further studies should focus on the interaction between MSC-produced azurin and the activation of such signalling pathways.

MSC are emerging as promising anti-cancer agents, fundamentally due to their innate tropism towards proinflammatory environments, such as the tumor microenvironment in both primary and metastatic sites[300]. In this context, we demonstrated the migratory capacity of hazu-MSC towards MCF-7 and A549 cancer cell lines through indirect co-cultures. The results demonstrated no differences in the migratory potential of engineered when compared to unmodified cells. Furthermore, we evaluated the expression of four cytokines expressed by naïve MSC that play a pivotal role in the hallmarks of cancer progression in processes such as cancer cell proliferation, invasion, migration, angiogenesis, apoptosis, and development of metastases[301]. Microporation seems to be inducing an effect in the expression of such cytokines to a certain extent, however we observed no significant differences between engineered MSC and naïve MSC, which may suggest that the results observed in cancer regression might be associated to the expression of azurin independently, rather than due to a crosstalk of azurin and the naïve MSC secretome.

The majority of the studies evaluating the effect of naïve MSC on tumor development, employ MSC from the BM, UCM and AT[281–283]. When analysing the outcome from these studies it seems to be a conspicuous pattern of tumorigenicity, with BM MSC being more pro-tumorigenic and UCM MSC being more tumor suppressive. And this pattern seems to be more pronounced when evaluating breast cancer, the most popular type of cancer tested with MSC cytotherapy[302]. For this reason, in the present study all experiments were validated using MSC isolated from two different donors of two tissue sources, BM and UCM.

Although BM has been the main source for MSC isolation, the harvest of BM is a highly invasive procedure and the number, differentiation potential, and maximal life span of BM MSC decline with increasing age[25]. In this regard, a significant advantage of the neonatal tissues, such as the UCM, as sources of MSC is that they are readily available, thus avoiding invasive procedures and ethical problems associated to adult tissues, and several studies have reported superior proliferative capacity, life span and differentiation potential over BM MSC[25]. Considering the ease of harvest, culture and transfection of MSC, the use of autologous cells may be realistic. However, the number and quality of MSC differ from patient to patient, making the quantification of the therapeutic effect difficult to interpret. Therefore, the use of allogeneic MSC from healthy donors would allow greater cell numbers of better characterized cells[124]. Moreover, envisioning an MSC cell line that stably expresses the transgene could overcome some issues related to the translation of MSC therapies to a clinical setting. Therefore, the establishment of a stable hazu-MSC cell line represents a more flexible system both in terms of manufacturing and the therapeutic perspectives (cell-based product or cell-free approach based on CM).

III. XENO-FREE PROTOCOL FOR THE PRECISE GENE EDITING OF HUMAN MESENCHYMAL STROMAL CELLS USING THE CRISPR/CAS9 TECHNOLOGY

Manuscript in preparation

III.1. Summary

Mesenchymal stromal cells (MSC) are an attractive cell population extensively studied for diverse therapeutic applications in the last decade due to their low immunogenicity, ability to selectively migrate towards inflammatory sites, as well as their ability to differentiate into several cell types and to secrete immunomodulatory and trophic factors, contributing for tissue regeneration. These cells have already demonstrated to be safe upon administration and effective in multiple clinical trial studies for several diseases. However, despite the great biomedical potential, further investigation is needed focused on the enhancement of the therapeutic features of MSC.

Though viral vectors have been widely explored as effective engineering tools, efforts towards safer and more controllable nonviral methods are recently being made in the field of cell engineering. In this context, the CRISPR-Cas9 system is a novel technique for gene editing that is being explored to improve MSC therapeutic usage. In this study, we report an entirely non-viral, microporation-based delivery protocol capable of delivering a Cas9 RNP complex into the hard-to-transfect human MSC (bone marrow (BM)- and umbilical cord matrix (UCM)-derived) under serum-free (SF)/ xenogeneic-free (XF) culture conditions, reaching an overall 50% on-target (the AAVS1 genomic safe harbor) efficiency, while preserving cell viability (>70%). Overall, we present a clinically oriented genetic toolbox to edit human MSC, opening a window of opportunities to design a more robust MSC cell product in terms of manufacturing and therapeutic options.

III.2. Background

MSC are highly attractive and valuable candidates for biomedical applications including for the development of cell and gene therapies, due to their high proliferative capacity[1], ability to differentiate into multiple lineages[1], and ability to migrate into injured organs[40], including cancer sites[131,227,243]. In this field, programmable nuclease technologies have shown great potential for disease modelling and development of new therapeutics. Among these technologies, the CRISPR-associated Cas9 (CRISPR/Cas9) has now become the tool of choice due to its simplicity and versatility[200]. One of the key points for efficient gene editing is the successful delivery of sufficient amounts of CRISPR/Cas9 elements into target cells. Molecular delivery methods can be broadly classified into viral, chemical, and physical. Viral delivery methods have been the most commonly used vehicles to deliver transgenes into MSC to develop cell lines for therapeutic application in the most diverse range of pathologies such as bone defects[95], stroke[100], cancer[106,108,303], acute kidney injury[111], diabetic peripheral neurovascular disease[115], and others. Though, overall, viral systems allow efficient and long

term-gene expression into cells, being the primordial delivery route for cell engineering, these still pose safety concerns that are critical when considering clinical applications[304,305]. Furthermore, their use sometimes causes significant changes in the characteristics of genetically modified stem cells, including their homing capacity[306]. Therefore, alternative non-viral delivery methods, have gained significant importance. These methods can be advantageous over viral methods since they are non-infectious, relatively non-immunogenic, can accommodate large DNA plasmids, and can be produced simply on a large scale[305]. Among the non-viral methods, electroporation is the most widely used physical method, being firstly introduced in 1982[307]. Electroporation is easy to perform and is generally applicable to a wide range of cell types, without requiring additional viral or cytotoxic chemical components. However, with the high electric field strength and derived electrochemical reactions, electroporation often leads to high post-transfection mortality[308]. An adaptation from the conventional electroporation method is microporation, which is a unique technology that uses a pipette tip as an electroporation space and a capillary type of electric chamber instead of a cuvette, which counteracts the harmful effects of cuvette-based electroporation gene transfer techniques such as pH variation, increasing in temperature, and metal ion generation, greatly increasing transfection efficiency and cell viability[308]. In our group, previous work has been conducted towards the development of complete XF microporation protocols in MSC from different tissue sources towards efficient transgene expression, while uncompromising cell recovery and the innate MSC features, envisioning future clinical application compliance[36,280].Though in preliminary stages, there are some studies exploiting MSC microporation towards the application of the CRISPR/Cas9 technology, specifically aiming at the improvement of their innate potentialities[207].

The power of CRISPR/Cas9 depends on several variables being strongly reliant on the quality of the delivery protocol for the Cas9 enzyme, along with the efficiency of the designed sgRNA, into the target cells. This is particularly critical for sensitive cells resilient to transfection protocols, such as MSC. Regardless of the delivery method, there are several challenges inherent to the delivery of Cas9 specifically. The Cas9 protein is a very large molecule (about 160kDa)[309] and is highly negatively charged. These features make it exactly the type of structure that the cell membrane has evolved to reject entering the cell[310].

Moreover, the CRISPR complex must also evade cellular degradation mechanisms, including proteases, RNAases, and lysosomes[311]. The Cas9 gene varies from 4 to 7kB, depending on the species of origin and the inclusion of intracellular tags[312]. Plasmid DNA is stable and inexpensive, making a plasmid encoding Cas9 an appealing delivery route[313314]. In order to be effective in eukaryotic cells, for this strategy, the plasmid DNA must cross both cellular and nuclear membranes. Single plasmids containing both the sgRNA and a Cas9 protein are

developed to act as an all-in-one vector giving the recipient cell all the information to generate the CRISPR complex in a compatible way. However, the introduction of plasmids increases the expression time compared with other modes of delivery, which may be advantageous if sustained expression is required for editing, but it could also lead to increased off-target effects, raising safety concerns[315]. An alternative to encoding Cas9 in plasmid DNA is instead to encode it as mRNA, which can be expressed by ribosomes found in the cytoplasm. This avoids the challenge of crossing the nuclear membrane and translation can be initiated immediately, while Cas9 plasmid DNA must be transcribed into mRNA first[313]. This strategy allows for a transient protein expression and a better control on the dosage or duration of Cas9 activity in the cell, which may help limit off-target editing events. On the downside, mRNA is less stable than DNA and is susceptible to degradation by RNAses both in the laboratory and inside the cells. One important consideration for mRNA delivery is the route of delivery of the sgRNA. As both mRNA and sgRNA are typically single-stranded RNA molecules, often the same delivery vector is appropriate for these molecules; however, the timing of delivery may be a concern[316]. Intact sgRNA must be present in the cell at the same time as functional Cas9 protein, however the delivered Cas9 mRNA molecule must first be translated into protein in situ. If the sgRNA and mRNA molecules are co-delivered, the sgRNA may begin to degrade by the time the mRNA has been translated. It was demonstrated previously that delaying the delivery of the sgRNA by up to 6h after the mRNA may enhance editing efficiency[316]. The third option is to deliver Cas9 in its ultimate protein form. This is often the most difficult delivery format due to the large size and charge of the protein, but several Cas9 protein delivery studies have been demonstrated *in vitro* and *in vivo*[317,318]. This format offers the most transient expression time, but also has the least delay in therapeutic activity, likely since transcription and translation are both circumvented[313]. Both Cas9 and sgRNA are produced *in vitro*, and then complexed into a RNP and delivered as a single unit.

Here, we report a microporation method capable of delivering nucleic acids and proteins of the CRISPR/Cas9 system into the hard-to-transfect human MSC under SF/XF culture conditions with high efficiency and low cytotoxicity, towards stable expression of therapeutic transgenes. As the CRISPR/Cas9 genome editing technology has been evolving, the scope of stem cell research and its therapeutic applications has widened at the same pace. By developing a streamline to stably edit MSC, we open a window of opportunities to design a more robust MSC cell product in terms of manufacturing and therapeutic perspectives.

III.3. Materials and Methods

III.3.1. Cell culture

All cell lines were grown in a humidified atmosphere at 37ºC with 5% CO_2 (Binder CO_2 incubator C150).

HEK293T (isolated cells from human embryonic kidneys, transformed with large T antigen) were obtained from ECACC and cultured in T-flasks with DMEM medium (GIBCO™) supplemented with 10% of heat-inactivated FBS (GIBCO™), 100IU/ml penicillin, and 100mg/ml streptomycin (PenStrep, GIBCO™). For their maintenance, cells were passaged 3 times per week by chemical detaching with Trypsin 0.05% (Corning™).

Human MSC used in this study are part of the cell bank available at the Stem Cell Engineering Research Group (SCERG), Institute for Bioengineering and Biosciences at Instituto Superior Técnico (iBB-IST). MSC were previously isolated/expanded according to protocols previously established at iBB-IST[286,287]. Originally, human tissue samples were obtained from local hospitals under collaboration agreements with iBB-IST (BM: Instituto Português de Oncologia Francisco Gentil, Lisbon; UCM: Hospital São Francisco Xavier, Lisbon, Centro Hospitalar Lisboa Ocidental, Lisbon). All human samples were obtained from healthy donors after written informed consent according to the Directive 2004/23/EC of the European Parliament and of the Council of 31 March 2004 on setting standards of quality and safety for the donation, procurement, testing, processing, preservation, storage, and distribution of human tissues and cells (Portuguese Law 22/2007, June 29), with the approval of the Ethics Committee of the respective clinical institution. Human MSC from the different tissue sources (BM and UCM) were kept cryopreserved in a liquid/vapor-phase nitrogen container. Upon thawing, cells were cultured in StemPro® Serum-free (SFM) medium and passaged two times per week, by chemical detachment with TrypLE™ Select (Gibco). Cells were cultured in StemPro® MSC SFM Xeno-free medium (GIBCO™) (XF medium). For their maintenance, cells were passaged 1-2 times per week by chemical detaching with Tryple Select (ThermoFisher™).

III.3.2. DNA purification

III.3.2.1. Genomic DNA

Total DNA from HEK293T cells and MSC was isolated with DNeasy® Blood & Tissue Kit (Qiagen), according to manufacturer's instructions. Cultured cells were lysed with proteinase K and buffer AL, containing a chaotropic salt, at 56ºC for 10min. After the addition of ethanol, the sample was loaded onto the DNeasy Mini spin column, centrifuged at 6.000xg (VWR) for

1min and washed in two steps to purify DNA. Purified DNA was eluted in 100µl of water and quantified by NanoDrop™ 2,000 (ThermoFisher ND-2,000).

III.3.2.2. Plasmid DNA

Plasmid DNA was extracted using NZYMiniprep Kit (NZYTech) according to manufacturer's instructions. Briefly, bacteria were pelleted and resuspended in buffer A1 containing RNase A. Cells were lysed by addition of buffer A2 containing NaOH and SDS. After neutralization by addition of buffer A3, cleared lysate was obtained by centrifugation at 18,000xg for 7min. Purified DNA was eluted in 30µl of elution buffer and quantified by NanoDrop™ 2,000 (ThermoFisher ND-2,000).

III.3.2.3. PCR products

PCR products were precipitated with 1/10 of the volume of sodium acetate, 3M pH 5.2, and 2.5 volumes of 100% ethanol, vortexed and stored at -20ºC overnight. All samples were centrifuged at 18,000xg (Microfuge® 18 Centrifuge, Beckman Coulter™) for 30min. The supernatant was removed, the pellets were washed with 70% ethanol (500µl), centrifuged for 10min, and the pellet was dissolved in 15µl of TE. Samples were separated by electrophoresis in 1.5% agarose gel (75V) and the bands of interest were excised from the gel with a scalpel. NZYGelpure kit (NZYTech) was used to purify DNA from agarose in agreement with the manufacturer's instructions. Briefly, each gel slice was melted in 3 volumes (v/w) of binding buffer at 55-60ºC and loaded onto a mini-column with silica-gel based membrane. DNA was eluted in 30µl of elution buffer and quantified by NanoDrop™ 2,000 (ThermoFisher ND-2,000).

III.3.3. Guide design, cloning and testing

III.3.3.1. Guide design

The 20 nucleotides followed by a NGG corresponding to the sgRNA sequence were designed with the help of online CRISPR design tools (CRISPOR - http://crispor.tefor.net/ and CRISPR Design from Zhang Lab, MIT - https://zlab.bio/guide-design-resources) considering the highest score and the lowest number of predicted off-targets in exonic regions. The genome location selected to target was the first intron of the protein phosphatase 1 regulatory subunit (*PPP1R12C)* gene known as the adeno-associated virus integration site 1 (AAVS1) locus. The

pairs of oligonucleotides corresponding to both strands of each guide sequence were synthetized by Sigma-Aldrich.

III.3.3.2. Guide cloning

The oligonucleotides were resuspended in Tris-HCl 10mM pH 8.0 to a final concentration of 1mM by incubation for 15min at room temperature with shaking. The oligonucleotides were diluted to 100µM with ultrapure water and phosphorylated and annealed in a reaction containing 10µM of both sense and antisense oligonucleotides (Table III.3.1), 1x T4 DNA Ligase Buffer (ThermoFisher), 1mM of ATP, 10U of PNK (ThermoFisher), and ultrapure water to a final volume of 10µl, incubated for 30-40min at 37ºC and for 5 min at 95ºC. Then, the reactions were cooled down on the bench (~2,5h) to the room temperature, allowing the efficient annealing of the oligonucleotide pairs.

Table III.3.1 - Guide sequences (indicated in uppercase) with BbsI linkers (indicated in lowercase) for cloning into pX459 plasmid.

Guide	Sense strand	Antisense strand	Target region
1	caccgCGAATTGGAGCCGCTTCAAC	aaacGTTGAAGCGGCTCCAATTCGc	Intronic
2	caccgCCAGCGAGTGAAGACGGCAT	aaacATGCCGTCTTCACTCGCTGGc	Intronic
3	caccgCAATCCTATTATAGCCGAAT	aaacATTCGGCTATAATAGGATTGc	Exonic
4	caccgCGGCCAGCGGTTTGGTAACG	aaacCGTTACCAAACCGCTGGCCGc	Intronic

Prior to the ligation step, all annealed oligonucleotides were diluted 1:250 with ultrapure water. The mixes for ligation step were prepared in 0.5ml microcentrifuge tubes containing in a final volume of 10µl: 50ng of vector pX459 [pSpCas9(BB)-2A-Puro (PX459, Addgene plasmid # 62988)] previously digested with BbsI restriction enzyme; 1µl of oligo duplex (1:250); 1x T4 DNA Ligase Buffer (ThermoFisher); 0.5mM of ATP; and 5U of T4 DNA Ligase (ThermoFisher). As a control, 50ng of vector pX459 were ligated without an insert in the same conditions. All tubes were incubated overnight at 8ºC. Competent *E. coli* DH5α bacteria were used to transform with 1/2 of ligation products on the next day: 5µl of each ligation were incubated on ice with 100µl of competent bacteria in 2ml microcentrifuge tubes during 15-30min; after 1min30s of heat shock at 42ºC cells were cooled down on ice for 1-2min. 900µl of LB medium

were added to tubes, and these were left to recover for 1h at 37ºC with shaking (220rpm). Bacteria were pelleted by brief centrifugation, supernatant was discarded, and the pellet resuspended in the remaining liquid and plated onto LB agar plates with 100µg/ml of ampicillin. Cells were incubated overnight at 37ºC and isolated colonies were picked in 3ml of ampicillin-containing LB medium and grown overnight at 37ºC and 220rpm. Plasmid DNA was extracted using NZYMiniprep Kit as described previously in section 3.2.2. Sanger sequencing was performed at GATC Biotech. After the sequence confirmation, the correct cells were stored in 15% glycerol at -80ºC.

III.3.4. Cleavage efficiency test of the guides in HEK293T cells

Approximately, 130,000 HEK293T cells/well were plated in a final volume of 1ml in a 24-well plate and incubated until reaching 70-80% of confluence. Cells were then transfected using Lipofectamine® 2,000 Transfection Reagent (Invitrogen™). The pX459 plasmids with cloned single guides (sgRNA plasmids) and the control empty px459 plasmid were diluted to final concentration of 200ng/µl and ~500ng were transfected per well. Firstly, 50µl of Opti-MEM™ medium (GIBCO™) were mixed, with 2µl of Lipofectamine® 2,000 (A), or with 3µl of diluted plasmid (B) and incubated for 5min at room temperature, before mixing both A and B, in dropwise manner and incubating for more 15min at room temperature. The final 100µl were added to the cells dropwise to the correspondent well containing 1ml of medium. The selection of transfected cells with puromycin started 24h after transfection by replacing the medium in each well with medium containing puromycin (2µg/ml) with exception of the control well that has only cells. This selection was performed during 48h, so after 24h the medium containing puromycin was renewed. After selection, cells were collected and pelleted by centrifugation and stored at -80ºC for further analysis. The cleavage efficiency of the guides was tested with GeneArt™ Genomic Cleavage Detection Kit (Invitrogen™), following the manufacturer's instructions. Firstly, a mix with cell lysis buffer (50µl) and protein degrader (2µl) per each cell pellet was prepared. The respective cell pellet was resuspended in 52µl in 0.2ml microcentrifuge tubes, vortexed and incubated in thermocycler first for 15min at 68ºC and then for 10min at 95ºC. Meanwhile, 1:1 (FW/RV) mix of each pair of primers (Table III.3.2) that amplify the region where Cas9 cuts was prepared.

Table III.3.2 - Primers used in Guides' Cleavage efficiency test.

Name	Sequence 5' to 3'	Type	Tm [ºC]	%GC	Reaction
Cut1.FW	TTCCCCGTTGCCAGTCTCGAT	Forward	66	57	Guide test
Cut1.RV	AGAGAGACGGCAGCGTTAGA	Reverse	63	55	
Cut2.FW	CAGGTTCCGTCTTCCTCCAC	Forward	64	60	
Cut2.RV	CAGGTTCCGTCTTCCTCCAC	Reverse	62	55	
Cut3.FW	GGCAAGGGCTCTGTCTACAG	Forward	64	60	
Cut3.RV	CAGGACCTCACACTGTCACC	Reverse	62	60	
Cut4.FW	GCTCTTTACCAGCCTGTCCA	Forward	64	55	
Cut4.RV	ACAATGAAGGAGGTGCTGGG	Reverse	62	55	

Mixes for PCR amplification of the cutting site were performed in a final volume of 25µl, adding each pair of primers (0.5µl of 10µM FW/RV mix) and 12.5µl of Amplitaq Gold® 360 Master Mix. 2µl of each cell lysate were added to 24µl of respective mix, while for the PCR control kit 1µl of control template and primers was added also to 12.5µl of Amplitaq Gold® 360 Master Mix to a final volume of 25µl. A control tube with 2µl of water instead of lysate was used for each pair of primers. The conditions used in the thermocycler are presented in Table III.3.3. PCR products were separated in a 2% agarose gel to confirm amplification.

Table III.3.3 - PCR conditions to verify the amplification of the regions of interest.

Stage	Temperature (ºC)	Time	Cycles
Initial denaturation	95	10min	1x
Denaturation	95	30sec	40x
Annealing	61	30sec	
Extension	72	30sec	
Final extension	72	7min	1x

The cleavage assay was performed GeneArt® Genomic Cleavage Detection Kit according to manufacturer's protocol. Briefly, a thermal cycler program randomly annealed the PCR

fragments with and without indels to form heterogeneous DNA duplexes. Conditions used in thermocycler were the following: a first step at 95ºC for 5min; a second step with a temperature drop between 95ºC-85ºC at -2ºC/s; and a third step with a temperature drop between 85ºC-25ºC at -0.1ºC/s. After denaturation and re-annealing, 1µl of Detection Enzyme was added to all test samples whereas 1µl of water was added to all negative control samples and incubated at 37ºC for 1h. Resulting fragments were loaded on 2% agarose gel (EtBr, 0.5xTBE) to verify the cleavage efficiency by observing the cleavage pattern. Efficiency ratios were obtained by Image J software (ratio of [cleaved/non-cleaved]).

III.3.5. MSC transfection with all-in-one CRISPR plasmids

MSC were transfected with 0.5µg of pX459 pSpCas9(BB)-2A-GFP plasmid (kindly gifted by Feng Zhang (Addgene plasmid # 48138; http://n2t.net/addgene:48138; RRID:Addgene_48138) through microporation [Microporator MP10 (Neon/Invitrogen-Life Technologies)] according to Madeira et al. (2011)[280]. 100,000 cells were resuspended in Buffer R (provided by the manufacturer) and microporated with 0.5µg of plasmid DNA in a final volume of 10µL. For microporation optimization with pX458 vector, 22 microporation conditions (Table III.3.4) were tested varying pulse voltage (mV), pulse width (ms) and pulse number. Afterwards, cells were immediately transferred to Opti-MEM™ medium (GIBCO™) and plated in 24-well-plates, previously coated with CELLstart (ThermoFisher™), in StemPro® MSC SFM XF medium (GIBCO™). 48h post-transfection, cell viability and GFP expression was determined by flow cytometry (FACSCalibur equipment, Becton Dickinson; FL1 filter (533/30nm)). Microporated cells were then selected 48h post-transfection with puromycin in concentrations ranging from 0.1 to 6ug/ml.

Table III.3.4 - Microporation optimization conditions for MSC transfection with the all-in-one CRISPR plasmids.

	Condition Name	**Voltage**	**Pulse Width (ms)**	**Pulse Number**
Opt 1	A1 (Control)	No microporation		
Opt 2	A2	1,400	20	1
Opt 3	A3	1,500	20	1
Opt 4	A4/A5	1,650	20	1
Opt 5	A6	1,100	30	1

Table III.3.4 (continued)

	Condition Name	Voltage	Pulse Width (ms)	Pulse Number
Opt 6	B1	1,200	30	1
Opt 7	B2	1,300	30	1
Opt 8	B3	1,400	30	1
Opt 9	B4	1,000	40	1
Opt 10	B5	1,100	40	1
Opt 11	B6	1,200	40	1
Opt 12	C1	1,100	20	2
Opt 13	C2	1,200	20	2
Opt 14	C3	1,300	20	2
Opt 15	C4	1,400	20	2
Opt 16	C5	850	30	2
Opt 17	C6	950	30	2
Opt 18	D1	1,050	30	2
Opt 19	D2	1,150	30	2
Opt 20	D3	1,300	10	3
Opt 21	D4	1,400	10	3

Table III.3.4 (continued)

	Condition Name	Voltage	Pulse Width (ms)	Pulse Number
Opt 22	D5	1,500	10	3
Opt 23	D6	1,600	10	3

III.3.6. MSC transfection with RNP complexes

III.3.6.1. RNP assembly

gRNA preparation was achieved by mixing 200µM Alt-R CRISPR Cas9 crRNA (Guide 2 – 5' CCAGCGAGTGAAGACGGCAT 3'; IDT Technologies) and 200µM Alt-R CRISPR-Cas9 tracrRNA (IDT technologies) in equimolar concentrations to a final duplex concentration of 44µM in nuclease free duplex buffer (IDT Technologies) and heated for 5min at 95ºC. Duplexes were cooled at room temperature and combined with 36µM Cas9 (IDT Technologies) in molar ratio of 1:1.2 for 20min at room temperature. 2.2µM of gRNA complexed to 1.8µM of Cas9 were used per electroporation reaction.

III.3.6.2. MSC transfection

MSC were transfected with RNP complexes through microporation [Microporator MP10 (Neon/Invitrogen-Life Technologies)] according to Madeira et al. (2011)[280]. 200,000 cells were resuspended in Buffer R (provided by the manufacturer) and microporated with RNP complexes adding 1.8µM Cas9 electroporation enhancer (IDT Technologies) in a final volume of 10µL. Microporation conditions tested were the following: Condition A – 1,600V, 10 ms, 3 pulses, according to Turk R and Prediger[319]; Condition B – 1,300V, 30ms, 1 pulse; and Condition C – 1,700V, 20ms and 1 pulse. Afterwards, cells were immediately transferred to Opti-MEM™ medium (GIBCO™) and plated in 24-well-plates, previously coated with CELLstart (ThermoFisher™), in StemPro® MSC SFM XF medium (GIBCO™). 48h post-transfection, cells were collected and the GeneArt™ Genomic Cleavage Detection Kit (Invitrogen™) protocol was executed as stated in the previous section III.3.4.

III.3.7. Sequencing analysis

To determine Cas9 efficiency (%), DNA was amplified from samples of RNP microporated MSC, in the genomic region of interest (sgRNA targeted region) using the GeneArt™ Genomic Cleavage Detection Kit (Invitrogen™) protocol. DNA control and test samples were Sanger sequenced to be further analysed with TIDE (available online at https://tide.deskgen.com/), according to the instructions.

III.3.8. Overexpression and production of in-house produced Cas9

Transformed *E. coli* BL21 (DE3) was cultured in SB medium with ampicillin (150µg/mL) at 37ºC with constant agitation of 250 rpm until it reaches exponential phase (OD between 0.6-0.8). Samples were taken at this point for SDS-PAGE and Western blot analysis (Time zero samples). Isopropyl-β-D-thiogalactopyranoside (IPTG) was added at a final concentration of 0.2mM for the induction of Cas9 expression and incubated at 25ºC with constant agitation of 250rpm, for 5-6h. Samples were taken at the end of this time for SDS-PAGE analysis and Western blot. Cells were centrifuged at 4ºC, 8,000rpm for 10min (Beckman J2-MC Centrifuge) and the pellet was resuspended in Binding buffer (20mM Tris-Cl, pH 8.0, 250mM NaCl, 10mM imidazole) and conserved at -80 ºC. 8% SDS gels and Western blots were made to visualize Cas9 expression. The same was applied for each step of purification.

Per purification, 6-8L of cell suspension were resuspended in Binding Buffer for sonication. The parameters used in BRANSON SONIFIER 250 were the following: Duty cycle of 50% and Output of 10, 9 cycles, 15 pulses each cycle, with intervals of 5-10min. After the sonication, the lysate was centrifuged at 4ºC, 17,600xg for 5min., and the resulting supernatant was centrifuged again in the same conditions for 1h. The supernatant was applied in an immobilized metal affinity chromatography (IMAC) column in which the His tag will bind to the nickel from the column HisTrap™ FF 5mL (GE Healthcare). IMAC was performed in AKTA start (GE Healthcare) after washing the system with dH_2O and equilibrated with Binding Buffer. After multiple sample applications and washouts to avoid column clogging, the protein was eluted with Elution Buffer B (20mM Tris-Cl, pH 8.0, 250mM NaCl, 250mM imidazole) in a linear gradient from 0-100% of Elution Buffer.

Table III.3.5 - Parameters of IMAC program for Cas9 purification.

Column volume	5.027mL
Pressure limit	0.30MPa
Flow rate	5mL/min.
Equilibrium with	1CV
Sample volume	20mL
Wash column with	6CV
Elution type	Gradient
Start %B	0.0%
Set target concentration	100% B
Gradient volume	20mL
Equilibrium with	5CV

Protein purity along the purification was analysed with 8% SDS-PAGE gels. The fractions containing higher levels of the target protein were concentrated with Amicon Ultra Centrifugal (Milipore), with a molecular weight cut-off of 10,000Da, at 4000rpm, 4ºC (Epp. Centrifuge) with a final volume of 3mL. Imidazole was removed by dialysis with Dialysis Buffer (20mM HEPES-KOH, pH 7.5, 150mM KCl, 10% (v/v) glycerol, 1mM dithiothreitol (DTT), 1mM EDTA). The Cas9 fusion protein produced has a TEV sequence for MBP-6His cleavage and in order to do both steps together, the purified Cas9 is inserted in a Slide-A-Lyzer™ G2 Dialysis Cassette (ThermoFisher Scientific), 10K MWCO, 3mL with 1.5µM of TEV and left with smooth agitation at 4ºC. Dialysis was extended for 2-3 days for higher cleavage efficiency. After dialysis, Cas9 was further purified by IEX using HiTrap™ 5mL SF HP (GE Healthcare) that was first washed with dH_2O and IEX Buffer A (20mM HEPES-KOH, pH 7.5, 100mM KCl), before protein application. Elution is performed with a linear gradient of IEX Buffer B (20mM HEPES-KOH, pH 7.5, 1M KCl) form 0-50%. Fractions containing Cas9 were pooled and concentrated with Amicon Ultra Centrifugal (Milipore), with a molecular weight cut-off of 50,000Da, at 4,000rpm and 4ºC until a final volume of 500µL.

The last step for Cas9 purification was Size Exclusion Chromatography (SEC). The column Superdex 200™ 10/300 was previously washed with dH_2O and SEC Buffer (20mM HEPES-

KOH, pH 7.5, 500mM KCl, 1mM DTT) and the parameters used in the program are represented in Table III.3.7.

Table III.3.6 - Parameters of IEX program for Cas9 purification.

Column volume	5.027mL
Pressure limit	0.30MPa
Flow rate	5mL/min.
Equilibrium with	2CV
Sample volume	2mL
Wash column with	5CV
Elution type	Gradient
Target %B concentration (0-100%)	50%
Volume 0-100 (CV)	12
Start %B concentration	0%
Equilibrium with	5CV

After SEC, concentration of the enriched fractions was made with Milipore 50,000 MWCO Amicon and Cas9 quantification was made with spectrophotometer at 280nm and an extinction coefficient of 120,450$M^{-1}cm^{-1}$, according to C. Anders and M. Jinek [320]. The resultant Purified Cas9-mCherry protein was divided into 300µL aliquots for further flash freeze with liquid nitrogen and storage at -80ºC, until is use.

Table III.3.7 - Parameters of SEC program for Cas9 purification.

Colum volume	24mL (30cm x 100mm)
Pressure limit	1.5MPa
Flow rate	0.5mL/min
Equilibrium with	1CV
Sample volume	500mL
Wash column with	5CV

III.4. Results

III.4.1. Cas9 guide construction and test

We chose the adeno-associated virus integration site 1 (AAVS1) genomic safe harbour, within the first intron of the protein phosphatase 1 regulatory subunit 12C (*PPP1R12C*) gene, to precisely insert the gene coding for azurin into the genome of MSC using the CRISPR/Cas9 technology. The AAVS1 locus resides in the first intron of the *PPP1R12C* gene and has been used as a safe harbor for transgene integration [321–325].

Three sgRNAs (sgRNA - 1, 2 and 4; G1, G2 and G4, respectively) were designed bioinformatically, targeting different regions of the first intron of *PPP1R12C* gene, considering the overall score and the number of exonic off-targets. As a control, a sgRNA targeting an exonic region of the *PPP1R12C* gene was also designed (gRNA 3; G3).

The selected sgRNAs were synthetized and cloned into an all-in-one Cas9-expressing vector pX459 (pSpCas9(BB)-2A-Puro) and tested in target cells for their cleavage efficiency using the GeneArt™ Genomic Cleavage Detection Kit (Invitrogen™).

III.4.1.1. Bioinformatic design and cleavage efficiency test

The selected gRNAs obtained by CRISPOR[326], and CRISPR Design from Zhang Lab, MIT, are presented in Table III.4.1, with the score and number of exonic off-targets presented in Table III.4.2, and the respective localization of each indicated exonic off-target in Table III.4.3.

Table III.4.1 - AAVS1 targeting Cas9 sgRNAs designed in this work with respective target and PAM sequences.

	G1 (Reverse strand)	**G2 (Forward strand)**	**G3 (Forward strand)**	**G4 (Forward strand)**
Sequence[1] 5'-3'	CGAATTGGAGCC GCTTCAAC	CCAGCGAGTGA AGACGGCAT	CAATCCTATTATA GCCGAAT	CGGCCAGCGGTT TGGTAACG
PAM[2]	TGG	GGG	GGG	AGG

[1] A – Adenine, T – Thymine, C – Cytosine, G - Guanine; [2] proto-spacer adjacent motif.

Table III.4.2 - Number of exonic off-targets sites and score value for four sgRNA tested in this work, obtained from two different bioinformatics tools (CRISPOR, and CRISPR Design).

	Tools	**G1**	**G2**	**G3**	**G4**
Number of Exonic off-target sites	CRISPOR	0	1	0	1
	CRISPR Design	2	7	0	3
Score	CRISPOR	94	92	96	97
	CRISPR Design	94	89	92	95

Table III.4.3 - Exonic off-target genes for the four sgRNA tested in this work, obtained from two different bioinformatics tools (CRISPOR, and CRISPR Design) verified in NCBI (https://www.ncbi.nlm.nih.gov/).

	Tools	**G1**	**G2**	**G3**	**G4**
Exonic off-target sites	CRISPOR	-	*CASP16*	-	*FBLN7*
	CRISPR Design	*SBK1*	*EDEM3*	-	*LOC148696*
		SMAD6	*MYBPC2*		*ECI1*
			LRRC4C		*FBLN7*
			DIO2-AS1		
			CLN3		
			DBNDD1		
			LMO4		

The selected sgRNAs were cloned into the pX459 vector with a codon-optimized *SpCas9* sequence for expression in human cells and the sgRNA under the control of the U6 promoter. The correct insertion of sgRNA sequences into the pX459 vector was verified by Sanger sequencing.

Firstly, HEK 293T cells were transfected to detect the cleavage efficiency of each selected sgRNA prior to the design of the homology arms for the introduction of the *azurin* cassette in MSC cells. HEK293T are widely used as a model for the development of genome-editing approaches as well as the study of DNA repair mechanisms in general[327], due to their ease of expansion and resilience to the DNA damage arising from editing techniques. Cells were transfected with all-in-one CRISPR pX459 plasmids with Lipofectamine 2,000 upon which, successfully transfected cells were selected with the addition of puromycin to the cell culture media at a concentration of 2µg/ml [328] with 48h of exposition. Then, target loci of harvested genomic DNA from pX459 transfected cells, was amplified by PCR (Figure III.4.1-A) and cleavage percentage was evaluated by the GeneArt™ Genomic Cleavage Detection protocol.

Through this method, we can directly correlate on-target insertion/deletion (indel) formation to the cleavage pattern of an endonuclease. As we can observe in Figure III.4.1-B, the sum of the intensity of the bands correspondent to cleaved fragments in cells transfected with G2 is about three-fold higher than the intensity of the bands correspondent to uncleaved fragments (uncleaved fragments 372bp; cleaved fragments 197 bp + 175bp), hence it was selected as a targeting sequence to carry out our CRISPR strategy.

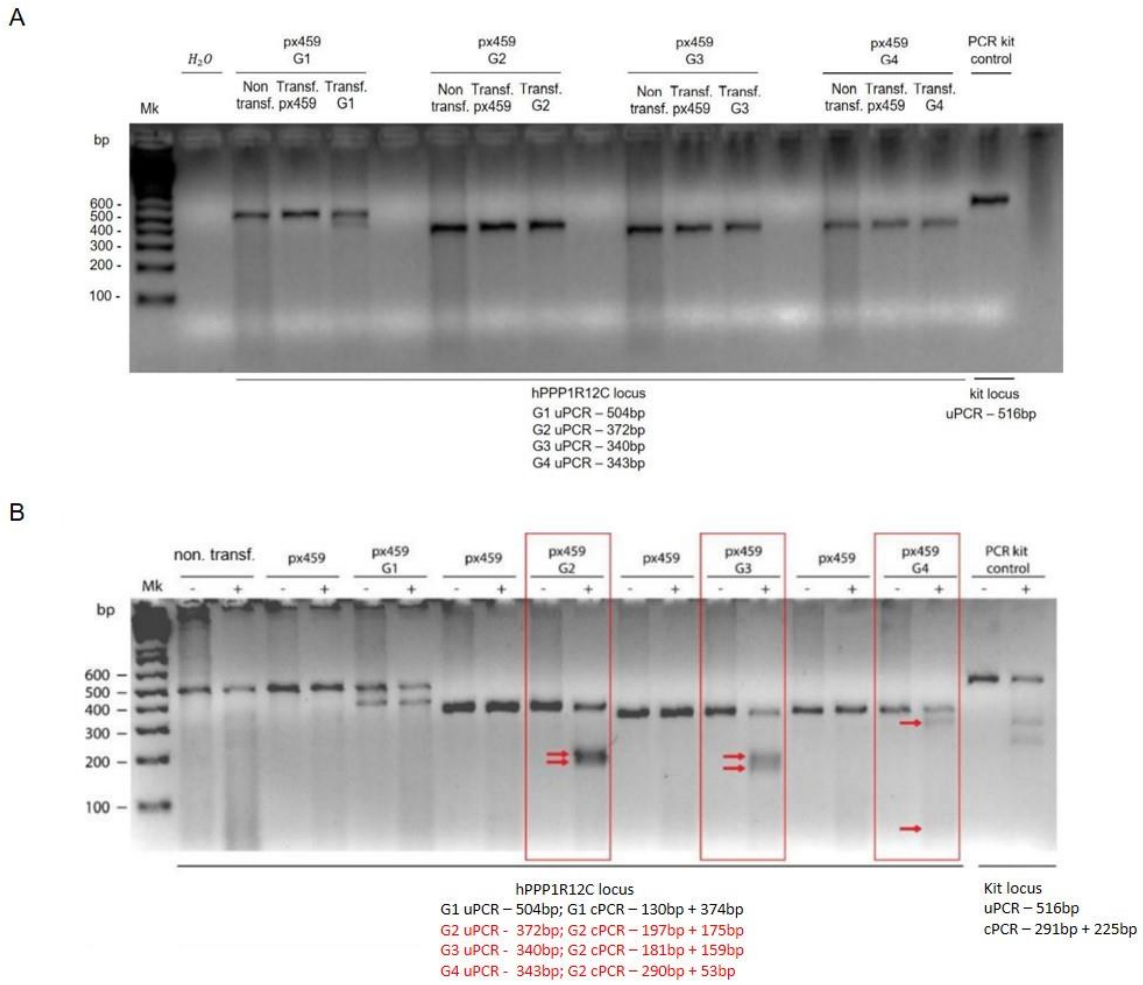

Figure III.4.1 - (A) Agarose gel electrophoresis of PCR products amplified with primers correspondent to each sgRNA. Guide 1: Cut1.Fw, Cut1.RV; Guide 2: Cut2.Fw, Cut2.RV; Guide 3: Cut3.Fw, Cut3.RV; Guide 4: Cut4.Fw, Cut4.RV (see Table 2 on section Material and Methods section). G1 - Guide 1; G2 - Guide 2; G3 - Guide 3; G4 - Guide 4; uPCR – uncleaved PCR; Mk – 1Kb Plus DNA Ladder (Invitrogen™). (B) Agarose gel electrophoresis of PCR products digested with Detection enzyme following the GeneArt™ Genomic Cleavage Detection Kit (Invitrogen™) to determine cleavage efficiency of the tested guides. Efficiency ratios were obtained by Image J software (ratio of [cleaved/noncleaved]): Guide 1: non-cutter; Guide 2: 51%; Guide 3: 55%; Guide 4: impossible to observe the second band. G1 - Guide 1; G2 - Guide 2; G3 - Guide 3; G4 - Guide 4; uPCR – uncleaved PCR; cPCR – cleaved PCR; Mk – 1Kb Plus DNA Ladder (Invitrogen™).

Figure III.4.2 highlights the relative localization of the selected G2 from our study, in parallel to other stem cell engineering studies which designed sgRNAs also targeting the AAVS1 locus[329–333].

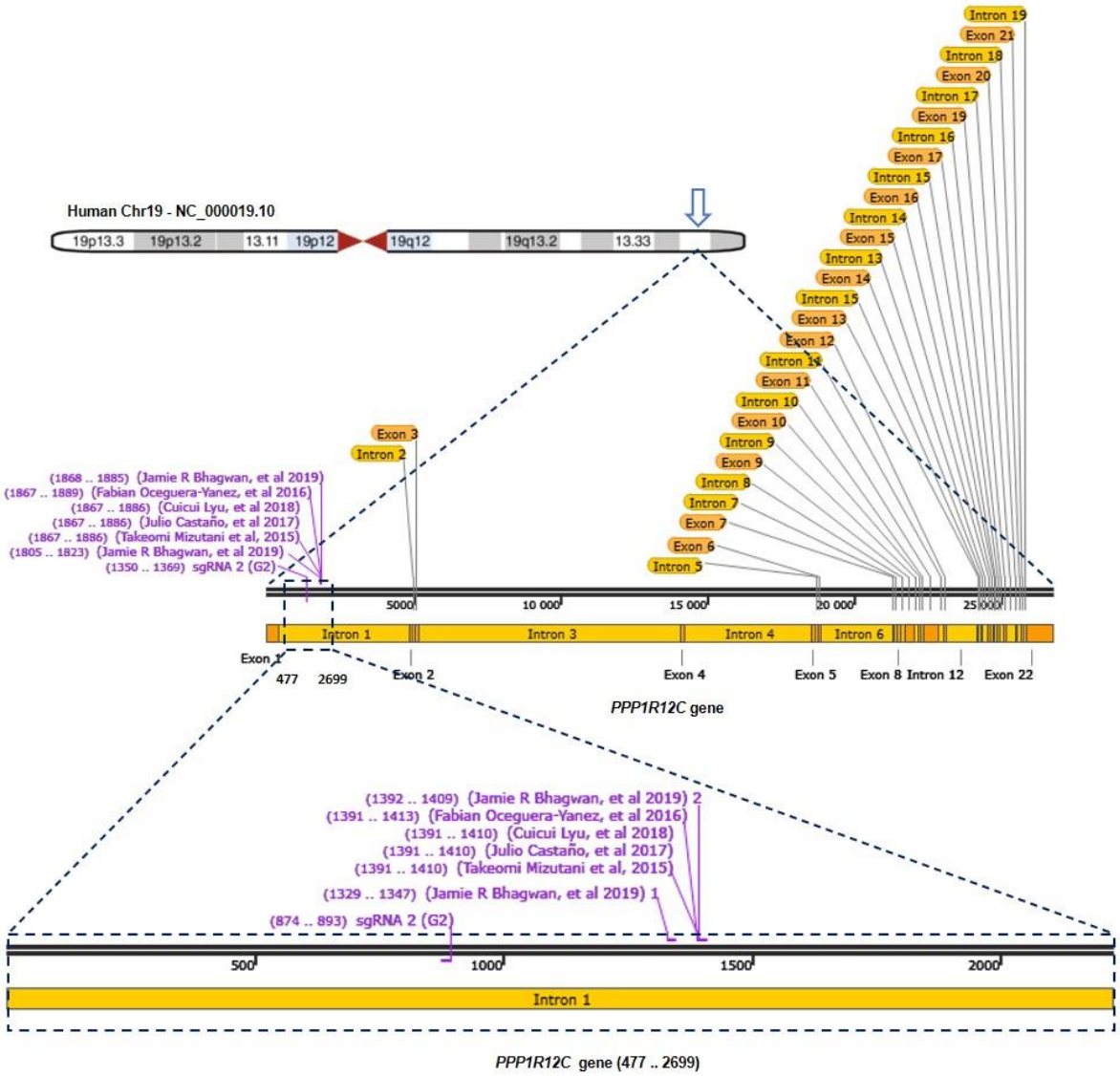

Figure III.4.2 - Schematic overview of the chromosomic location of the *AAVS1* locus genomic safe harbor in the PPP1R12C gene from chromosome 19. Selected targeting sgRNA (G2) relative localization to designed sgRNAs from other studies in induced pluripotent stem cells (iPSCs) (represented in purple).

III.4.1.2. Optimization of the microporation conditions for the all-in-one Cas9 plasmid in mesenchymal stromal cells

As for HEK 293T cells, MSC were microporated with the all-in-one CRISPR pX459 plasmid harbouring the selected G2 and puromycin selection was initiated 48h after with concentrations ranging from 0.5 to 6µg/ml (Figure III.4.3). We observed that cells were extremely sensitive to low puromycin concentrations (0.5µg/mL), a dosage that insufficiently selects microporated cells.

A

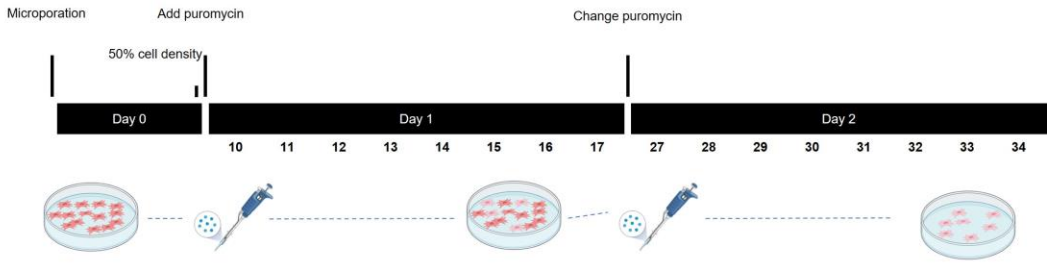

Concentration (µg/ml)	Day 0	Day 1							Day 2		
	hours (h)										
	0	10	11	12	13	14	15	16	17	27	28	34
0	100	100	100	100	100	100	100	100	100	100	100	100
0.5	100	100	100	100	100	100	100	100	60	20	0	0
1	100	70	70	70	70	70	70	60	50	0	0	0
2	100	60	50	50	50	50	50	50	40	0	0	0
2.5	100	50	40	40	40	40	40	20	0	0	0	0
3	100	40	40	40	40	40	40	20	0	0	0	0
4	100	40	40	30	30	30	30	20	0	0	0	0
6	100	20	20	20	20	10	10	10	0	0	0	0

B

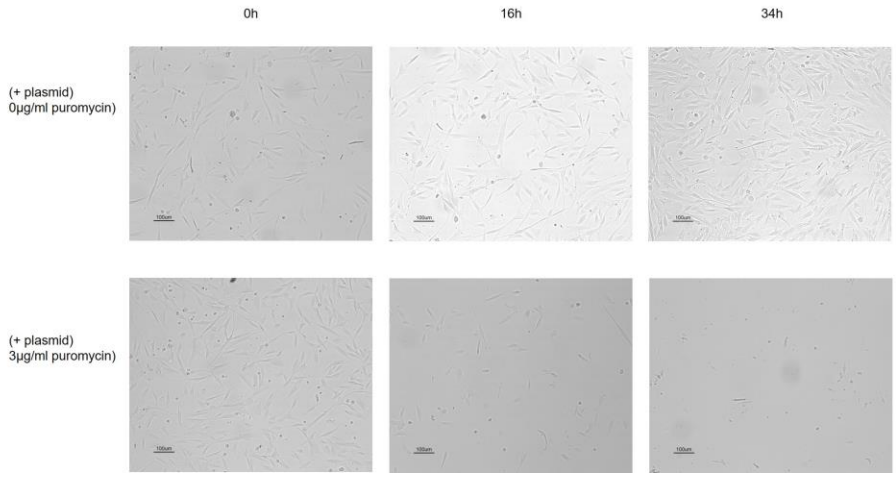

Figure III.4.3 - *(*A) MSC sensitivity to puromycin after electroporation with 0.5µg of pX459 all-in-one CRISPR plasmid through microporation. Initial density at day 0 of 4,000 cells/cm^2. At day 1 cells reached a confluency of 40-50% and selection was initiated with puromycin concentrations ranging from 0.1 to 6ug/ml. Cell confluency was observed and quantified from 10 to 34h post-transfection. Depicted cell confluency percentages are referred to 50% initial cell density. Green: cells presented a confluence equal to or greater than the initial; Yellow: some cells died; Orange: mostly cells died; Brown: almost all cells died; Red: all cells died. (B) Representative images of transient puromycin selection 16 and 34h post-transfection with pX459 all-in-one CRISPR plasmid. 0µg/ml puromycin condition was electroporated under same conditions as experimental treatment.

As these results demonstrated that MSC are highly susceptible to puromycin, we hypothesized that the cause for that could be an insufficient number of cells transfected with the plasmid

carrying the gene conferring resistance for the antibiotic. Thus, we attempted to optimize the parameters for microporation with an alternative all-in-one plasmid were the puromycin resistance marker is replaced by the enhanced green fluorescence protein (*eGFP*) gene as a reporter (pX458 - Addgene # 48138). The presence of a reporter gene allows for the identification by flow cytometry of the best microporation protocol leading to high transfection efficiencies while maintaining cell viability. For that, 22 different parameter conditions were tested with voltages ranging from 850 to 1,600 V, and pulse widths ranging from 10 to 30ms in 1 to 3 pulses, following the manufacturers standard optimization protocol.

We identified conditions B2 (1,300V, 30ms, 1 pulse), B1 (1,200V, 30ms, 1 pulse) and A3 (1,500V, 20ms, 1 pulse) as the conditions allowing for the highest GFP^+ percentage (41, 26.6 and 20%, respectively; measured by flow cytometry) and cell viability, being more efficient than our first employed protocol B4 (1,000V, 40ms, 1 pulse) with only 10% GFP^+ cells (Table III.4.4).

Table III.4.4 - Parameters tested for MSC DNA microporation by Neon transfection System, transfection efficiency by GFP expression evaluation and cell density post-transfection. Cell density is represented in a range from 1 to 4 and a green scale, being 4 and darkest green representative of the highest cell density. Previous adopted microporation parameters are highlighted in blue and the selected new protocols are highlighted in grey.

	Condition name	Cell Density	GFP^+ (%)	Pulse		
				Voltage (V)	Width (ms)	Number
Opt 1	A1 (control)	4	-	No microporation		
Opt 2	A2	4	10	1,400	20	1
Opt 3	A3	2	20	1,500	20	1
Opt 4	A4/ A5	2	10	1,650	20	1
Opt 5	A6	3	11	1,100	30	1
Opt 6	B1	3	9	1,200	30	1
Opt 7	B2	3	26.6	1,300	30	1
Opt 8	B3	3	41	1,400	30	1
Opt 9	B4	3	10	1,000	40	1
Opt 10	B5	2	17	1,100	40	1
Opt 11	B6	2	8.6	1,200	40	1
Opt 12	C1	1	Not enough cells	1,100	20	2
Opt 13	C2	1	Not enough cells	1,200	20	2
Opt 14	C3	1	Not enough cells	1,300	20	2
Opt 15	C4	1	Not enough cells	1,400	20	2
Opt 16	C5	1	Not enough cells	850	30	2

Table III.4.4 (continued)

	Condition name	Cell Density	GFP⁺ (%)	Pulse		
				Voltage (V)	Width (ms)	Number
Opt 17	C6	1	Not enough cells	950	30	2
Opt 18	D1	1	Not enough cells	1,050	30	2
Opt 19	D2	1	Not enough cells	1,150	30	2
Opt 20	D3	1	Not enough cells	1,300	10	3
Opt 21	D4	1	Not enough cells	1,400	10	3
Opt 22	D5	1	Not enough cells	1,500	10	3
Opt 23	D6	1	Not enough cells	1,600	10	3

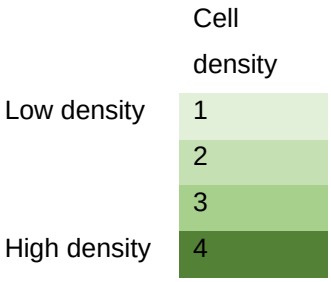

Applying these optimized conditions, MSC were microporated with pX459 harbouring the custom designed G2, following puromycin selection at concentrations lower than 0.5µg/mL (0.1, 0.25 and 0.5µg/mL). After one week of a modest increase in confluence cells ceased to grow, never reaching confluence levels necessary to realize the cleavage efficiency test. Several attempts were made to improve cell survival upon selection with puromycin, however cell sensitivity required extended culture time, ultimately leading to a not observable cleavage after the GeneArt™ Genomic Cleavage Detection protocol.

III.4.2. Direct delivery of the CRISPR/Cas9 system into MSC as a RNP complex

As demonstrated in the previous section, employing a plasmid based CRISPR strategy and microporation protocol pose an excessive sensitization to MSC under the SF/XF growing conditions used, leading to an unsuccessful protocol. As such we redesigned our strategy towards a RNP-mediated CRISPR genome editing, which is stated to be more effective, avoiding the problems associated with using plasmids[334–336]. An electroporation protocol allows the RNP to enter the cell nucleus quickly, so it can immediately start its endonuclease activity towards the genome[337]. The RNP complex is active immediately because it is already

developed by complexing a recombinant Cas9 enzyme and the chemically synthesized G2, whereas when delivered through a plasmid formulation, Cas9 is available in the cell for an extended period of time increasing the chances of off-target effects[335]. Also, the natural cellular mechanisms of protein and RNA turnover ensure that the RNP will be digested by the cells, also decreasing the chances of off-targets being introduced. With this system the antibiotic selection step is also unnecessary, avoiding increased cytotoxicity.

III.4.3. Optimization of microporation conditions for the RNP complex and validation in different MSC donors

To deliver the RNP complex to MSC with high efficiency, three different Neon Transfection System protocol conditions (Conditions A, B and C) were tested (Table III.4.5)[319].

Table III.4.5 - Parameters for MSC RNP transfection using the Neon transfection System (Invitrogen™).

	Condition Name	Voltage	Pulse Width (ms)	Pulse Number
Opt 1	A	1,600	10	3
Opt 2	B	1,300	30	1
Opt 3	C	1,700	20	1

We evaluated Cas9 cleavage efficiency (%) as an indirect measure for microporation efficiency by using the GeneArt Genomic Cleavage Detection protocol, as previously. By using the ImageJ software, the efficiency was estimated determining the intensity of the parental uncleaved band (372bp) and the cleaved bands (175bp and 197bp), that appear to be merged into one single band due to their sizes being very similar.

Though microporation conditions A and C, proved to be effective in transfecting MSC with a full protein RNP complex, we acknowledged condition C as the most efficient allowing for 51% of Cas9 cleavage efficiency, while maintaining a sustainable cell viability (over 70% cell viability, data not shown) (Table III.4.6; Figure III.4.4-A), thus being selected for further experiments. We then proceeded to validate our optimized protocol in 4 different donors of BM- and UCM-MSC reaching an average Cas9 efficiency of 45% and 35%, respectively (Figure III.4.4-B).

Table III.4.6 - Parameters for MSC RNP transfection with correspondent Cas9 cutting efficiencies (%) and cell confluencies (%) 48h post-transfection. Microporation condition A – 1,600V, 10ms, 3 pulses; microporation condition B – 1,300V, 30ms, 1 pulse and microporation condition C – 1,700V, 20ms, 1 pulse. Opt – Optimization.

	Condition name	Cell Density (48h post-transfection)	Cutting Efficiency (%)	Pulse		
				Voltage (V)	Width (ms)	Number
Opt 1	A	3	26	1,600	10	3
Opt 2	B	3	-	1,300	30	1
Opt 3	C	2	51	1,700	20	1

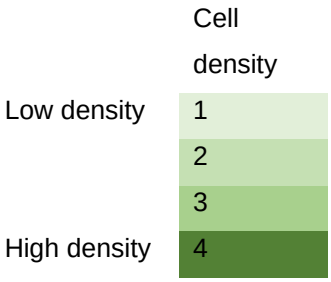

Using the TIDE (Tracking of Indels by Decomposition) software analysis (https://tide.deskgen.com/) as a complementary tool, we evaluated Cas9 efficiency across several MSC donors from different tissue sources. As seen in Figure III.4.4-C;D, transfection of the RNP into BM-MSC and UCM-MSC resulted in an efficiency of 52% and 30%, respectively using TIDE analysis. Moreover, a tendency for inserting a thymine (T) was observed as an indel mutation event after NHEJ (Figure III.4.4-C; VIII Appendix section - Figure VII.2.1).

Both analysis techniques indicated similar Cas9 cutting efficiency percentages, being the highest with BM-derived MSC. Moreover, results were congruent between the 4 MSC donors tested, being the highest with BM donor 1 and UCM donor 1, which might be partially associated with differences in the microporation efficiency.

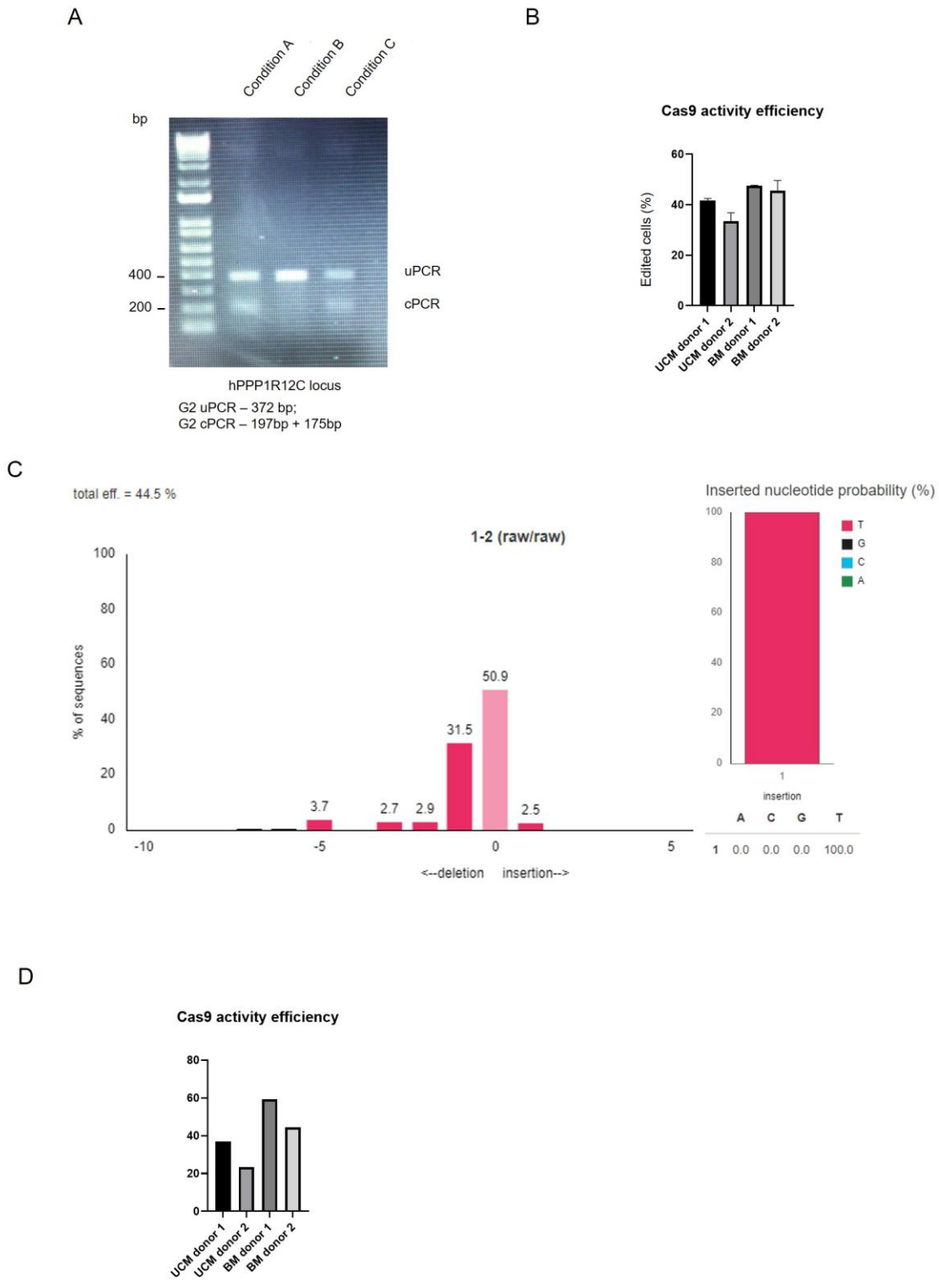

Figure III.4.4 - *(*A) Representative agarose gel electrophoresis containing MSC cleavage assay results for RNP transfection optimization. Well 1: 1Kb Plus DNA Ladder (Invitrogen™); Well 2: cells microporated with condition A; Well 3: cells microporated with condition B; Well 4: cells microporated with condition C. For cells microporated with conditions A and C two bands, corresponding to the uncut parental band - 372bp and to the cleaved fragments– 175bp and 197b, are observed. Condition B led to a non-observable cleavage event, only being possible to detect the parental band, ultimately being discarded from further experiments; uPCR – uncut PCR; cPCR – cut PCR. B) Cas9 cutting efficiencies (%) calculated for two donors of BM (BM) and UCM (UCM)-MSC (n = 2).

Figure III.4.4 - (continued) Efficiency was estimated using Image J software by determining the intensity of the parental uncut band (372bp) and the cleaved bands (175bp and 197bp) (ratio of [cut/noncut]), that appear to be merged into one single band due to their proximity in size. C) Representative output graph obtained for BM donor 1 with TIDE software depicting the calculated percentage of sequences with no genomic alterations and indels, the Cas9 cleavage efficiency (total efficiency, %) and inserted nucleotide (%) probability. A – adenine; T- thymine; G – guanine; C- cytosine. D) TIDE software analysis results illustrating total Cas9 efficiency (%) calculated for two donors of BM- and UCM-MSC.

III.4.5. *In-house* production and purification of Cas9

In the course of this thesis, an optimized protocol for the production and purification of Cas9 in our laboratory was obtained. An *E.coli* BL21(DE3) strain was employed for the over-expression of Cas9 protein, by transformation of this strain through electroporation with the pMJ923 plasmid.

In-house Cas9 complexed with G2 proved to be effective in targeting and generating a DSB in the target locus with very similar efficiencies to the commercially obtained Cas9 in both BM- and UCM-MSC (Figure III.4.5).

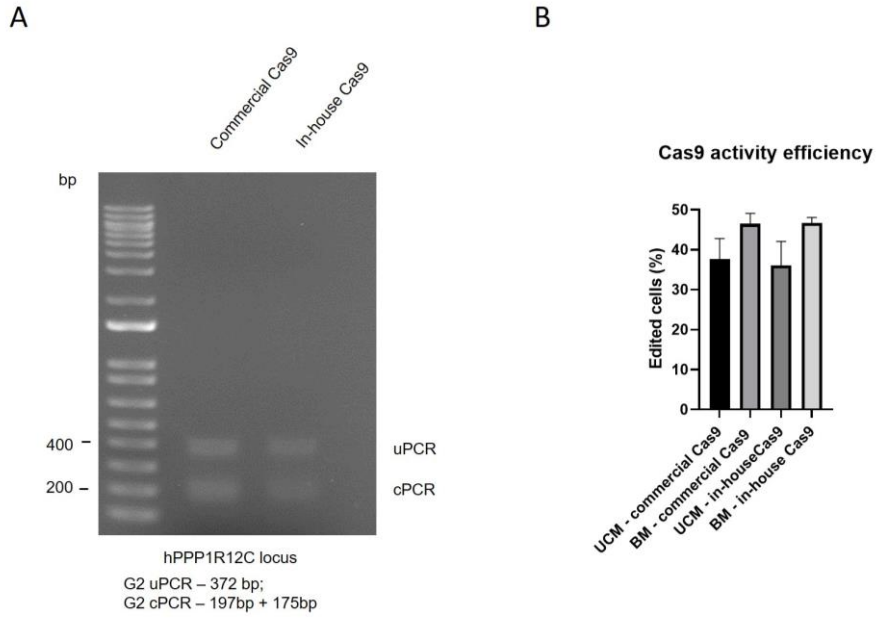

Figure III.4.5 - *(*A) Representative agarose gel electrophoresis of PCR products digested with Detection enzyme following the GeneArt™ Genomic Cleavage Detection Kit (Invitrogen™) to determine cleavage efficiency after MSC RNP transfection. Well 1: 1Kb Plus DNA Ladder (Invitrogen™); Well 2: two bands, corresponding to the uncut parental band - 372bp and to the cleaved fragments– 175bp and 197b obtained with a commercially acquired Cas9 protein; Well 2: two bands, corresponding to the uncut parental band - 372bp and to the cleaved fragments– 175bp and 197b obtained with an in-house produced and purified Cas9 protein. uPCR – uncut PCR; cPCR – cut PCR. B) Commercially acquired versus in-house produced- Cas9 cutting efficiencies (%) calculated for two donors of BM (BM) and UCM (UCM)-MSC (n = 2).

Figure III.4.5 - (continued) Efficiency was estimated using Image J software (ratio of [cut/noncut]) by determining the intensity of the parental uncut band (372bp) and the cleaved bands (175bp and 197bp), which appear to be merged into one single band due to their proximity in size.

III.5. Discussion

The CRISPR/Cas9 system has emerged as a very promising tool for multiple arears, including gene and cell therapies by enabling precise genome editing with technological plasticity and simplicity. Compared to previous developed TALENs and the ZFNs, CRISPR/Cas9 technology is faster, more economically efficient, and user-friendly[338]. The use of such methodology could comprise, for example, harvesting cells from an unhealthy individual, editing the genome of injured cells, and reintroducing the edited cells back into the body via autologous transplantation[339]. It could also represent a pathway to develop therapeutic cell lines with improved or new functions that could be applied as autologous off-the-shelf products in the most varied biological contexts. In addition to its use in gene and cell therapies, the CRISPR/Cas9 system may be used for disease modelling, drug screening studies, and specific diseases diagnosis[340]. In fact, several studies have been carried out on the use of the CRISPR/Cas9 system for the treatment of different diseases, both in animal and human models[340–342]. Studies in the context of cardiovascular diseases[343], haematological diseases[344,345], immunological diseases[346], inborn error diseases[347], cancer[348], muscular dystrophy[349], neurological disorders[350], and others[351,352] have shown great progress in the application of CRISPR/Cas9 system in preclinical disease models and *in vitro* culture of human cells.

The therapeutic effect of MSC is based on their integration into an injured target tissue and strong paracrine effect, with no generation of an immune response[353]. Though, apart from their therapeutic potential and the progress in the clinical employment, their poor engraftment and low survival rate in the target organ receiving the transplant are among the main obstacles to be surpassed so that the cellular therapy with MSC brings significant benefits[354]. The variety of works using genome-editing in human cells with CRISPR/Cas9 suggest how this technology can be applied to MSC, for instance, altering the self-renewal potential and commitment of these cells with certain lineage[355,356], which would contribute to increase their engraftment and regenerative potential, or by introducing therapeutic transgenes stably into their genome, transforming these cells into tailored active drug delivery systems.

In this work, we developed an entirely non-viral protocol to deliver nucleic acids and proteins of the CRISPR/Cas9 system into the hard-to-transfect MSC, under SF/XF culture conditions with high efficiency while preserving cell viability, towards stable expression of therapeutic transgenes. We designed three sgRNA sequences, resorting to the CRISPOR and CRISPR

Design bioinformatics tools, targeting the *AAVS1* genomic safe harbour, within the first intron of the *PPP1R12C* gene. These designing tools allow to visualize, optimize, and annotate multiple sgRNA sequences at a time, get on- and off-target scores to compare and optimize for higher activity and lower off-target effects, allowing the users to select the best putative sgRNAs for a given locus. The *AAVS1* locus is known as a safe harbor to introduce transgenes, because its disruption does not have any described adverse effect on the cell, and robust transcription can be used to maintain the expression of an exogenously inserted gene[321–325]. A microporation protocol was optimized in MSC, with a fluorescently labelled all-in-one CRISPR plasmid, (pX458 (2A-*EGFP*, Addgene plasmid # 48138)), aiming to determine the best transfection conditions, measured by GFP expression and cell recovery, to further test the cleavage efficiency of G2 into MSC with primary pX459. However, we were unable to apply a puromycin selection protocol, as previously optimized in HEK293T cells, since the cells were extremely sensitive to low puromycin concentrations (0.1µg/mL), a dosage that insufficiently ablates non-targeted cells. CRISPR plasmids expressing Cas enzymes and sgRNAs have been used for several years, but these plasmids have several limitations, including cytotoxicity and unpredictability of expression. Some cell types are more sensitive to plasmid transfection due to direct cytotoxicity of the plasmid transfection itself, adding to the toxicity arising from the transfection reagents[357]. Moreover, when a plasmid is transfected into a cell, the plasmid must first be transported into the nucleus for RNA transcription of both sgRNA and Cas-encoding mRNA. The resulting mRNA must be exported from the nucleus for translation of the Cas protein. The Cas protein binds the sgRNA and the complex is transported into the nucleus for access to the genome, where editing occurs, in a process that may require around 24h[341]. Moreover, plasmids support prolonged expression, allowing for the Cas enzyme and sgRNA to remain active in the cells for extended periods of time, leading to increased probabilities of off-targeting effects and prolonged toxicity[311]. The longer the Cas protein and sgRNA persist, the greater the chance that genomic DNA in non-targeted sites will be targeted[311]. Therefore, even the lowest concentrations of puromycin may act synergistically with the basal toxicity that arises from the transfection protocol itself. In addition, due to the waiting time before the CRISPR genome editing can begin, an uncertainty of when the enzyme is expressed may be problematic for experiments that require other manipulations such the delivery of a donor template in HDR studies. For these reasons, we redesigned our strategy towards the microporation of a RNP-mediated CRISPR genome editing system, which is stated to be more effective, avoiding many pitfalls associated with pDNA or mRNA delivery[311]. RNP delivery enables the fastest genome editing by reason of eliminating the need for intracellular transcription and translation. Meanwhile, the transient genome editing not only permits high editing efficiency, but also reduces off-target effects and insertional mutagenesis[311]. However, considering the unique characteristics of RNP complexes, *i.e.* the

complex molecular composition and negative charge property, transfection efficiency is lower when compared with nucleic acids[191]. It is worth noting that enhancing sgRNA stability by chemical modification could further improve the genome editing efficiency of microporation-mediated RNP delivery[358]. As such, we optimized a microporation protocol to deliver an RNP complex carrying the selected G2, and directly determined the ability and specificity of Cas9 to create double-strand breaks in the DNA at the correct target with this formulation, without the need for antibiotic selection.

The pioneering technique for determining the efficiency of engineered nucleases is Sanger DNA sequencing, which can identify and locate induced mutations, being well suited for testing the functionality of newly engineered Cas9 and sgRNAs. To get fast results using Sanger sequencing, a software was introduced in 2014[359] to identify DNA mismatches more readily. The tracking of indels by decomposition (TIDE) technique is a three-step method whereby the region targeted by the engineered nuclease is PCR amplified from DNA isolated from transfected cells. Controls are provided by non-transfected cells. Amplicons of 500-1,500bp generated around the target site are then subjected to conventional Sanger DNA sequencing followed by analysis using the TIDE Web-based tool[359]. The presence of aberrant base signals along the sequence is revealed in a graph allowing for the identification of the modifications induced by Cas9 and designed sgRNA. The precise localization of break sites is also facilitated by the software, which additionally estimates the statistical significance of each indel. TIDE also reduces costs as sequence chromatograms can be generated from mixed cell populations, thus circumventing the need for isolation of multiple clones. A great advantage of TIDE resides in the fact that this approach can provide ‘absolute’ estimates of cutting efficiency and information about the pattern of the indels[205]. Such information is crucial to analyse the results generated with engineered nucleases. However, for TIDE to be reliable, the PCR products and the sequence reads must be of high quality. If lower quality reads are produced, errors can readily result from arbitrary modifications to the decomposition parameters introduced to lower the detection threshold of possible indels[359]. Other techniques currently employed to assess the efficiency of engineered nucleases are denaturation-based techniques, like the mismatch-sensitive endonucleases, such as the T7 and Surveyor nucleases, that can recognize and cut double-stranded DNA fragments with a mismatch. These techniques are easy, fast, cheap, and relatively sensitive. Target sequences are PCR amplified from genomic DNA of edited and control cells, and then amplicons are denatured, reannealed, and treated with the endonuclease. If a mutation has been introduced on one strand by the NHEJ repair process, DNA amplicons will be cleaved on both strands and detectable in an agarose gel. Sanger sequencing can then be used to further confirm that the mutation has been created at the correct cleavage site. However, false positives can result

from a confusion between mutations and naturally occurring polymorphisms. Moreover, these techniques cannot detect homozygous variations of genomic sequences[360]. According to such evaluation techniques, our protocol originated between 40-50% on-target Cas9 cleavage efficiency, a higher percentage when comparing to other published studies (between 12-25% in induced pluripotent stem cells (iPSC), analysed with Surveyor assays)[361,362]. Interestingly, TIDE analysis revealed a preferential indel repair pattern by inserting a T in the DSB site. This finding is in agreement with previous studies showing that indel profiles are non-random, being an intrinsic feature of the target site, with some targets showing one highly-preferred sequence alteration and others displaying a wide range of infrequent, yet reproducible, indels[363].

MSC gene editing has been described using both viral and nonviral (physical and chemical) genetic constructions delivery[201]. Although viral systems give the higher molecular delivery efficiency, they still hold safety concerns[132] that are critical when considering clinical applications. This view tended us to select an entirely non-viral engineering and delivery procedure. Microporation provides the most predictable and reproducible transfection rates and cell survival[308], with a low consumables cost, with the optimal electrical pulse conditions easily optimizable to the convenience of our study, allowing for the delivery of DNA molecules and full-size proteins, such as Cas9. Moreover, our protocol was optimized towards complete SF/XF culture conditions, according to good manufacturing practices (GMP)[31]. As such, our protocol is fully designed to be readily incorporable in a clinically focused streamline to safely and predictably engineer MSC, towards the establishment of cell lines with elevated therapeutic potentialities for the most varied clinical applications, either by silencing genes, enhance gene expression, or add a new function by employing a HDR strategy towards the insertion of exogenous transgenes in a selected locus in the genome.

IV. ESTABLISHMENT OF STABLE CAS9-ENGINEERED HUMAN BONE MARROW-DERIVED MESENCHYMAL STROMAL CELLS EXPRESSING AZURIN IN SERUM/XENO-FREE CONDITIONS

Manuscript in preparation

IV.1. Summary

Mesenchymal stromal cells (MSC) are a promising source for engineered cell-based therapies for which genetic engineering could enhance therapeutic efficacy. With this view, CRISPR/Cas9 is an easily designing tool, which has already been successful in stem cell engineering studies in diverse biological contexts. Here, we report a non-viral, GMP compliant, CRISPR/Cas9-mediated homology directed repair system for the insertion of exogenous DNA up to 3 kilobases into a genomic safe harbor of bone marrow (BM)-MSC. Co-microporation of a Cas9 RNP complex with a single-stranded DNA donor cassette, resulted in efficient targeted integration of the anti-tumoral *azurin* gene sequence into a genomic safe harbor of MSC genome. With this system, we aim to obtain a stable tumor-targeted cell system for the specific delivery of anti-tumoral proteins directly into the tumor microenvironment, taking advantage of the innate tumor tropism features of MSC. Given the relative simplicity and plasticity of this approach, we predict that it should be a valuable resource for basic and translational research in diverse contexts of MSC biology, by providing more robust or novel cellular functions to these promising therapeutic agents.

IV.2. Background

MSC are a promising source for cell-based therapies. However, despite promising preclinical therapeutic benefits shown with naïve[364] and engineered MSC versions[37], there are still some questions raised regarding MSC-based therapies, mainly due to the lack of knowledge of some of their mechanisms of action and contradictions in clinical outcomes[364,365]. Hence, genetic engineering of these cells could strengthen their innate therapeutic potential with known mechanisms of action and help filling the current gap in the knowledge of their biological properties, while establishing a MSC safety profile. In clinical settings, while transient gene expression or random gene integration could be adequate considering short term presence of MSC *in vivo*, it might not be highly effective due to the engineering methods' drawbacks, mainly concerning safety[132]. Moreover, there are some data regarding the adverse impact of viral transduction on the stem cell properties of engineered cell lines[366]. Thus, in this scenario, precise genome editing, as provided by the CRISPR/Cas9 technology, is an important tool by allowing stable and predictable functional manipulations by gene disruption, DNA sequence editing, and transgene integration at a desired locus within the genome[367]. An area in which engineered MSC can be used therapeutically is in anti-cancer cell-based therapies. These cells present inherent tumor-directed migratory properties[40], which allows them to serve as vehicles for effective delivery of therapies to the tumor microenvironment and possibly metastases as well. Indeed, MSC have been genetically engineered to express

anti-proliferative, pro-apoptotic, and anti-angiogenic agents that specifically target different cancer models, with promising preclinical[40,106,108,241,243] and preliminary clinical results[247].

Numerous studies have identified “safe harbor” *loci* in the human genome, which can be specifically targeted without causing significant detrimental effects on host genes while maintaining a high level of gene expression [329]. The AAVS1 is an exemplary locus within the first intron of the *PPP1R12C* gene of a “safe harbor” locus for targeted integration that has been previously explored in CRISPR/Cas9 studies in stem cell research[329–333]. The AAVS1 locus is not susceptible to gene silencing effects and provides improved targeting efficiency and ubiquitous transgene expression without alteration of the cell viability or phenotype[323]. Therefore, this site can represent a potential engineering target for the introduction of anti-tumor therapeutic transgenes into MSC to circumvent the problem with the duality of their influence on the tumor microenvironment[368], by developing more predictable functions and converting them into unequivocal therapeutic tools.

In Chapter II, we demonstrated that after cell microporation with a recombinant plasmid, the conditioned medium of MSC transiently expressing a human optimized version of the anti-tumoral protein azurin (*hazu*-MSC), induced a decrease in cancer cell viability, migration and invasion, and an increase in cell death in breast (MCF-7) and lung (A549) cancer cell lines[369]. These results provided the foundation for the present study in which we optimized BM- derived MSC non-viral transfection by microporation under SF/XF cell culture conditions to a apply a CRISPR/Cas9- mediated HDR system for exogenous DNA insertion to up to 3 kilobases to stably introduce the simultaneously expression of azurin and GFP proteins by a 2A self-cleaving peptide coding sequence into MSC genome, aiming at a more robust determination of the therapeutic potential of *hazu*-MSC in anti-cancer therapies along with a clearer interpretation of MSC interaction within the different cellular elements of the tumor microenvironment. Our methodology was also used to integrate a single GFP reporter expression cassette, allowing for a deeper MSC characterization within diverse biological contexts. As such, the following protocol should be a valuable resource for basic and translational research in the fields of MSC biology and tumor therapy.

IV.3. Materials and Methods

IV.3.1. Cell culture

Cells were cultured as previously described in Chapter III (section III.3.1).

IV.3.2. DNA purification

IV.3.2.1. Genomic DNA

Genomic DNA was purified as previously described in Chapter III (section III.3.2.1.).

IV.3.2.2. Plasmid DNA

Plasmid DNA was purified as previously described in Chapter III (section III.3.2.2.).

IV.3.2.3. PCR products

PCR products were purified as previously described in Chapter III (section III.3.2.3.).

IV.3.3. HDR donor templates production

Full length fluorescently labelled CMV-*azurin* HDR cassette (HDR donor 1) was obtained by gene synthesis (pUC57_*template*, Nzytech). We then generated linear and shorter versions using HDR donor 1 as template, by PCR amplification with the primers presented in Table IV.3.1, obtaining HDR donors 2 and 3.

HDR donors 4 and 5 were obtained by PCR amplification of pVAX-*hazu* and pVAX-*GFP* (previously employed in Chapter III) as templates, a consecutive double digested with NotI and NcoI and subcloning into pUC57 between the synthetized homology arms. The obtained plasmid HDR cassettes were then used as templates for PCR amplification generating HDR donors 4 and 5.

All PCR fragments were obtained amplified with 2.5U of NZYLong DNA Polymerase (NZYTech) in a final volume of 25µl containing: 1x Reaction Buffer (NZYTech), 0.4mM of dNTPs, 0.4µM of each primer, forward and reverse, and 15ng of correspondent DNA. PCR products were further purified as described in section III.3.2.3. The conditions used in the thermocycler are presented in Table IV.3.2.

Table IV.3.1 - Primers used to obtain HDR donor templates. Restriction enzyme linkers (indicated in lowercase).

Name	Sequence 5'to 3'	Type	Tm[ºC]	%GC	Reaction
FullDonor.FW	TAGCCACTCTGTGCTGACCA CTCTGCCCCA	Forward	68	60	Production of donor 2
FullDonor.RV	TCTCCCTCCCAGGATCCTCT CTGGCTCCAT	Reverse	68	60	
5HAshorter.FW	ATCTGCCTGGCCCTGGCCAT TGTCACTTTGCGCT	Forward	70	58	Production of donor 3
3HAshorter.RV	CAGAGCCACATTAACCGGCC CTGGGAATATAAG	Reverse	68	51	
5HA-CMVpVAX-az.FW	GCTGCACCACGTGATGTCCT CTGAGCGGATCATATATGGA GTTCCGCGTTACATAACTTA	Forward	72	48	Production of CMV-AZ fragment
AzpVAXNotI.Rv	gcggccgcCTTCAAGGTCAGGG TTCCTTTCATA	Reverse	69	57	
5HA-CMVpVAX-az.FW	GCTGCACCACGTGATGTCCT CTGAGCGGATCATATATGGA GTTCCGCGTTACATAACTTA	Forward	72	48	Production of CMV-GFP fragment
pVAXGFPNotI.Rv	gcggccgcTACTTGTACAGCTC GTCCATGCCGAGAGT	Reverse	72	60	
FullDonor.FW	TAGCCACTCTGTGCTGACCA CTCTGCCCCA	Forward	72	48	Production of donors 4 and 5
FullDonor.RV	TCTCCCTCCCAGGATCCTCT CTGGCTCCAT	Reverse	72	60	

Table IV.3.2 - PCR conditions used to obtain HDR donor templates.

Stage	Temperature (ºC)	Time	Cycles
Initial denaturation	95	2min	1x
Denaturation	95	30sec	35x
Annealing	65	45sec	
Extension	68	2.5min	
Final extension	68	5min	1x

IV.3.4. Single-stranded DNA production and purification

Single-stranded DNA (ssDNA) fragments were obtained via the Guide-it™ Long ssDNA Production System v2 kit (Takara). The dsDNA fragments were generated by PCR amplification using one of the primers (forward or reverse) with a 5' phosphorylation in order to generate the antisense or sense ssDNA, respectively (Table IV.3.1). The PCR amplification conditions were applied as stated on the previous section IV.3.3. For each reaction, 40ng of obtained dsDNA fragments were combined with PrimeSTAR Max Premix (2X) in a total volume of 100µl with 2µL of each primer (40µM). The conditions used in the thermocycler are presented in Table IV.3.3.

Table IV.3.3 - PCR conditions to obtain dsDNA fragments with 5' phosphorylated ends.

Temperature (ºC)	Time	Cycles
98	10sec	40x
65	5sec	
72	15sec	

Subsequently, dsDNA substrates were column purified using NucleoSpin Gel and PCR Clean-Up kit (Macherey-Nagel™). 15µg of dsDNA were subjected to two independent and consecutive strandase reactions (Strandase A and Strandase B reactions) following the thermocycler conditions presented in Table IV.3.4 and Table IV.3.5, respectively.

Table IV.3.4 - Thermocycler conditions for the Strandase A reaction.

Temperature (ºC)	Time	Cycles
37	15min	1x
80	5min	1x

Table IV.3.5 - Thermocycler conditions for the Strandase B reaction.

Temperature (ºC)	Time	Cycles
37	15min	1x
80	5min	1x

After strandase reaction, the ssDNA products were column-purified to remove free nucleotides using the NucleoSpin Gel and PCR Clean-Up kit together with Buffer NTC (a binding buffer specific for ssDNA) (Macherey-Nagel™).

IV.3.5. MSC transfection with HDR-RNP complexes

IV.3.5.1. RNP assembly

RNP assembly was performed as in See Chapter III (section III.3.6.1.).

IV.3.5.2. MSC transfection

MSC were transfected with RNP complexes through microporation [Microporator MP10 (Neon/Invitrogen-Life Technologies)] adapted from Madeira et al. (2011)[280]. Cells were washed with PBS and detached from plastic surface using TripLE Select. 200,000 cells were resuspended in Buffer R (provided by the manufacturer) and microporated with RNP complexes adding 1.8µM Cas9 electroporation enhancer (IDT technologies) and 200 to 500 ng of HDR DNA templates as plasmid or in linear (dsDNA or ssDNA) formulation in a final volume of 10µL. Microporation conditions were 1,700V, 20ms and 1 pulse, as established in Chapter III. Afterwards, cells were immediately transferred to Opti-MEM™ medium (GIBCO™) and plated in 24-well-plates, previously coated with CELLstart™, in StemPro® MSC SFM XF medium (GIBCO™). Cells were passaged and collected for flow cytometry (FACSCalibur

equipment, Becton Dickinson; FL1 filter (533/30nm) at 7- and 14-days post-microporation, acquiring a minimum of 50,000 total events.

IV.3.5.3. DNA genotyping

Genomic DNA was extracted from edited and control MSC as described previously (section III.3.2.1.) and the on-target genomic region was amplified by PCR with primers positioned inside and outside (Table IV.3.6) of the homology arms contained in the HDR repair template sequence to confirm the insertion at the correct location. PCR amplification was accomplished using NZYLong DNA Polymerase (NZYTech), following thermocycler conditions present in Table IV.3.7. PCR products were separated by electrophoresis in agarose gel, purified as described previously (Section III.3.2.3.) and 25–100ng of pooled PCR products were sequenced by Sanger sequencing.

Table IV.3.6 - Primers for HDR donor template integration into MSC genome.

Name	Sequence 5'to 3'	Type	Tm[ºC]	%GC	Reaction
Cut2.FW	CAGGTTCCGTCTTCCTCCAC	Forward	64	60	Verify insertion inside the homology arm of the donor template
Cut2.RV	CAGGTTCCGTCTTCCTCCAC	Reverse	62	55	
verifyHDRout2.FW	ATTCCCCTTCGACCACCCCA	Forward	60	60	Verify insertion outside the homology arm of the donor template
verifyHDRout3.RV	CACCAGGATCAGTGAAACG CACCAG	Reverse	62	56	

Table IV.3.7 - PCR conditions used to verify HDR donor template integration into the target locus in MSC genome.

Stage	Temperature (ºC)	Time	Cycles
Initial denaturation	95	2min	1x
Denaturation	95	30sec	35x
Annealing	60-62	45sec	
Extension	68	2.5min	
Final extension	68	5min	1x

IV.4. Results

IV.4.1 HDR template design and construction

Our overall goal was to insert the full-length *azurin* gene into the *AAVS1* genomic safe harbour of MSC, to acquire stable transgene expression. We generated a fluorescently labelled CMV-*azurin* HDR cassette through gene synthesis (Figure IV.4.1-A) cloned into a vector plasmid (HDR donor 1). Knock-in efficiencies can vary widely, depending in part on the species or cell type, the genomic region being targeted, and the size of the insertion[370]. A constraint that could lower substantially the knock-in efficiency of our strategy is the considerable size of the insertion cassette (~3kb). Therefore, having HDR donor 1 as DNA template, we additionally generated linear and shorter versions, by designing a donor template with shorter homology arms (HA) (HDR donor 3), and insertion cassettes holding each transgene (*azurin* or *eGFP*) separately (HDR donor 4 and 5, respectively). We obtained these different donor cassette formulations by a combination of PCR and restriction enzyme genetic engineering (Figure IV.4.1-B;C). It has been demonstrated that there is a clear relationship between homology arm length and knock-in efficiency, with DNA templates including homology arms between 350–700bp in length providing the best performance[371], and therefore our knock-in cassettes ranged in HA size between 410–660bp.

The donor template used for HDR may be double-stranded DNA (dsDNA, linear or plasmid) or single-stranded DNA (ssDNA), and recent findings have suggested that the repair mechanism varies depending on the type of template used[372]. Therefore, we systematically examined the use of ssDNA donors for CRISPR-based knock-in and compared the performance of ssDNA versions of donors 2, 3, 4 and 5 to the other forms of templates. Moreover, ssDNA has been associated with lower toxicity and a reduced probability of off-target integration relative to dsDNA[372]. We generated long (~3kb) ssDNA donor templates employing the optimized Guide-it Long ssDNA Production System v2 (Takara), which provides the production of ssDNA up to 5kb in length from a double-stranded PCR product via selective digestion of either the sense or antisense strand (Figure IV.4.1-D;E).

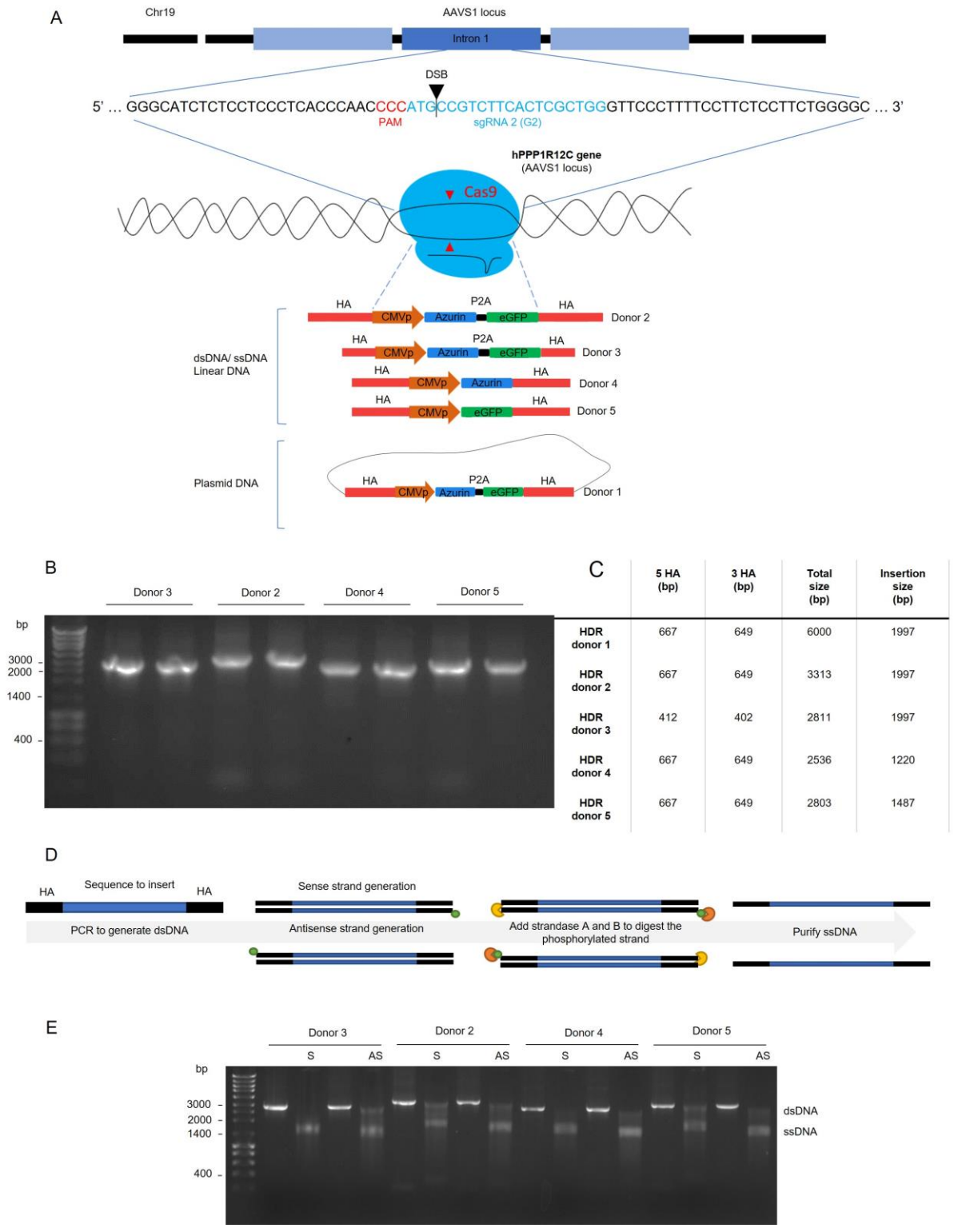

Figure IV.4.1 - (A) Schematic illustration of CRISPR/Cas9-mediated gene knock-in of the full-length azurin gene into the *AAVS1* genomic safe harbour of MSC within the PPP1R12C gene. PAM site is marked in red and sgRNA targeting sequence is marked in blue. Template design formulation schematics are depicted as HDR donor 1, 2, 3, 4 and 5. A – adenine; T- thymine; G – guanine; C- cytosine. DSB – double strand break. B) Agarose gel electrophoresis of PCR amplified HDR donors 2, 3, 4 and 5 (see table 1 on the Materials and Methods section). Well 1 - NZYDNA Ladder III (Nzytech^{TM}). C) Predicted molecular weight of HDR donor templates (bp), along with their corresponding homology arm (HA) size (bp) and insertion template size (bp) (Total size minus HA size). D) Single-stranded DNA (ssDNA) preparation using exonucleases.

Figure IV.4.1 - (continued) Both of exonuclease A and exonuclease B recognize double-stranded DNA's (dsDNA) specific ends and digest one of the strands along the chain. This consecutive digestion produces ssDNA molecules of either sense or antisense nature, that are further purified. E) Gel image showing the dsDNA starting material (wells 2; 4; 6; 8; 10; 12; 14 and 16) and sense (SS) or antisense (AS) ssDNA products for several HDR templates generated using the Guide-it Long ssDNA Production System (wells 3; 5; 7; 9; 11; 13; 15 and 17). The dsDNA and ssDNA were analyzed via agarose gel electrophoresis. ssDNA products run at a smaller molecular weight than corresponding dsDNA substrates. Well 1 - NZYDNA Ladder III (Nzytech^{TM}).

IV.4.2. Simultaneous delivery of RNP complexes and repair templates to MSC by microporation and identification of most efficient HDR CRISPR knock-in conditions

Co-microporation of Cas9 complexed with the sgRNA (G2) in tandem with all HDR templates from the previous section was performed as previously optimized in Chapter IV. Cas9-sgRNA RNPs were prepared by co-incubating recombinant Cas9 protein with *in vitro*-transcribed G2 designed to target the *AAVS1* locus, and the RNPs were then combined with corresponding HDR templates consisting of either plasmid DNA, dsDNA or ssDNA (sense or antisense). The various RNP-HDR template combinations and associated negative-controls without Cas9 were then electroporated into BM-MSC using optimized conditions. Forty-eight hours later imaging was performed on each cell population and sporadic GFP-positive cells could be observed. Moreover, we assessed the relative toxicity of each RNP-HDR template combination. While co-microporation of plasmid, dsDNA or ssDNA HDR templates and RNPs yielded noticeable toxicity relative to the application of HDR templates alone or microporation controls (cells microporated without RNP-HDR), the level of toxicity associated with plasmid and dsDNA was much greater than what was observed for ssDNA (data not shown).

Being CMV a constitutive promoter designed in all our HDR templates, we could predict transient transgene expression to a certain extent. For this reason, the observation of cells microporated solely with HDR templates were used as a visual measurement of HDR probability, by observing a decrease in fluorescence through time, contrasting with a more stable GFP expression in our RNP-HDR microporated cells.

Following culture, the edited and control cell populations were analysed using flow cytometry 7- and 14- days post-microporation (Table IV.4.1) (Figure IV.4.2). In these analyses, the percentage of fluorescent-positive cells could be considered equivalent to the percentage of successful knock-in's. It was observed that the use of sense or antisense ssDNA templates yielded different knock-in efficiencies, being the highest with the antisense strands (8.87 and 11.6%, respectively). Moreover, a difference in efficiency was attributed to the insertion sequence size, being the highest with the smaller template (donor 5). Knock-in efficiency was supported by the absent fluorescence in the correspondent cells microporated with HDR templates alone (Table IV.4.2).

Table IV.4.1 - Knock-in efficiency estimation by GFP expression percentage, accessed by flow cytometry in two consecutive culture passages at day 7 and 14 post-microporation. MSC were microporated with a ribonucleoprotein (RNP) and 500 or 200ng of HDR donor template with different molecular formulations (linear double-stranded DNA (dsDNA) and linear single-stranded DNA (ssDNA) with sense or anti-sense chains) (n = 2). SS -sense strand; AS- antisense strand; dsDNA – double-stranded DNA; ssDNA – single-stranded DNA; WT – wild type MSC.

DNA amount (ng)	**WT**	**Donor 5 dsDNA**	**Donor 3 dsDNA**	**Donor 2 dsDNA**	**DNA amount (ng)/ DNA formulation**	**Donor 5 ssDNA**	**Donor 3 ssDNA**	**Donor 2 ssDNA**
	% GFP$^+$ cells					% GFP$^+$ cells		
	Passage 1 – 7 days post-microporation					Passage 1 – 7 days post-microporation		
500	0.031	8.94	1.60	0.17	500/ SS	8.67	0.97	1.72
					500/ AS	10.8	2.84	2.84
					200/ SS	8.24	0.49	0.59
					200/ AS	9.60	2.09	1.05
DNA amount (ng)	Passage 2 – 14 days post-microporation				**DNA amount (ng)/ DNA formulation**	Passage 2 – 14 days post-microporation		
500	0.031	9.72	1.39	0.13	500/ SS	8.87	1.07	1.52
					500/ AS	11.6	2.50	2.54
					200/ SS	8.52	0.54	0.51
					200/ AS	9.75	2.07	1.06

Table IV.4.2 - GFP expression percentage quantification accessed by flow cytometry at day 7 post-microporation. MSC were microporated with 500ng of HDR donor template with different molecular formulations (linear double-stranded DNA (dsDNA) and linear single-stranded DNA (ssDNA) with the antisense chains) without a ribonucleoprotein (RNP) (n = 2).

DNA amount (ng)	WT	Donor 5 dsDNA	Donor 3 dsDNA	Donor 2 dsDNA	Donor 5 ssDNA	Donor 3 ssDNA	Donor 2 ssDNA
	% GFP^+ cells						
500	0.031	0.038	0.037	0.048	0.13	0.085	0.069

HDR template designated in a plasmid formulation (donor1) was discarded due to severe toxicity. Although it was possible to observe GFP-positive cells, in very low percentage (<2%), this was the most aggressive protocol disabling cells from recovery.

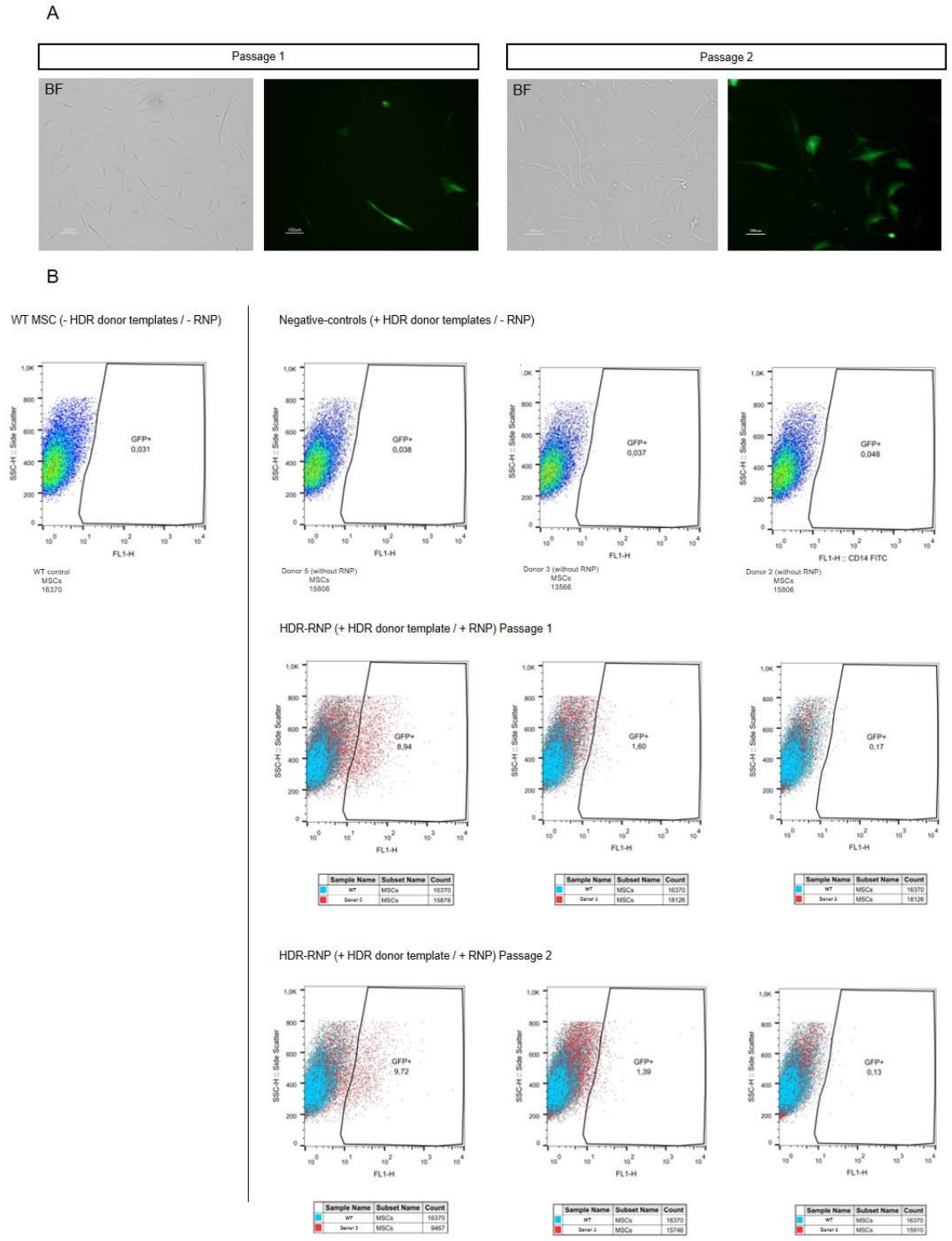

Figure IV.4.2 - (A) Representative imagens of bright-field and fluorescence of RNP-HDR donor 5 (double-stranded (dsDNA) DNA formulation) microporated cells after 2 rounds of culture passage (7 and 14 days post-microporation). B) Representative quantitative analysis of the percentage (%) of the fluorescent cell population obtained by flow cytometry of RNP-HDR donor 5, 3 and 2 (dsDNA formulation), and the respective negative controls (cells microporated with HDR donor templates and without Cas9 protein) and WT control cells (cells microporated without HDR donor templates or Cas9 protein).

Overall, we can verify that HDR efficiency is the highest with antisense ssDNA donor templates, achieving a maximum of 11.6% HDR knock-in efficiency. Biologically, there is no rule regarding the preferential use of sense or antisense ssDNA for HDR templates longer than 200nt, but in the case of shorter single-stranded oligodeoxynucleotide (ssODN) templates, template polarity has been found to influence efficiency[373]. *GFP* expression was stable over two consecutive passages, up until cells entered senescence. This premature entry into cell senescence was also observed in control cells microporated with HDR templates alone (data not shown) that could be linked to foreign DNA toxicity or to the microporation protocol applied. These results imply a fine-tuning of the presented protocol in the near future.

IV.4.3. DNA genotyping

Genomic DNA was extracted from all conditions 14 days post-microporation and amplified by PCR with primers annealing inside the homology arms of the donor template (Cut2_FW + Cut2_RV) and a combination of inside the donor template at the CMV promotor region and outside the donor template (VerifyHDRCMV_FW + VerifyHDRout3_RV) (Figure IV.4.3-A). Agarose gel analysis of the resulting PCR products indicated that the majority of cell lines took the knock-ins and that comparable editing outcomes were obtained using (ds) dsDNA, sense (ss) or antisense (as) ssDNA templates. The obtained PCR products are accordingly with the predicted PCR fragment sizes (depicted in Table IV.4.3) for the intra-cassette amplification reaction (Cut2_FW + Cut2_RV – Figure IV.4.3-B). PCR amplicons were further sequenced confirming correct target DNA insertion (VIII Appendix section – Figures VII.3). Importantly, after 14 days of post-microporation, exogenously delivered HDR template DNA should be degraded by the cell machinery. As such, potential PCR amplification from non-integrated donor template fragments is highly unlikely[374]. For the intra- and extra-cassette genotyping PCR (VerifyHDRCMV_FW + VerifyHDRout3_RV – Figure IV.4.3-C) not all samples presented the predicted amplification fragments (correctly targeted samples are depicted in green). Nevertheless, is important to note that the presented PCR results were performed with mixed cell populations, with maximum knock-in percentages of 11%. As such, further enrichment of the knock-in cell population is necessary for more accurate conclusions.

Table IV.4.3 - Predicted molecular weight of amplified PCR products using the primers described in Table IV.3.6 from Materials and Methods (Section IV.3).

HDR donor template	Cut2_FW + Cut2_RV	VerifyHDRCMV_FW + VerifyHDRout3_RV
	bp	
HDR donor 2	2,240	2,634
HDR donor 3	2,240	2,634
HDR donor 4	1,463	2,057
HDR donor 5	1,730	2,324
No insert (WT)	372	0

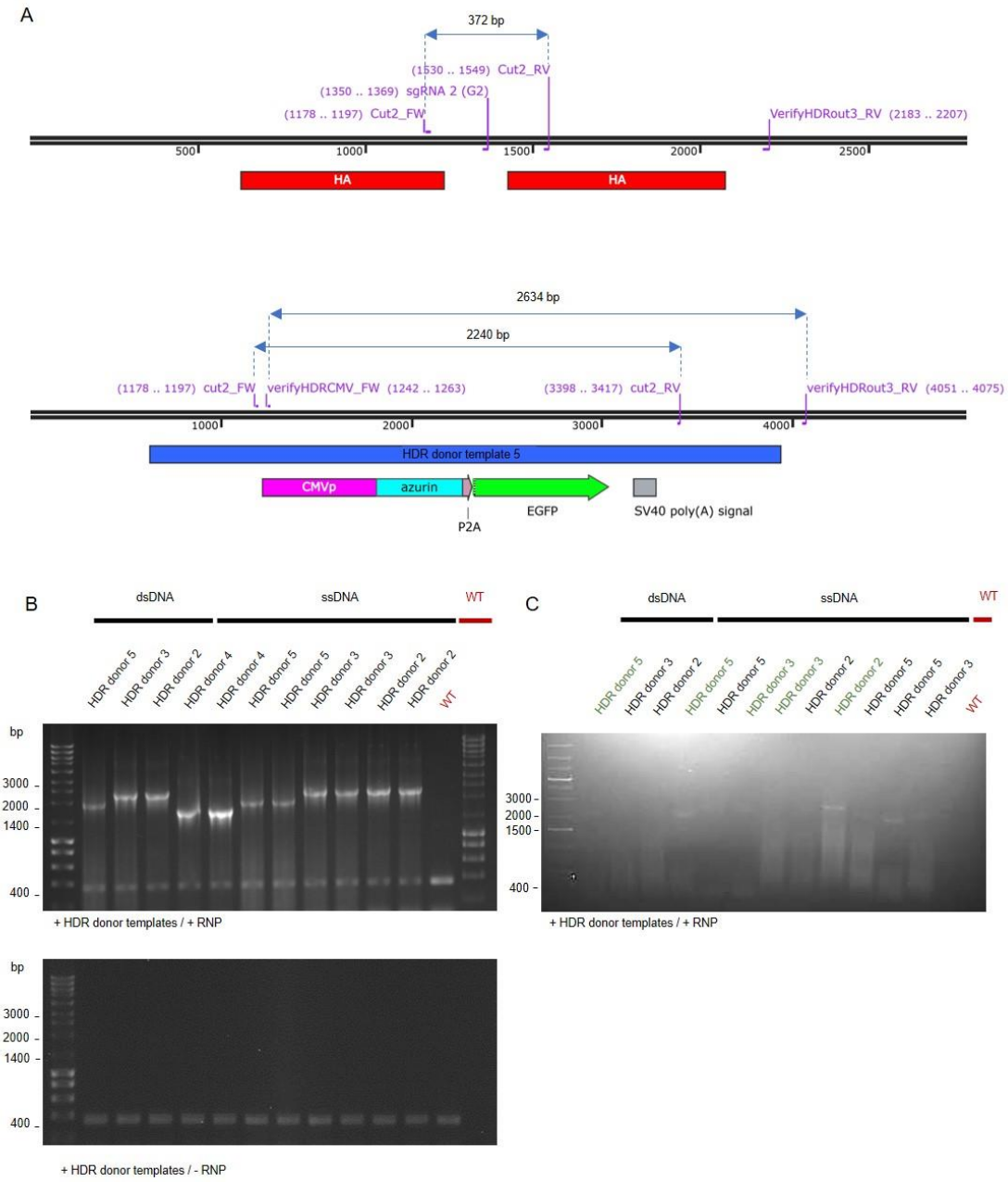

Figure IV.4.3 - *(*A) Schematic illustration and predicted molecular weight of the fragments after PCR amplification with genotyping primers (see Table 6 from the Materials and Methods section) to verify knock-in success at the target locus. B) Agarose gel electrophoresis of HDR knock-in intra-cassette targeting PCR (Cut2_FW + Cut2_RV) screen using genomic DNA isolated from HDR-RNP transfected cells (top gel) and respective negative controls (microporated cells with HDR donor templates and without Cas9 protein) (bottom gel). Well 1 - NZYDNA Ladder III (Nzytech™). C) Agarose gel electrophoresis of HDR knock-in combining intra- and extra-cassette targeting PCR (VerifyHDRCMV_FW + VerifyHDRout3_RV) screen using genomic DNA isolated from HDR-RNP transfected cells. Correctly targeted knock-in samples are depicted in green. Well 1 - NZYDNA Ladder III (Nzytech™).

IV.5. Discussion

MSC have a broad application prospect in the field of regenerative medicine[48,240]. Adding to their already clinically demonstrated capabilities[39,121], their potential use in personalized medicinal applications may be augmented by genetic engineering[36], including the insertion of genes towards expression of constitutive cell fluorescent labels, towards induced differentiation and engraftment into target sites, or acquirement of new therapeutic functions. To this end, the CRISPR/Cas9 technology promises to be a powerful asset due to its flexibility and ease of manipulation[310,367]. A common application of CRISPR/Cas9 technology involves engineering gene knock-ins in which DNA sequences are substituted or inserted at specific genomic *loci*[327]. In contrast with CRISPR-mediated indels, which result from the error-prone NHEJ pathway, gene knock-ins are often engineered via HDR, typically through the use of CRISPR elements (Cas9 enzyme and sgRNA) in tandem with a DNA template that shares homology with the target site and encodes for the desired modification[375]. Though in preliminary stages, the employment of this technique already demonstrated to be feasible and valuable in MSC studies aiming at their therapeutic improvement, while uncompromising their innate MSC features[202,204,207]. As such, in this study, we employed our previously developed CRISPR/Cas9 protocol (See Chapter III), under non-viral and xeno-free conditions, towards a HDR pathway and insertion of a fluorescently labelled *azurin* cassette targeting the genomic safe harbor *AAVS1*[329], into MSC genome. The template used to accomplish HDR, and ultimately insert the exogenous DNA in the target locus, may be provided in the format of double-stranded DNA (dsDNA, linear or plasmid) or single-stranded DNA (ssDNA), and recent findings have suggested that the repair mechanism varies depending on the type of template used; dsDNA triggers a RAD51-dependent mechanism that mirrors meiotic homologous recombination, whereas HDR involving ssDNA (referred to as single-stranded template repair) is RAD51-independent and requires multiple components of the Fanconi Anemia (FA) repair pathway[376]. Moreover, ssDNA has been associated with lower toxicity and a reduced likelihood of off-target integration relative to dsDNA[372]. As such, in our study, we co-microporated a Cas9-sgRNA RNP complex alongside DNA HDR templates consisting of either dsDNA or ssDNA (obtained by selective digestion of either the sense or antisense strand of the double-stranded PCR product), aiming to identify the optimal experimental settings, specifically for our biological system. Additionally, as knock-in efficiencies can vary widely, depending on the species or cell type, and the size of the insertion[372], we tested different formulations for the HDR donor templates, by designing two fluorescently labelled *azurin* cassettes with different homology arm size (~700bp – donor 2; ~400bp – donor 3), a *gfp* expression cassette (donor 5) and an *azurin* expression cassette (donor 4). We observed that the level of toxicity associated with plasmid and dsDNA was much greater than what was observed for ssDNA.

This finding is consistent with the results of previous studies performed by others[372]. It is also important to note that the higher the molecular weight of the HDR template, and since the amounts of HDR template used for electroporation are measured in µg, the fewer moles (copies) will be delivered to transfected cells. Furthermore, HDR template formulated in a plasmid (donor 1), was discarded from additional experiments due to due to severe toxicity to recipient cells. A possible explanation for this outcome could be the toxicity profile of transfecting a large plasmid (>6kbp), which is largely dependent on the cell type and dosage of exogenous nucleic acid. Transfection of larger plasmids (from 6 to 16kbp) is stated to result in very low viability and transfection efficacy[357]. Moreover, the use of sense or antisense ssDNA templates yielded different knock-in efficiencies, being the highest with the antisense strands (11.6% knock-in efficiency, assessed by the percentage of GFP-positive cells 14 days post-microporation) of the smaller HDR donor template (donor 5), contrasting to an absent GFP expression in the control conditions, where HDR donor templates were microporated without a RNP complex, suggesting that overtime non-integrated HDR donor templates have been degraded by the cell machinery. Although higher levels of gene targeting can often be achieved via NHEJ in cell lines[377,378], the efficiency of precise gene modification via HDR generally occurs at significantly lower rate than NHEJ and account for no more than one-third (usually much lower) of the total editing events[379,380]. Even more so, the efficiencies in the more clinically relevant human stem cells and primary cells are usually substantially lower, when compared to more stable cell lines. For example, in human induced pluripotent stem cells (iPSC) the overall gene targeting rates are typically only between 1–25% without subsequent selection[190,381,382]. In primary human T cells the efficiencies have been reported to be 4- to 10-fold lower than HEK293T cells for the various sgRNAs and transfection methods tested[313,383]. Others reported that, for MSC, targeting rates could potentially achieve 30%, when employing viral delivery methods for CRISPR components[205]. Even though our method provided lower knock-in efficiencies, is important to mention that the absence of viral vectors represents an advantage when considering future clinical applications. Moreover, at such efficiencies, subsequent positive population enrichment by fluorescence-activated cell sorting (FACS) or subcloning is required to isolate the edited cells for further studies[384].

In our study, the combination of a CRISPR/Cas9 technology with the application of DNA templates for homology-directed repair in MSC could potentially allow for precise genome editing that can be employed in a wide array of experimental contexts. A promising application of this CRISPR-mediated knock-in technology involves site-specific insertion of fluorescent protein sequences to obtain fusion proteins that are expressed under the same promoter and subject to the same regulatory and cell-signalling mechanisms as their endogenous counterparts, as opposed to expressing the fusion protein from a plasmid under a different

promoter or from a non-native genomic context via random integration. It may also be useful for bioimaging studies relative to MSC interaction within the cellular components of different biological contexts, such as the tumor stroma, potentially getting clues about the role of naïve MSC in cancer development, by recapitulating more accurately the tumor microenvironment, for example with the development of 3D MSC models. Moreover, using our system, other therapeutic transgenes could potentially be employed aiming at different disease contexts, other than anti-cancer therapies. Given the relative simplicity and plasticity of the approach presented here, we anticipate that it will continue to drive greater usage for precise MSC genome editing, under GMP compliance, envisioning a clinical application scenario.

V. FINAL DISCUSSION AND FUTURE PERSPECTIVES

V.1. General Discussion

Most anti-cancer therapies to date have been designed to interfere with the molecular drivers of tumorigenesis, *i.e.*, the molecules necessary for tumor growth and progression. Traditional cytotoxic chemotherapies usually target rapidly proliferating cancer cells by interfering with cell division[385]. However, this strategy also targets, non-specifically, rapidly-dividing healthy cells such as BM, liver and hair cells, producing the well-recognized side effects of chemotherapy[385]. Therefore, a primary goal of targeted anti-cancer therapies is to act with greater specificity to reduce these side effects, by developing tumor-targeted therapies. Novel approaches have recently focused on applying various artificial drug delivery systems[214] and also, tumor targeting cells[116,214]. These drug carriers not only transport the chemotherapeutic agents to tumors, avoiding normal tissues and reducing toxicity in the rest of the body, but also protect cytotoxic drugs from degradation, increase their half-life, payload and solubility, and reduce renal clearance[214]. Particularly, the field of targeted cell-based therapies has been evolving rapidly with novel therapeutic modalities, including administration of MSC[220], based on the remarkable tumor homing capacity of these cells. Hence, in this thesis, it was proposed that MSC could serve as tumor-targeted vehicles for the enriched expression of the anti-tumoral protein azurin, directly into the tumor microenvironment. Azurin mediates high-affinity interactions with several independent signalling pathways relevant in different steps of tumor development, while inducing little side effects *in vivo,* and its complex and broad anti-tumoral effect has been deeply studied by our group[249–251,256,261]. This ability makes it distinct and promising relatively to other antitumor agents, which have a more limited range of action. To our knowledge, the present work is pioneer in combining a stem cell-based approach to deliver a bacterial protein for anti-cancer therapies. Nevertheless, the bacterial strain *Escherichia coli (E. coli)* Nissle has been previously employed as a transient cell-delivery system for azurin, taking advantage of the tumor-targeting properties of these cells, demonstrating promising results in mice models[386]. In this thesis, nonviral strategies were developed aiming at the establishment of a human codon optimized azurin (*hazu*)-expressing MSC line. The first line of research was to engineer a recombinant plasmid containing the *hazu* gene and a engineered secretory sequence, and to deliver it to MSC by microporation, based on previous studies of our group focused on the optimization of non-viral gene delivery to MSC of different human tissue sources using a reporter fluorescent protein (green fluorescence protein - GFP)[280,387], towards the transient expression of *hazu*. We observed that MSC are capable to express and secrete a non-native humanized version of azurin, delivering it to the extracellular environment (*i.e.*, CM), and upon treatment with this *hazu*-enriched CM, cancer cells demonstrated a decrease in cell viability, migration and invasion, and an increase in cell death. MSC secrete a variety of proteins, peptides, RNA, and lipid mediators, which are adaptable to

the biological conditions to which MSC are exposed[40,53]. In this thesis, the anti-tumoral effect observed after treatment with *hazu*-enriched CM is in fact a result from the complex panoply of factors produced by *hazu*-MSC, and not only to the sole effect of hazu. Due to the natural promiscuity of azurin to interact with several proteins of non-related biological pathways[258], the hypothesis of a crosstalk between azurin and other protein components of MSC' secretome should not be excluded.

MSC-derived CM concentrates and EV isolates are gaining more focus, representing a new class of cell-free therapeutics that could obviate the technical problems associated with living products in a clinical scenario[60,79]. As such, in parallel with cellular therapy development, cell-free therapies based on MSC-secreted bioactive factors are also significant. In Chapter II, a transient gene delivery method was developed as a proof-of-concept for the value of *hazu*-expressing MSC-CM in anti-cancer treatment. However, when envisioning a clinically focused product, the generation of a stable transgene-expressing MSC cell line is imperative. In this context, Chapters III and IV were oriented towards the establishment of a stable *hazu*-MSC line employing the CRISPR/Cas9 technology. By defining a strategy to stably edit the genome of MSC, we could potentially reach one extra level of the tremendous potential of these cells, making them undoubtedly effective cell-based therapeutic products. By stably inserting the *hazu* gene into MSC genome, we could take advantage of MSC as a tailored cellular therapy, taking advantage of their innate tumor tropism[37] and secretory potential; and we could also disclose a streamline for the production of a bioactive anti-tumoral CM product, by employing *hazu*-MSC as a continuous living factory. By developing a protocol to manipulate the genome of MSC, we could also work on promoting the effective engraftment of these cells upon administration, as low engraftment has been reported as the major cause of the therapeutic limitations of MSC observed in clinical trials[388]. Moreover, it could be applied to increase/diversify the production of the MSC secretome constituents towards a given therapeutic context – pro-angiogenic[58], anti-fibrotic[4], anti-apoptotic[5], and immunomodulatory factors[3] – by enhancing gene expression. The induced delay of the senescence process of MSC, previous to their administration in a clinical setting, could also be a study target, which besides prolonging the therapeutic effect of these cells, would improve their feasibility, also potentiating the engraftment to the target-tissue. For this purpose, with gene editing, the telomere shortening could be delayed, reducing histones deacetylation, as well as the DNA methylation, alterations characteristic of the cell senescence process[389]. Additionally, immortalizing transgenes could be introduced into the MCS genome improving the technical challenge of maintaining primary MSC lines in long-term culture. The combination of an immortalized MSC technology to a cell-free approach based on the production of MSC-secreted bioactive factors could represent a strong improvement in this class of therapeutic

products. In the literature, the vast majority of studies on MSC immortalization were accomplished based on viral gene transfer methods[70,390–392], nevertheless by precisely predicting the engineering target site, we avoid the unpredictability of random integration, that could represent safety issues[132]. Moreover, this genetic engineering technology could be used to favour the expression of receptors to chemokines and pro-inflammatory factors, increasing the homing and MSC adhesion to the target-tissue[393]. It is still unclear what is the fate of MSC after exogenous administration, with some reports suggesting that MSC are phagocytosed by the host immune system as a possible mechanism of their clearance[394]. Another potential method of MSC clearance is that, under stress, these cells may undergo apoptosis and break up into microparticles[395]. The development of stable MSC lines with a fluorescent label (i.e., to facilitate cell detection and further cell enrichment) could represent a significant improvement in such studies. The employment of CRISPR could be advantageous over the use of transiently expressing recombinant plasmids or viral vectors allowing for a non-toxic system, that does not alter the cell morphology or phenotype, and is reliable in terms of labelling method, signal strength, and has long-lasting effect[396]. The generation of stable fluorescent MSC lines could also allow to get insights about the MSC *in vivo* biodistribution between fresh and frozen cells[397]. Importantly, $NG2^+$/$Nestin^+$ MSC is a rare subset of BM-MSC that has recently been demonstrated to induce dormancy in disseminated tumor cells (DTC) from multiple cancers. Stable fluorescently labelled MSC could get insights regarding MSC interaction specifically within this microenvironment context, representing a tool for its accurate recapitulation, and understanding on how this MSC subset instruct cancer cells to enter dormancy[398] (Figure V.1.1).

As MSC products are moving from early development to clinical translation[15], culture conditions must shift to SF/XF systems, aiming at a defined and safe clinical-grade cell-product profile[29,399,400]. As MSC-based therapies have been used to treat patients in clinical trials, it has become clear that adopting GMP early at the research phase can hasten the transition from the bench to the clinic[365,399,401,402]. As such, all work accomplished throughout this thesis was optimized and performed under complete SF/XF culture conditions. The impact of isolation and culture-expansion methods on the long-term resiliency of MSC within challenging transplant environments is still not fully understood. Nevertheless, some studies report that more consistent growth characteristics during the isolation and expansion of MSC arise from xeno-free conditions, resulting in faster doubling times and higher cell yields compared to culturing with FBS. Other than enhanced cell yield[403–405], rapid growth kinetics[400,404], lower overall variance in performance between donors[400] – suggesting that variance often attributed to “inherent” donor characteristics could actually be heavily influenced by early bioprocessing decisions – and improved genetic stability over extended

culture periods[405,406], are also reported in studies with xeno-free cultures over xeno-based (e.g. using FBS supplementation) cultures. To the best of our knowledge, the results provided in Chapters III and IV, are the first in the literature to employ an entirely non-viral CRISPR/Cas9 protocol for the genetic engineering of MSC under SF/XF culture conditions.

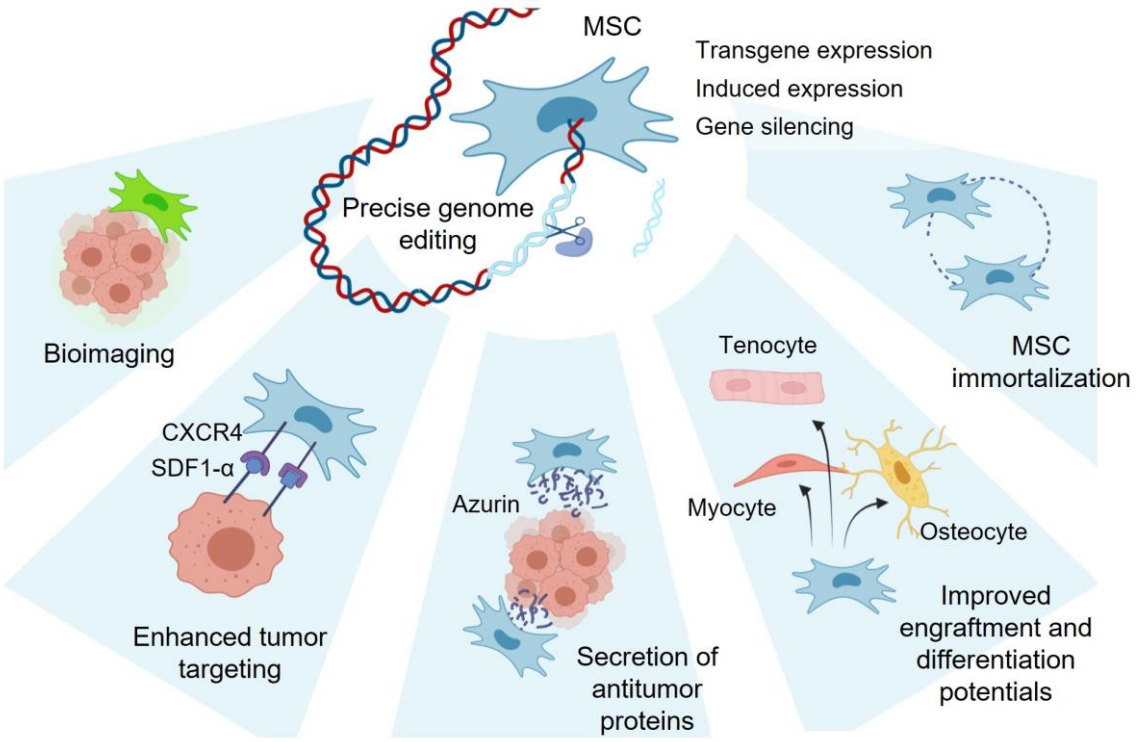

Figure V.1.1 - The scope of MSC potentialities in diverse biological contexts after precise genome editing. Created with *BioRender.com*.

V.2. Future Perspectives

A question that still arises is the identification of the mechanisms of action that make *hazu*-MSC CM antitumorigenic. One of the primordial mechanisms of azurin action is at its internalization step into the cancer cell through endocytosis, a process that disturb caveolae and removes from the cell membrane selective receptors that may be over-activated and are crucial for cancer progression[256]. In fact, we were unable to detect the azurin uptake by cancer cells, upon treatment with hazu-enriched CM. This may suggest that, even at low concentrations, azurin produced by engineered-MSC may act synergistically within the naïve components of MSC secretome. Being azurin a natural scaffold protein[258], we could expect a crosstalk with factors naturally produced by MSC that are associated with their pro/ antitumorigenic features[368]. In Chapter II, we evaluated the expression of four cytokines expressed by naïve MSC that play an important role in processes such as cancer cell

proliferation, invasion, migration, angiogenesis, apoptosis, and development of metastases[407]. However, we did not observe significant differences between engineered and naïve MSC, which may at a first sight suggest that the results observed in cancer regression are associated to the expression of azurin independently, though it would be necessary to perform a whole secretome analysis in the future to get further conclusions. Moreover, we observed the presence of a glycosylated azurin in the CM of *hazu*-MSC. This brings us to hypothesize that the activity of this glycosylated form of azurin may differ from the native protein. Therefore, in future studies, it would be important to characterize this modified protein in terms of structure, functionality, *in vivo* immune response and anti-tumoral activity[408].

In this thesis, a nonviral method to edit MCS genome with the CRISPR/Cas9 system was successfully established, yet some points remain to be optimized. In our mediated homology-directed-repair (HDR) system, the insertion transgene was designed under the control of the CMV constitutive promoter. Alternatively, in the repair template, the IL6 promoter sequence (~1.2 kb upstream of the gene) could be used to control the expression of knocked-in *hazu*. IL6 was identified in a study as one of the genes which is more up-regulated when MSC were exposed to TGFα[409] one of the most potent ligands of epidermal growth factor receptor (EGFR), secreted by cancer cells[409]. Also, MSC express a functional EGFR, therefore, the activation of this signalling pathway could be, in our hypothesis, likely to increase the expression of the therapeutic gene once MSC reach the tumor microenvironment. Additionally, other tumor-responsive promoters could add an extra layer of specificity for enhancing our tumor targeted therapeutic system, such as the use of hypoxia-response elements (HRE) in combination with a minimal promoter or a tissue-specific promoter[410,411], to restrict the gene expression in the hypoxic tumor environment[74,412,413]. This dual-specific expression system has been previously applied in cancer gene therapy[414–416]. Also, low-pH-inducible promoters, supporting minimal gene expression at pH values above 5.0[417–419], or the use of tetracycline-controlled (Tet-On) gene expression systems, with doxycycline induction[420], could be potentially applied. Moreover, additional target sites could be explored other than the GSH AAVS1 locus. Due to the relatively low success rate of accurate HDR-mediated donor integration, the end result is often a monoallelic modification[322,421]. In the particular case of our strategy, a heterozygous insertion of *hazu* is sufficient. Therefore, targeting MSC genes closely related to a pro-tumorigenic MSC profile could represent an interesting strategy to further modulate MSC interaction with the tumor microenvironment. However, in this strategy, the perturbation of the 'secondary' non recombined allele should not be detrimental and thus 'functional loss of-heterozygosity' should be tested for the selected target gene. Examples of such potential target genes are the CCL25 or the CXCL3.

An important line of further improvement of the protocol presented in this thesis concerns the subsequent selection via FACS[422]. FACS enrichment will further allow us to detect correctly targeted cells by a combination of PCR and southern blot genotyping, for identification of the possible editing outcomes: homozygously or heterozygoulsy targeted, heterozygoulsy targeted with an NHEJ event in the non-targeted allele, or all above with random vector integration, and identification of potential off-targets. This approach will prevent the occurrence of false positives in cases where the donor template incorrectly integrated into MSC genome. Importantly, further clarification on MSC innate features after gene editing must be undertaken, by performing tri-lineage differentiation protocols and assessment of immunophenotype (by flow cytometry) as identity criteria readouts, as well as *in vitro* functional assays (e.g., hematopoietic supportive capacity, mixed lymphocyte reactions (MLR))[13]. Moreover, *hazu* knock-in enriched populations will allow further anti-cancer functional assays, in the light of the results presented in Chapter III, after confirming the secreted hazu presence in *hazu*-MSC' CM.

Alternatively, complementary strategies could be applied to further improve the efficiency of the CRISPR/Cas9 protocol presented in this thesis, by inhibition of NHEJ events when delivering the RNP and HDR fragments to MSC, either via co-expression of adenovirus 4 proteins[423] or via small molecule inhibitors of DNA ligase IV[423–426], that could potentially enhance HDR-mediated genome editing; and cell cycle synchronization in the G2/M-phase combined with timed RNP delivery[427,428] could potentially increase nuclease activity in the HDR dominant phase of the cell cycle.

There are still several challenges when translating genetically modified MSC therapy into the clinics, particularly related to the manufacturing of a clinical-grade product. Cell and gene therapies are inherently based on heterogenous living products, and their characteristics can be affected by multiple variables associated with their *ex vivo* manipulation to achieve clinically meaningful cell numbers. Differences in the techniques available for the large-scale expansion of MSC, such as the culture medium used, matrices to support cell anchorage and devices for cell propagation (such as bioreactors), could probably influence the heterogeneity, senescence, secretome and multilineage differentiation potential of MSC, as well as *in vivo* homing, survival and integration into target tissues[429]. Most clinical protocols to date implement extensive MSC expansion *ex vivo*, using a variety of conditions, which may impact cell identity and phenotype, and consequently the therapeutic potential of these cells[272,429], making comparison among studies difficult. Thus, a universal, streamlined manufacturing process needs to be developed, to allow translation to clinical use. Another point of crucial importance concerns the challenges of using autologous cell-based therapies. The use of autologous MSC has proven to be feasible and a safe approach in numerous cell-based therapy clinical

studies[430]. However, it is difficult to isolate enough numbers of autologous MSC, with high activity and low variability, from patients with advanced age or comorbidities. Additionally, applying genetic engineering protocols in autologous MSC populations may not be suited for the treatment of acute diseases or conditions that require the generation of engineered MSC-based therapies because their extraction and subsequent *ex vivo* expansion to produce the high number of cells required is extremely time-consuming[430]. Allogeneic MSC, featuring immunomodulatory properties and low immunogenicity, have been studied as an alternative to autologous cells, as these can be obtained in advance from young healthy donors, expanded and/or engineered and kept cryopreserved in cell banks enabling their immediate off-the-shelf use. Allogeneic MSC-based therapies are thus a promising alternative to autologous cells, with advantages in what concerns time, cost, and quality assurance[430].

Overall, the recent advances in genetic engineering protocols for MSC and clinical studies assessing MSC-based therapy products, including the work presented in this thesis, will certainly contribute to increase our knowledge on the safety and therapeutic potential of MSC, instructing future trials to further develop this rapidly expanding field. However, further studies are required before therapies with genetically engineered MSC can be routinely used in a clinical setting.

VI.PUBLICATIONS AND COMUNICATIONS

Scientific publications:

Papers in Journals

Silva, M., Monteiro, G.A., Fialho, A.M., Bernardes, N., da Silva, C.L. Conditioned Medium From Azurin-Expressing Human Mesenchymal Stromal Cells Demonstrates Antitumor Activity Against Breast and Lung Cancer Cell Lines. Front Cell Dev Biol 8:471 (2020)

Books and Book Chapters

Silva, M., Ulpiano, C., Bernardes, N., Monteiro, G.A., da Silva, C.L. Gene delivery as a tool to improve the therapeutic features of mesenchymal stromal cells: methods and applications in Gene Delivery: Methods and Applications, Zimmer, V. (ed.), Nova Science Publishers, ISBN 9781536162684 (2019)

Scientific Communications (Platform Presentations, Posters, Abstracts):

Oral Communications

Selected oral communication for the 11th meeting of the Portuguese Society for Stem Cell and Cell Therapies, Lisbon, Portugal, October (2019)

Poster Communications

Silva M, Almeida A, Beckman E, Cabral JMS, Fialho A, Bernardes N, Silva CL, "Development of an anti-cancer cell therapy with genetically-modified mesenchymal stem/stromal cells expressing azurin", ASPIC- Associação Portuguesa de Investigação em Cancro, Lisbon, Portugal, May (2018)

Silva M, Almeida A, Beckman E, Cabral JMS, Fialho A, Bernardes N, Silva CL, "Development of an anti-cancer cell therapy with genetically-modified mesenchymal stem/stromal cells expressing azurin", Ciência 2018 - Encontro de Ciência e Tecnologia , Lisbon, Portugal, July (2018)

Silva M, Beckman E, Cabral JMS, Fialho A, Bernardes N, Silva CL, "Genome engineering of mesenchymal stem/stromal cells to express the anti-cancer protein azurin ", PhD Open Days, Lisbon, Portugal, April (2019)

VII. REFERENCES

1. Xie, L. *et al. In vitro* mesenchymal trilineage differentiation and extracellular matrix production by adipose and bone marrow derived adult equine multipotent stromal cells on a collagen scaffold. *Stem Cell Rev. Reports* **9**, 858–872 (2013).

2. Hofer, H. R. & Tuan, R. S. Secreted trophic factors of mesenchymal stem cells support neurovascular and musculoskeletal therapies. *Stem Cell Res. Ther.* **7**, 1–14 (2016).

3. Gao, F. *et al.* Mesenchymal stem cells and immunomodulation: current status and future prospects. *Cell Death Dis.* **7**, e2062 (2016).

4. Hiwatashi, N. *et al*. Mesenchymal stem cells have anti-fibrotic effects on Transforming Growth Factor-β1-stimulated vocal fold fibroblasts. *Laryngoscope* **127**, 35–41 (2017).

5. He, A. *et al.* The antiapoptotic effect of mesenchymal stem cell transplantation on ischemic myocardium is enhanced by anoxic preconditioning. *Can. J. Cardiol.* **25**, 353–358 (2009).

6. Murray, I. R. & Péault, B. Q&A: Mesenchymal stem cells - where do they come from and is it important? *BMC Biol.* **13**, 4–9 (2015).

7. Friedenstein, A. F. *et al*. The development of fibroblast colonies in marrow and spleen cells monolayer cultures of guinea-pig bone. *Development* **38**, 1–6 (1970).

8. Gorskaya, Y. F. *et al*. Precursor cells of fibroblasts detected by *in vitro* cloning of cells from hematopoietic organs of normal and irradiated mice. *Bull. Exp. Biol. Med.* **81**, 195–198 (1976).

9. Caplan, A. I. Mesenchymal Stem Cells. *J. Orthop. Res.* 641–650 (1991).

10. Cohnheim, J. Ueber Entzündung & Eiterung. Arch. für Pathol. Anat. und Physiol. und für Klin. Med*.* **40 (1–2)**, 1–79 (1867).

11. Hernigou, P. Bone transplantation and tissue engineering, part IV. Mesenchymal stem cells: history in orthopedic surgery from Cohnheim and Goujon to the Nobel Prize of Yamanaka. *Int. Orthop.* **39**, 807–817 (2015).

12. Dominici, M. *et al.* Minimal criteria for defining multipotent mesenchymal stromal cells . The International Society for Cellular Therapy position statement. *Cytoth.* **8**, 315–317 (2006).

13. Murray, I. R. *et al.* Natural history of mesenchymal stem cells, from vessel walls to culture vessels. *Cell. Mol. Life Sci.* **71**, 1353–1374 (2014).

14. Pontikoglou, C. *et al*. Bone Marrow Mesenchymal Stem Cells: Biological Properties and

Their Role in Hematopoiesis and Hematopoietic Stem Cell Transplantation. *Stem Cell Rev. Reports* **7**, 569–589 (2011).

15. Nagamura-Inoue, T. Umbilical cord-derived mesenchymal stem cells: Their advantages and potential clinical utility. *World J. Stem Cells* **6**, 195 (2014).

16. Kim, D. W. *et al.* Wharton's jelly-derived mesenchymal stem cells: Phenotypic characterization and Optimizing their therapeutic potential for clinical applications. *Int. J. Mol. Sci.* **14**, 11692–11712 (2013).

17. Abumaree, M. H. *et al.* Phenotypic and Functional Characterization of Mesenchymal Stem Cells from Chorionic Villi of Human Term Placenta. *Stem Cell Rev. Reports* **9**, 16–31 (2013).

18. Uzieliene, I. *et al*. The Potential of Menstrual Blood-Derived Mesenchymal Stem Cells for Cartilage Repair and Regeneration: Novel Aspects. *Stem Cells Int.* **2018**, 1–10 (2018).

19. Minteer, D. *et al*. Adipose-Derived Mesenchymal Stem Cells: Biology and Potential Applications. *Adv. Biochem. Eng. 59–71* 59–70 (2012).

20. El-sayed, K. M. F. & Dörfer, C. E. Gingival Mesenchymal Stem / Progenitor Cells : A Unique Tissue Engineering Gem. *Stem Cells Int.* **2016**, (2016).

21. Ledesma-Martínez, E. *et al*. Mesenchymal stem cells derived from dental pulp: A review. *Stem Cells Int.* **2016**, 1–12 (2016).

22. Elahi, K. C. *et al.* Human Mesenchymal Stromal Cells from Different Sources Diverge in Their Expression of Cell Surface Proteins and Display Distinct Differentiation Patterns. *Stem Cells Int.* **2016**, 1–9 (2016).

23. Hass, R. *et al*. Different populations and sources of human mesenchymal stem cells (MSC): A comparison of adult and neonatal tissue-derived MSC. *Cell Commun. Signal.* **9(1)**, 1–14 (2011).

24. Rebelatto, C. K. *et al.* Dissimilar Differentiation of Mesenchymal Stem Cells from Bone Marrow, Umbilical Cord Blood, and Adipose Tissue. *Exp. Biol. Med.* **233**, 901–913 (2008).

25. Kern, S. *et al*. Comparative Analysis of Mesenchymal Stem Cells from Bone Marrow, Umbilical Cord Blood, or Adipose Tissue. *Stem Cells* **24**, 1294–1301 (2006).

26. Shih, D. T. & Burnouf, T. Preparation , quality criteria , and properties of human blood platelet lysate supplements for *ex vivo* stem cell expansion. *Nat. Biotechnol.* (2016).

27. Witzenedera, K. *et al.* Human-Derived Alternatives to Fetal Bovine Serum in Cell Culture. *Transfus. Ther. Hematotherapy* 417–423 (2013).

28. Laitinen, A. *et al.* A robust and reproducible animal serum-free culture method for clinical-grade bone marrow-derived mesenchymal stromal cells. *Cytotechnology* 891–906 (2016).

29. Panchalingam, K. M. *et al*. Bioprocessing strategies for the large-scale production of human mesenchymal stem cells : a review. *Stem Cell Res. Ther.* 1–10 (2015).

30. Sotiropoulou, P. A. *et al*. Technology Development Characterization of the Optimal Culture Conditions for Clinical Scale Production of Human Mesenchymal Stem Cells. *Stem Cells Technol. Dev.* 462–471 (2006).

31. Ikebe, C. & Suzuki, K. Mesenchymal Stem Cells for Regenerative Therapy : Optimization of Cell Preparation Protocols. *Biomed. Res. Int.* **2014**, (2014).

32. Patrikoski, M. *et al.* Development of fully defined xeno-free culture system for the preparation and propagation of cell therapy-compliant human adipose stem cells. *Stem Cell Res. Ther.* (2013).

33. Bakopoulou, A. *et al.* Isolation and prolonged expansion of oral mesenchymal stem cells under clinical- grade , GMP-compliant conditions differentially affects " stemness " properties. *Stem Cell Res. Ther.* 1–21 (2017).

34. Tozetti, P. A. *et al.* Expansion strategies for human mesenchymal stromal cells culture under xeno-free conditions. *Cell Cult. Tissue Eng.* (2017).

35. Carmelo, J. G. *et al*. A xeno-free microcarrier-based stirred culture system for the scalable expansion of human mesenchymal stem / stromal cells isolated from bone marrow and adipose tissue. *Biotechnol. J.* 1235–1247 (2015).

36. Serra, J. *et al.* Engineering of human mesenchymal stem / stromal cells (MSC) with VEGF-encoding minicircles for angiogenic *ex vivo* gene. *Hum. Gene Ther.* 1–32 (2018).

37. Chulpanova, D. S. *et al.* Application of Mesenchymal stem cells for therapeutic agent delivery in anti-tumor treatment. *Front. Pharmacol.* **9**, 1–10 (2018).

38. Aysegul, O. S. & Buitenhuis, M. Molecular mechanisms underlying adhesion and migration of hematopoietic stem cells. *Cell Adh. Migr.* 39–48 (2012).

39. Hsuan, Y. C. *et al*. Mesenchymal stem cell-based treatments for stroke, neural trauma, and heat stroke. *Brain Behav.* **6**, 1–11 (2016).

40. Zhao, R. C. Essentials of mesenchymal stem cell biology and its clinical translation. Essentials of Mesenchymal Stem Cell Biology and Its Clinical Translation (2013).

41. Zachar, L. *et al*. Activation, homing, and role of the mesenchymal stem cells in the inflammatory environment. *J. Inflamm. Res.* **9**, 231–240 (2016).

42. Yin, F. *et al.* Bone marrow mesenchymal stromal cells to treat tissue damage in allogeneic stem cell transplant recipients. *Stem Cell* **32**, 1278–1288 (2014).

43. Katuchova, J. *et al.* Impact of different pancreatic microenvironments on improvement in hyperglycemia and insulin deficiency in diabetic rats after transplantation of allogeneic mesenchymal stromal cells. *J. Surg. Res.* **178**, 188–195 (2012).

44. Glenn, J. D. *et al*. HHS Public Access. *Stem Cells* **32**, 2744–2755 (2014).

45. Cizkova, D. *et al.* Repetitive Intrathecal Catheter Delivery of Bone Marrow Mesenchymal Stromal Cells Improves Functional Recovery in a Rat Model of Contusive Spinal Cord Injury. *J. Neurotrauma* **28**, 1951–1961 (2010).

46. Ankrum, J. A. *et al*. Perspective Mesenchymal stem cells : immune evasive , not immune privileged. *Nat. Biotechnol.* **32**, (2014).

47. Tse, W. T. *et al*. Suppression of allogeneic T-cell proliferation by human marrow stromal cells: implications in transplantation. *Transplantation* **75**, 389–97 (2003).

48. Sharma, R. R. *et al*. Mesenchymal stem or stromal cells: a review of clinical applications and manufacturing practices. *Transfusion* **5**, 1418–1437 (2016).

49. Undale, A. H. *et al*. Mesenchymal stem cells for bone repair and metabolic bone diseases. *Mayo Clin. Proc.* **84**, 893–902 (2009).

50. Orlic, D. *et al.* Mobilized bone marrow cells repair the infarcted heart, improving function and survival. *Proc. Natl. Acad. Sci.* **98**, 10344–10349 (2002).

51. Freyman, T. *et al.* A quantitative , randomized study evaluating three methods of mesenchymal stem cell delivery following myocardial infarction. *Eur. Heart J.* **27**, 1114–1122 (2006).

52. Ryan, S. T. *et al.* Extracellular Vesicles from Mesenchymal Stromal Cells for the Treatment of Inflammation-Related Conditions. *Int. J. Mol. Sci.* (2021).

53. Sarvar, D. P. *et al*. Mesenchymal stem cell-derived exosomes: New opportunity in cell-free therapy. *Adv. Pharm. Bull.* **6**, 293–299 (2016).

54. Bruno, S. *et al.* Microvesicles Derived from Human Bone MarrowInhibit Tumor Growth.

Stem Cells Dev. **22**, (2013).

55. Wu, S. *et al*. Microvesicles Derived from Human Umbilical Cord Wharton ' s Jelly Mesenchymal Stem Cells Attenuate Bladder Tumor Cell Growth *In vitro* and In Vivo. *PLoS One* **8**, 1–12 (2013).

56. Harrell, C. R. *et al.* Therapeutic potential of mesenchymal stem cell-derived exosomes in the treatment of eye diseases. *Adv. Exp. Med. Biol.* **1089**, 47–57 (2018).

57. Han, C. *et al.* Human umbilical cord mesenchymal stem cell derived exosomes encapsulated in functional peptide hydrogels promote cardiac repair. *Biomater. Sci.* (2019).

58. Shi, Y. *et al.* Mesenchymal stem cell–derived extracellular vesicles: a new impetus of promoting angiogenesis in tissue regeneration. *Cytoth.* **21**, 497–508 (2019).

59. Deng, H. *et al.* Lipid, Protein, and MicroRNA Composition Within Mesenchymal Stem Cell-Derived Exosomes. *Cell Reprog.* **20**, 1–9 (2018).

60. Zhou, B. *et al.* The Effect of Conditioned Media of Adipose-Derived Stem Cells on Wound Healing after Ablative Fractional Carbon Dioxide Laser Resurfacing. *BioMed Res. Int.* **2013**, (2013).

61. Fukuoka, H. *et al*. Hair Regeneration Therapy: Application of Adipose-Derived Stem Cells. *Curr. Stem Cell Res. Ther.* **1**, 531–534 (2017).

62. Katagiri, W. *et al*. Clinical Study of Bone Regeneration by. *Implant Dent.* **26**, (2017).

63. Al-radaideh, D. A. A. *et al.* Mesenchymal stem cells and conditioned media in the treatment of multiple sclerosis patients : Clinical , ophthalmological and radiological assessments of safety and efficacy. *CNS Neurosci. Ther.* 1–9 (2017).

64. Kordelas, L. *et al.* Accepted Article Preview : Published ahead of advance online publication. *Leukemia* 1–12 (2014).

65. Nassar, W. *et al.* Umbilical cord mesenchymal stem cells derived extracellular vesicles can safely ameliorate the progression of chronic kidney diseases. *Biomater. Res.* 1–11 (2016).

66. Fujita, Y. *et al*. Clinical Application of Mesenchymal Stem Cell-Derived Extracellular Vesicle-Based Therapeutics for Inflammatory Lung Diseases. *J. Clin. Med.* (2018).

67. Takahara, K. *et al.* 245 MicroRNA-145 mediates the inhibitory effect of adipose-derived stem cells on androgen-independent prostate cancer. *Eur. Urol. Suppl.* **15**, e245 (2016).

68. Roccaro, A. M. *et al.* BM mesenchymal stromal cell – derived exosomes facilitate multiple myeloma progression. *J. Clin. Invest.* **123**, (2013).

69. Lee, J. *et al.* Exosomes Derived from Mesenchymal Stem Cells Suppress Angiogenesis by Down-Regulating VEGF Expression in Breast Cancer Cells. *PLoS One* **8**, (2013).

70. Balducci, L. *et al.* Immortalization of human adipose-derived stromal cells : production of cell lines with high growth rate , mesenchymal marker expression and capability to secrete high levels of angiogenic factors. *Stem Cell Res. Ther.* 1–15 (2014).

71. Gnecchi, M. *et al.* Evidence supporting paracrine hypothesis for Akt- modified mesenchymal stem cell-mediated cardiac protection and functional improvement. *FASEB J.* 661–669 (2006).

72. Wang, X. *et al.* Engineered Exosomes With Ischemic Myocardium-Targeting Peptide. *J. Am. Heart Assoc.* 1–16 (2018).

73. Rathinasabapathy, A. *et al.* Therapeutic potential of adipose stem cells derived conditioned medium against pulmonary hypertension and lung fibrosis. *Br. J. Pharmacol.* (2016).

74. Bhang, S. H. *et al*. Efficacious and Clinically Relevant Conditioned-medium of Human Adipose-derived Stem Cells for Therapeutic Angiogenesis. *Mol. Ther.* (2014).

75. Linero, I. & Chaparro, O. Paracrine Effect of Mesenchymal Stem Cells Derived from Human Adipose Tissue in Bone Regeneration. *PLoS One* **9**, 1–12 (2014).

76. Fontanilla, C. V *et al.* Adipose-derived Stem Cell Conditioned Media Extends Survival time of a mouse model of Amyotrophic Lateral Sclerosis. *Nat. Publ. Gr.* 1–11 (2015).

77. Bi, B. *et al*. Stromal Cells Protect against Acute Tubular Injury via an Endocrine Effect. *Soc. Nephrol.* 2486–2496 (2007).

78. Ionescu, L. *et al.* Stem cell conditioned medium improves acute lung injury in mice : *in vivo*evidence for stem cell paracrine action Stem cell conditioned medium improves acute lung injury in mice : *in vivo*evidence for stem cell paracrine action. *Lung Cell. Mol. Physiol.* (2013).

79. Ahmadi, M. *et al*. Bone marrow mesenchymal stem cells and their conditioned media could potentially ameliorate ovalbumin-induced asthmatic changes. *Biomed. Pharmacother.* **85**, 28–40 (2017).

80. Parekkadan, B. *et al*. Mesenchymal Stem Cell-Derived Molecules Reverse Fulminant Hepatic Failure. *PLoS One* (2007).

81. Kay, A. G. *et al.* Mesenchymal Stem Cell- Conditioned Medium Reduces Disease Severity and Immune Responses in Inflammatory Arthritis. *Sci. Rep.* 1–11 (2017).

82. Bai, L. *et al.* Hepatocyte growth factor mediates mesenchymal stem cell – induced recovery in multiple sclerosis models. *Nat. Neurosci.* **15**, (2012).

83. Suto, N. *et al*. Morphological and Functional Attenuation of Degeneration of Peripheral Neurons by Mesenchymal Stem Cell-Conditioned Medium in Spinocerebellar Ataxia Type 1-Knock-in Mice. *CNS Neurosci. Ther.* **2**, 1–7 (2016).

84. Yamagata, *et al*. Human Dental Pulp-Derived Stem Cells Protect Against Hypoxic-Ischemic Brain Injury in Neonatal Mice. *Stroke* 551–555 (2015).

85. Sun, J. *et al*. The Healing Effects of Conditioned Medium Derived from Mesenchymal Stem Cells on Radiation-Induced Skin Wounds in Rats. *Cell Transplant.* 1–11 (2018).

86. Zhang, W. W. *et al.* The First Approved Gene Therapy Product for Cancer Ad- *p53* (Gendicine): 12 Years in the Clinic. *Hum. Gene Ther.* **29**, 160–179 (2018).

87. Salmon, F. *et al*. Safety profile of recombinant adeno-associated viral vectors: Focus on alipogene tiparvovec (Glybera®). *Expert Rev. Clin. Pharmacol.* **7**, 53–65 (2014).

88. Mosca, J. D. *et al.* Mesenchymal stem cells as vehicles for gene delivery. *Clin Orthop* S71-90 (2000).

89. Gao, L. R. *et al.* Overexpression of apelin in Wharton' jelly mesenchymal stem cell reverses insulin resistance and promotes pancreatic β cell proliferation in type 2 diabetic rats (Stem Cell Research & Therapy. *Stem Cell Res. Ther.* **10**, 1–14 (2019).

90. Jin, S. *et al.* Mesenchymal Stem Cells with Enhanced Bcl-2 Expression Promote Liver Recovery in a Rat Model of Hepatic Cirrhosis. *Cell. Physiol. Biochem.* **40**, 1117–1128 (2016).

91. Zhang, F. *et al.* Role of FGF-2 Transfected Bone Marrow Mesenchymal Stem Cells in Engineered Bone Tissue for Repair of Avascular Necrosis of Femoral Head in Rabbits. *Cell. Physiol. Biochem.* **48**, 773–784 (2018).

92. Yin, T. *et al.* Genetically modified human placenta-derived mesenchymal stem cells with FGF-2 and PDGF-BB enhance neovascularization in a model of hindlimb ischemia. *Mol. Med. Rep.* **12**, 5093–5099 (2015).

93. Bougioukli, S. *et al.* Lentiviral Gene Therapy For Bone Repair Using Human Umbilical Cord Blood Derived-Mesenchymal Stem Cells. *Hum. Gene Ther.* 1–32 (2019).

94. Kumar, S. *et al*. Therapeutic potential of genetically modified adult stem cells for osteopenia. *Gene Ther.* **17**, 105–116 (2010).

95. Liao, H. *et al.* Bone mesenchymal stem cells co-expressing VEGF and BMP-6 genes to combat avascular necrosis of the femoral head. *Exp. Ther. Med.* **15**, 954–962 (2018).

96. Kim, Y. *et al*. Evaluation of mesenchymal stem cell sheets overexpressing BMP-7 in canine critical-sized bone defects. *Int. J. Mol. Sci.* **19**, (2018).

97. Yang, S. *et al.* Integration of C-type natriuretic peptide gene-modified bone marrow mesenchymal stem cells with chitosan/silk fibroin scaffolds as a promising strategy for articular cartilage regeneration. *Cell Tissue Bank.* **0123456789**, (2019).

98. Cheng, Z. *et al.* Targeted migration of mesenchymal stem cells modified with CXCR4 gene to infarcted myocardium improves cardiac performance. *Mol. Ther.* **16**, 571–579 (2008).

99. Liu, D. *et al.* Decorin-Modified Umbilical Cord Mesenchymal Stem Cells (MSC) Attenuate Radiation-Induced Lung Injuries via Regulating Inflammation, Fibrotic Factors, and Immune Responses. *Int. J. Radiat. Oncol. Biol. Phys.* **101**, 945–956 (2018).

100. Gao, X. *et al.* Protective effects of mesenchymal stem cells overexpressing extracellular regulating kinase 1/2 against stroke in rats. *Brain Res. Bull.* **149**, 42–52 (2019).

101. Kalimuthu, S. *et al.* Genetically engineered suicide gene in mesenchymal stem cells using a Tet-On system for anaplastic thyroid cancer. *PLoS One* **12**, 1–19 (2017).

102. Farrell, E. *et al.* IL-10-overexpressing human MSC modulate naïve and activated T lymphocytes following induction of collagenase-induced osteoarthritis. *Stem Cell Res. Ther.* **7**, 1–11 (2016).

103. Tian, S., Yan, Y., Qi, X., Li, X. & Li, Z. Treatment of Type II Collagen-Induced Rat Rheumatoid Arthritis Model by Interleukin 10 (IL10)-Mesenchymal Stem Cells (BMSC). *Med. Sci. Monit.* **25**, 2923–2934 (2019).

104. Nakajima, M. *et al.* Mesenchymal Stem Cells Overexpressing Interleukin-10 Promote Neuroprotection in Experimental Acute Ischemic Stroke. *Mol. Ther. - Methods Clin. Dev.* **6**, 102–111 (2017).

105. Changchun R. *et al*. Therapeutic potential of mesenchymal stem cells producing IFN-α in a mouse melanoma lung metastasis model. **26**, 2332–2338 (2008).

106. Chen, X. *et al*. Effects of mesenchymal stem cells harboring the Interferon-β gene on

A549 lung cancer in nude mice. *Pathol. Res. Pract.* **215**, 586–593 (2019).

107. Ahn, J. *et al.* Anti-Tumor Effect of Adipose Tissue Derived-Mesenchymal Stem Cells Expressing Interferon-β and Treatment with Cisplatin in a Xenograft Mouse Model for Canine Melanoma. *PLoS One* **8**, 1–11 (2013).

108. Dembinski, J. L. *et al.* Tumor stroma engraftment of gene-modified mesenchymal stem cells as anti-tumor therapy against ovarian cancer. *Cytotherapy* **15**, 20-32.e2 (2013).

109. Elzaouk, L., *et al*. Anti-tumor activity of mesenchymal stem cells producing IL-12 in a mouse melanoma model. *Exp. Dermatol.* **15**, 865–874 (2006).

110. Kanehira, M. *et al.* Targeted delivery of NK4 to multiple lung tumors by bone marrow-derived mesenchymal stem cells. *Cancer Gene Ther.* **14**, 894–903 (2007).

111. Zhang, F. *et al*. Klotho gene-modified BMSC showed elevated antifibrotic effects by inhibiting the Wnt/β-catenin pathway in kidneys after acute injury. *Cell Biol. Int.* **42**, 1670–1679 (2018).

112. Zhu, X. *et al.* Gene therapy of gastric cancer using LIGHT-secreting human umbilical cord blood-derived mesenchymal stem cells. *Gastric Cancer* **16**, 155–166 (2013).

113. Lang, F. M. *et al.* Mesenchymal stem cells as natural biofactories for exosomes carrying miR-124a in the treatment of gliomas. *Neuro. Oncol.* **20**, 380–390 (2018).

114. Liu, Z. *et al.* Lentivirus-mediated microRNA-26a overexpression in bone mesenchymal stem cells facilitates bone regeneration in bone defects of calvaria in mice. *Mol. Med. Rep.* **18**, 5317–5326 (2018).

115. Zhang, X. *et al.* Netrin-1 improves adipose-derived stem cell proliferation, migration, and treatment effect in type 2 diabetic mice with sciatic denervation 11 Medical and Health Sciences 1103 Clinical Sciences. *Stem Cell Res. Ther.* **9**, 1–13 (2018).

116. Qiao, B. *et al*. Human mesenchymal stem cells as delivery of osteoprotegerin gene: Homing and therapeutic effect for osteosarcoma. *Drug Des. Devel. Ther.* **9**, 969–976 (2015).

117. Chen, Q. *et al.* Therapeutic potential of bone marrow-derived mesenchymal stem cells producing pigment epithelium-derived factor in lung carcinoma. *Int. J. Mol. Med.* **30**, 527–534 (2012).

118. Chen, C. *et al*. Inhibiting PHD2 in bone marrow mesenchymal stem cells via lentiviral vector-mediated RNA interference facilitates the repair of periodontal tissue defects in SD rats. *Oncotar.* **8**, 72676–72699 (2017).

119. Mao, W. *et al.* TNF-α expression in the UCB-MSC as stable source inhibits gastric cancers growth in nude mice. *Cancer Invest.* **30**, 463–472 (2012).

120. Bao, C. *et al*. TNFR gene-modified mesenchymal stem cells attenuate inflammation and cardiac dysfunction following MI. *Scand. Cardiovasc. J.* **42**, 56–62 (2008).

121. Spano, C. *et al.* Soluble TRAIL Armed Human MSC As Gene Therapy For Pancreatic Cancer. *Sci. Rep.* **9**, 1–14 (2019).

122. Deng, Q. *et al.* TRAIL-secreting mesenchymal stem cells promote apoptosis in heat-shock-treated liver cancer cells and inhibit tumor growth in nude mice. *Br. Dent. J.* **217**, 317–327 (2014).

123. Yan, C. *et al.* Suppression of orthotopically implanted hepatocarcinoma in mice by umbilical cord-derived mesenchymal stem cells with sTRAIL gene expression driven by AFP promoter. *Biomat.* **35**, 3035–3043 (2014).

124. Loebinger, M. R. *et al*. Mesenchymal stem cell delivery of TRAIL can eliminate metastatic cancer. *Cancer Res.* **69**, 4134–4142 (2009).

125. Grisendi, G. *et al.* Adipose-derived mesenchymal stem cells as stable source of tumor necrosis factor-related apoptosis-inducing ligand delivery for cancer therapy. *Cancer Res.* **70**, 3718–3729 (2010).

126. Rossignoli, F. *et al.* MSC-delivered soluble TRAIl and paclitaxel as novel combinatory treatment for pancreatic adenocarcinoma. *Theranostics* **9**, 436–448 (2019).

127. Xia, L. *et al.* TRAIL-expressing gingival-derived mesenchymal stem cells inhibit tumorigenesis of tongue squamous cell carcinoma. *J. Dent. Res.* **94**, 219–228 (2015).

128. Luetzkendorf, J. *et al.* Growth inhibition of colorectal carcinoma by lentiviral TRAIL-transgenic human mesenchymal stem cells requires their substantial *intra-tumoral* presence. *J. Cell. Mol. Med.* **14**, 2292–2304 (2010).

129. C., Y. *et al.* Human umbilical cord mesenchymal stem cells as vehicles of CD20-specific TRAIL fusion protein delivery: A double-target therapy against non-Hodgkin's lymphoma. *Mol. Pharm.* **10**, 142–151 (2013).

130. Kaczorowski, A. *et al.* Delivery of improved oncolytic adenoviruses by mesenchymal stromal cells for elimination of tumorigenic pancreatic cancer cells. **7**, (2016).

131. Ursula, A. *et al.* Prodrug suicide gene therapy for cancer targeted intracellular by mesenchymal stem cell exosomes. *Int. J. Cancer* **144**, 897–908 (2019).

132. Yin, H. *et al.* Non-viral vectors for gene-based therapy. *Nat. Rev. Genet.* **15**, 541–555 (2014).

133. Ramamoorth, M. & Narvekar, A. Non Viral Vectors in Gene Therapy- An Overview. *J. Clin. Diagnostic Res.* **9**, 1–6 (2015).

134. Santos, J. L. *et al.* Non-Viral Gene Delivery to Mesenchymal Stem Cells : Methods , Strategies and Application in Bone Tissue Engineering and Regeneration. *Curr. Gene Ther.* 46–57 (2011).

135. Helal, N. A. *et al.* Non-viral gene delivery systems : hurdles for bench-to-bedside transformation. *Pharmazie* **72**, (2017).

136. Hamann, A. *et al*. Nucleic acid delivery to mesenchymal stem cells: A review of nonviral methods and applications. *J. Biol. Eng.* **13**, 1–16 (2019).

137. Xiang, S. *et al.* Uptake mechanisms of non-viral gene delivery. *J. Control. Release* **158**, 371–378 (2012).

138. Cho, J. W. *et al*. Therapeutic potential of mesenchymal stem cells overexpressing human forkhead box A2 gene in the regeneration of damaged liver tissues. *J. Gastroenterol. Hepatol.* **27**, 1362–1370 (2012).

139. Tsubokawa, T. *et al.* Impact of anti-apoptotic and anti-oxidative effects of bone marrow mesenchymal stem cells with transient overexpression of heme oxygenase-1 on myocardial ischemia. *Am. J. Physiol. Circ. Physiol.* **298**, H1320–H1329 (2010).

140. You, M. H. *et al.* Cytosine deaminase-producing human mesenchymal stem cells mediate an antitumor effect in a mouse xenograft model. *J. Gastroenterol. Hepatol.* **24**, 1393–1400 (2009).

141. Yu, Y. *et al.* Knockdown of MicroRNA Let-7a Improves the Functionality of Bone Marrow-Derived Mesenchymal Stem Cells in Immunotherapy. *Mol. Ther.* **25**, 480–493 (2017).

142. Teoh, H. K. *et al.* Small interfering RNA silencing of interleukin-6 in mesenchymal stromal cells inhibits multiple myeloma cell growth. *Leuk. Res.* **40**, 44–53 (2015).

143. LI, W. *et al.* Bcl-2 Engineered MSC Inhibited Apoptosis and Improved Heart AND. *Transl. Clin. Res. MESENCHYMAL STEM CELLS Ser.* **25(8)**, 2118–2127 (2007).

144. Rejman, J. *et al*. mRNA transfection of cervical carcinoma and mesenchymal stem cells mediated by cationic carriers. *J. Control. Release* **147**, 385–391 (2010).

145. Sun, J. *et al.* Biomaterials Chondrogenesis of human mesenchymal stem cells mediated by the combination of SOX trio SOX5 , 6 , and 9 genes complexed with PEI-modi fi ed PLGA nanoparticles. *Biomaterials* **32**, 3679–3688 (2011).

146. Cicerone, R. J. *et al.* Genetic engineering of human stem cells for enhanced angiogenesis using biodegradable polymeric nanoparticles. *Proc. Natl. Acad. Sci.* (2010).

147. Malik, Y. S. *et al.* Polylysine-modified polyethylenimine polymer can generate genetically engineered mesenchymal stem cells for combinational suicidal gene therapy in glioblastoma. *Acta Biomater.* (2018).

148. Zhang, T. *et al.* Gene recombinant bone marrow mesenchymal stem cells as a tumor-targeted suicide gene delivery vehicle in pulmonary metastasis therapy using non-viral transfection. *Nanomed. Nanot., Biol. Med.* 1–11 (2013).

149. Huang, B. *et al.* Peptide modified mesenchymal stem cells as targeting delivery system transfected with miR-133b for the treatment of cerebral ischemia. *Int. J. Pharm.* **531**, 90–100 (2017).

150. Kim, T. *et al.* Efficacy of mesoporous silica nanoparticles in delivering BMP-2 plasmid DNA for *in vitro* osteogenic stimulation of mesenchymal stem cells. *Soc. for Biom.* 1651–1660 (2012).

151. Zhu, K. *et al.* Nanoparticle-Enhanced Generation of Gene-Transfected Mesenchymal Stem Cells for *In vivo*Cardiac Repair. *Biomat.* (2015).

152. Joydeep, D. *et al.* Efficient delivery of C / EBP beta gene into human mesenchymal stem cells via polyethylenimine- coated gold nanoparticles enhances adipogenic differentiation. *Nat. Publ. Gr.* 1–16 (2016).

153. Muroski, M. E. *et al*. A gold nanoparticle pentapeptide: Gene fusion to induce therapeutic gene expression in mesenchymal stem cells. *J. Am. Chem. Soc.* **136**, 14763–14771 (2014).

154. Wu, H. C. *et al*. Novel magnetic hydroxyapatite nanoparticles as non-viral vectors for the glial cell line-derived neurotrophic factor gene. *Adv. Funct. Mater.* **20**, 67–77 (2010).

155. Sathy, B. N. *et al.* Mesenchymal Stem Cell Fate Following Non-viral Gene Transfection Strongly Depends on the Choice of Delivery Vector. *Acta Biomater.* (2017).

156. Li, W. *et al.* Bcl-2 Engineered MSC Inhibited Apoptosis and Improved Heart Function. *Stem Cells* **25**, 2118–2127 (2007).

157. Park, J. S. *et al.* Chondrogenesis of human mesenchymal stem cells mediated by the combination of SOX trio SOX5, 6, and 9 genes complexed with PEI-modified PLGA nanoparticles. *Biomat.* **32**, 3679–3688 (2011).

158. Yang, F. *et al.* Genetic engineering of human stem cells for enhanced angiogenesis using biodegradable polymeric nanoparticles. *Proc. Natl. Acad. Sci.* **107**, 3317–3322 (2009).

159. Malik, Y. S. *et al.* Polylysine-modified polyethylenimine polymer can generate genetically engineered mesenchymal stem cells for combinational suicidal gene therapy in glioblastoma. *Acta Biomater.* **80**, 144–153 (2018).

160. Zhang, T. Y. *et al.* Gene recombinant bone marrow mesenchymal stem cells as a tumor-targeted suicide gene delivery vehicle in pulmonary metastasis therapy using non-viral transfection. *Nanomed. Nanot. Biol. Med.* **10**, 257–267 (2014).

161. Kim, T. H. *et al.* Efficacy of mesoporous silica nanoparticles in delivering BMP-2 plasmid DNA for *in vitro* osteogenic stimulation of mesenchymal stem cells. *J. Biomed. Mater. Res. - Part A* **101 A**, 1651–1660 (2013).

162. Zhu, K. *et al.* Nanoparticle-enhanced generation of gene-transfected mesenchymal stem cells for *in vivo*cardiac repair. *Biomat.* **74**, 188–199 (2016).

163. Das, J. *et al*. Efficient delivery of C/EBP beta gene into human mesenchymal stem cells via polyethylenimine-coated gold nanoparticles enhances adipogenic differentiation. *Sci. Rep.* **6**, 1–17 (2016).

164. Gonzalez-Fernandez, T. *et al.* Mesenchymal stem cell fate following non-viral gene transfection strongly depends on the choice of delivery vector. *Acta Biomater.* **55**, 226–238 (2017).

165. Mehier-Humbert, S. & Guy, R. H. Physical methods for gene transfer: Improving the kinetics of gene delivery into cells. *Adv. Drug Deliv. Rev.* **57**, 733–753 (2005).

166. Kim, H. & Im, G. Electroporation-Mediated Transfer of SOX Trio Genes of Mesenchymal Stem Cells. *Stem Cells Dev.* **20**, (2011).

167. Lee, J. S. *et al*. Electroporation-mediated transfer of Runx2 and Osterix genes to enhance osteogenesis of adipose stem cells. *Biomat.* **32**, 760–768 (2011).

168. Kojima, R. *et al.* Designer exosomes produced by implanted cells intracerebrally deliver therapeutic cargo for Parkinson's disease treatment. *Nat. Commun.* (2018).

169. Liu, S. P. *et al.* Nonsenescent Hsp27-upregulated MSC implantation promotes

neuroplasticity in stroke model. *Cell Transplant.* **19**, 1261–1279 (2010).

170. Nakashima, S. *et al*. Highly Efficient Transfection of Human Marrow Stromal Cells by Nucleofection. *Transplant. Proc.* **37**, 2290–2292 (2005).

171. Pham, P. Van *et al.* Improved differentiation of umbilical cord blood-derived mesenchymal stem cells into insulin-producing cells by PDX-1 mRNA transfection. *Different.* 1–9 (2014).

172. Fakiruddin, K. S. *et al.* Nucleofection optimization and *in vitro* antitumorigenic effect of TRAIL-expressing human adipose-derived mesenchymal stromal cells. *Cancer Cell Int.* **14**, 1–13 (2014).

173. Seung, Y. K. *et al*. Growth-inhibitory effect of neurotrophin-3-secreting adipose tissue-derived mesenchymal stem cells on the D283-MED human medulloblastoma cell line. *J. Neurooncol.* 89–98 (2012).

174. Pelled, G. *et al.* BMP6-engineered MSC induce vertebral bone repair in a pig model: A pilot study. *Stem Cells Int.* **2016**, (2016).

175. Lim, J. Y. *et al.* Microporation is a valuable transfection method for efficient gene delivery into human umbilical cord blood-derived mesenchymal stem cells. *BMC Biotechnol.* (2010).

176. Mun, J. Y. *et al*. Minicircle microporation-based non-viral gene delivery improved the targeting of mesenchymal stem cells to an injury site. *Biomaterials* **101**, 310–320 (2016).

177. Serra, J. *et al*. Minicircle-based expression of vascular endothelial growth factor in mesenchymal stromal cells from diverse human tissues. *J. Gene Med.* (2021).

178. Nakashima, M. *et al.* Induction of Reparative Dentin Formation by Ultrasound-Mediated Gene Delivery of Growth/Differentiation Factor 11. *Hum. Gene Ther.* **14**, 591–597 (2003).

179. Otani, K. *et al.* Nonviral delivery of siRNA into mesenchymal stem cells by a combination of ultrasound and microbubbles. *J. Control. Release* **133**, 146–153 (2009).

180. Haber, T. *et al*. Ultrasound-Mediated Mesenchymal Stem Cells Transfection as a Targeted Cancer Therapy Platform. *Sci. Rep.* **7**, 1–13 (2017).

181. Ang, G. *et al.* Enhanced Homing of CXCR-4 Modified Bone Marrow–Derived Mesenchymal Stem Cells to Acute Kidney Injury Tissues by Micro-Bubble–Mediated Ultrasound Exposure. *Ultrasound Med. Biol.* **42**, 539–548 (2016).

182. Tsulaia, T. V. *et al.* Biomedical Science Glass Needle-Mediated Microinjection of Macromolecules and Transgenes into Primary Human Mesenchymal Stem Cells. *Biomed. Sci.* **77550**, 328–336 (2003).

183. Han, S.W. *et al.* High-efficiency DNA injection into a single human mesenchymal stem cell using a nanoneedle and atomic force microscopy. *Nanomedicine Nanotechnology, Biol. Med.* **4**, 215–225 (2008).

184. Kim, H.J. & Im, G.I. Electroporation-Mediated Transfer of SOX Trio Genes (SOX-5, SOX-6 , and SOX-9) to Enhance the Chondrogenesis of Mesenchymal Stem Cells . *Stem Cells Dev.* **20**, 2103–2114 (2011).

185. Kojima, R. *et al.* Designer exosomes produced by implanted cells intracerebrally deliver therapeutic cargo for Parkinson's disease treatment. *Nat. Commun.* **9**, (2018).

186. Van Pham, P. *et al.* Improved differentiation of umbilical cord blood-derived mesenchymal stem cells into insulin-producing cells by PDX-1 mRNA transfection. *Different.* **87**, 200–208 (2014).

187. Kim, Y. H. *et al.* Growth-inhibitory effect of neurotrophin-3-secreting adipose tissue-derived mesenchymal stem cells on the D283-MED human medulloblastoma cell line. *J. Neurooncol.* **106**, 89–98 (2012).

188. Serra, J. *et al.* Engineering of human mesenchymal stem/stromal cells (MSC) with VEGF-encoding minicircles for angiogenic gene therapy. *Hum. Gene Ther.* hum.2018.154 (2018).

189. Wang, G. *et al.* Enhanced Homing of CXCR-4 Modified Bone Marrow-Derived Mesenchymal Stem Cells to Acute Kidney Injury Tissues by Micro-Bubble-Mediated Ultrasound Exposure. *Ultrasound Med. Biol.* **42**, 539–548 (2016).

190. Byrne, S. M. & Church, G. M. Genome Editing in Human Stem Cells. The Use of CRISPR/cas9, ZFNs, TALENs in Generating Site Specific Genome Alterations. *Elsevier.* **546**, (2014).

191. Lino, C. A. *et al*. Delivering CRISPR : a review of the challenges and approaches. *Drug Deliv.* **25**, 1234–1257 (2018).

192. Saleh-gohari, N. & Helleday, T. Conservative homologous recombination preferentially repairs DNA double-strand breaks in the S phase of the cell cycle in human cells. *Nucleic Acids Res.* **32**, 3683–3688 (2004).

193. Pavletich, N. P. & Pabo, C. Zinc Finger-DNA Recognition : Crystal Structure of a Zif268-

DNA Complex at 2 .1.A. *Science.* (1991).

194. Kim, Y. G. *et al*. Hybrid restriction enzymes : Zinc finger fusions to Fok I cleavage domain. *Proc Natl Acad Sci U S A* **93**, 1156–1160 (1996).

195. Boch, J. *et al.* Breaking the Code of DNA Binding. *Science.* **1509**, (2012).

196. Moscou, M. J. *et al*. A Simple Cipher Governs DNA Recognition by TAL Effectors. *Science.* 50011 (2009).

197. Cong, L. *et al.* Multiplex Genome Engineering Using CRISPR/Cas Systems. *Science.* **339**, 819–823 (2013).

198. Dicarlo, J. E. *et al*. RNA-Guided Human Genome Engineering via Cas9. *Sci. Express* 9–13 (2013).

199. Liang, G. *et al*. Selection of highly efficient sgRNAs for CRISPR / Cas9-based plant genome editing. *Nat. Publ. Gr.* 1–8 (2016).

200. Kleinstiver, B. P. *et al.* Engineered CRISPR-Cas9 nucleases with altered PAM specificities. *Nature* **523**, 481–485 (2016).

201. Suresh, G. *et al*. Gene Delivery Approaches for Mesenchymal Stem Cell Therapy : Strategies to Increase Efficiency and Specificity. *Stem Cell Rev. Reports* **0**, 0 (2017).

202. Deryabin, P. *et al*. Optimization of lentiviral transduction parameters and its application for CRISPR-based secretome modification of human endometrial mesenchymal stem cells. *Cell Cycle* **18**, 742–758 (2019).

203. Sun, S. *et al.* Targeting ectodysplasin promotor by CRISPR / dCas9-effector effectively induces the reprogramming of human bone marrow-derived mesenchymal stem cells into sweat gland-like cells. *Stem Cell Res. Ther.* 1–10 (2018).

204. Kosaric, N. *et al.* Human Mesenchymal Stromal Cells Engineered to Overexpress PDGF-B Using CRISPR / Cas9 / rAAV6-based Tools Improve Wound Healing Nanoparticle Delivery of Keap1 siRNA Accelerates Diabetic Wound Healing. *Plast. Reconstr. Surg. Glob. Open* 2017 (2017).

205. Srifa, W. *et al.* Cas9-AAV6-engineered human mesenchymal stromal cells improved cutaneous wound healing in diabetic mice. *Nat. Commun.* 1–14 (2020).

206. Meca-Cortés, O. *et al.* CRISPR / Cas9-Mediated Knockin Application in Cell Therapy : A Non-viral Procedure for Bystander Treatment of Glioma in Mice. *Mol. Ther. Nucleic Acid* **8**, 395–403 (2017).

207. Xu, X. *et al.* Efficient homology-directed gene editing by CRISPR/Cas9 in human stem and primary cells using tube electroporation. *Sci. Rep.* **8**, 1–11 (2018).

208. Lee, J. *et al.* CRISPR/Cas9 Edited sRAGE-MSC Protect Neuronal Death in Parkinson's Disease Model. *Int. J. Stem Cells* **12**, 114–124 (2019).

209. Hu, X. *et al.* CRISPR / Cas9-mediated reversibly immortalized mouse bone marrow stromal stem cells (BMSC) retain multipotent features of mesenchymal stem cells (MSC). *Oncotar.* **8**, 111847–111865 (2017).

210. Meng, X. *et al.* Transplantation of CRISPRa system engineered IL10-overexpressing bone marrow-derived mesenchymal stem cells for the treatment of myocardial infarction in diabetic mice. *J. Biol. Eng.* **6**, 1–12 (2019).

211. Perry, M. W. *et al*. Report Precision of Hunchback Expression in the Drosophila Embryo. *Curr. Biol.* **22**, 2247–2252 (2012).

212. Jeong, K. *et al.* Irradiation-induced localization of IL-12-expressing mesenchymal stem cells to enhance the curative effect in murine metastatic hepatoma. *Int. J. Cancer* **00**, 00 (2015).

213. Hierro, C. *et al*. Unveiling changes in the landscape of patient populations in cancer early drug development. *Oncot.* **8**, 14158–14172 (2017).

214. Pelaz, B. *et al.* Nano Focus Diverse Applications of Nanomedicine. *NanoFocus* (2017).

215. Salgado, R. *et al.* Harmonization of the evaluation of tumor infiltrating lymphocytes (TILs) in breast cancer: recommendations by an international tilsworking group 2014. *Ann. Oncol.* (2014).

216. Li, D. *et al.* Genetically engineered T cells for cancer immunotherapy. *Signal Transduct. Target. Ther.* (2019).

217. Feins, S., *et al*. An Introduction to Chimeric Antigen Receptor (CAR) T cell Immunotherapy for Human Cancer. *Am. J. Hematol.* **94(S1):S3**, (2019).

218. Voutsadakis, I. A. Immune ligands for cytotoxic T Lymphocytes (CTLS) in cancer stem cells (CSCS). *Front. Biosci.* 563–583 (2018).

219. Wu, S. *et al*. Natural killer cells in cancer biology and therapy. *Mol. Cancer* 1–26 (2020).

220. Lin, W. *et al.* Mesenchymal Stem Cells and Cancer : Clinical Challenges and Opportunities. *Biomed Res. Int.* **2019**, (2019).

221. Studeny, M. *et al.* Advances in Brief Bone Marrow-derived Mesenchymal Stem Cells as

Vehicles for Interferon-b Delivery into Tumors 1. *Adv. Br.* **2**, 3603–3608 (2002).

222. Hung, S. *et al.* Mesenchymal Stem Cell T argeting of Microscopic Tumors and umor Stroma Development Monitored by Noninvasive *In vivo*Positron Emission Tomography Imaging. *Imaging, Diagnosis, Progn.* **11**, 7749–7757 (2005).

223. Ponte, A. *et al*. The *In vitro* Migration Capacity of Human Bone Marrow Mesenchymal Stem Cells : Comparison of Chemokine and Growth. *Stem Cells* 1737–1745 (2007).

224. Droujinine, I. A. *et al*. To grab the stroma by the horns : From biology to cancer therapy with mesenchymal stem cells. *Oncont.* **4**, 651–664 (2013).

225. Lüttichau, N. *et al.* Human Adult CD34- Progenitor Cells Functionally Express the Chemokine Receptors CCR1, CCR4, CCR7, CXCR5, and CCR10 but Not CXCR4. *Stem Cells Dev.* **336**, 329–336 (2005).

226. Fox, J. M. *et al*. Recent advances into the understanding of mesenchymal stem cell trafficking. *BJH* **4**, 491–502 (2007).

227. Bhoopathi, P. *et al.* MMP-2 mediates mesenchymal stem cell tropism towards medulloblastoma tumors. *Gene Ther.* **18**, 692–701 (2012).

228. Song, C. & Li, G. CXCR4 and matrix metalloproteinase-2 are involved in mesenchymal stromal cell homing and engraftment to tumors. *Cytot.* 549–561 (2011).

229. Ho, I. A. W. *et al.* Matrix metalloproteinase-1-mediated mesenchymal stem cell tumor tropism is dependent on crosstalk with stromal derived growth factor 1 / C-X-C chemokine receptor 4 axis. *FASEB J.* 4359–4368 (2014).

230. Maria, C. & Gomes, F. The dual role of mesenchymal stem cells in tumor progression. *Stem Cell Res. Ther.* (2013).

231. Ayuzawa, R. *et al.* Naïve human umbilical cord matrix derived stem cells significantly attenuate growth of human breast cancer cells *in vitro* and in vivo. *Cancer Lett.* **280**, 31–37 (2010).

232. Ganta, C. *et al.* Rat Umbilical Cord Stem Cells Completely Abolish Rat Mammary Carcinomas with No Evidence of Metastasis or Recurrence 100 Days Post – Tumor Cell Inoculation. *Cancer Res.* 1815–1821 (2009).

233. Chao, K. *et al*. Human umbilical cord mesenchymal stem cells suppress breast cancer tumorigenesis through direct cell – cell contact and internalization. *J. Mol. Med.* **16**, 1803–1815 (2012).

234. Ma, Y. *et al*. The *in vitro* and *in vivo*effects of human umbilical cord mesenchymal stem cells on the growth of breast cancer cells. *Breast Cancer Res. Treat.* 473–485 (2012).

235. Gauthaman, K. *et al.* Human Umbilical Cord Wharton's Jelly Stem Cell (hWJSC) Extracts Inhibit Cancer Cell Growth *In vitro* Kalamegam. *J. Cell. Biochem.* **2039**, 2027–2039 (2012).

236. Li, T. *et al.* Umbilical cord-derived mesenchymal stem cells promote proliferation and migration in MCF-7 and MDA - MB-231 breast cancer cells through activation of the ERK pathway. *Oncol. Rep.* 1469–1477 (2015).

237. Zhou, X. *et al.* Mesenchymal stem cell - derived extracellular vesicles promote the *in vitro* proliferation and migration of breast cancer cells through the activation of the ERK pathway. *Int. J. Oncol.* 1843–1852 (2019).

238. Silini, A. *et al*. Review Is Immune Modulation the Mechanism Underlying the Beneficial Effects of Amniotic Cells and Their Derivatives in Regenerative Medicine ? *Cell Transplant.* **26**, 531–539 (2017).

239. Ann K. *et al*. Concise Review : Dissecting a Discrepancy in the Literature : Do Mesenchymal Stem Cells Support or Suppress Tumor Growth? *Stem Cells* 11–19 (2011).

240. Mounayar, M. *et al*. Immunomodulation by mesenchymal stem cells - a potential therapeutic strategy for type 1 diabetes. *Stem Cell-Dependent Ther. Mesenchymal Stem Cells Chronic Inflamm. Disord.* **57**, 309–318 (2013).

241. Jing, W. *et al.* Human Umbilical Cord Blood − Derived Mesenchymal Stem Cells Producing IL15 Eradicate Established Pancreatic Tumor in Syngeneic Mice. *Mol. Cancer Ther.* (2014).

242. Ren, C. *et al.* Therapeutic potential of mesenchymal stem cells producing IFN- α in a mouse melanoma lung metastasis model. *Stem Cells.* **26**, 2332–2338 (2008).

243. Xin, H. *et al.* Targeted Delivery of CX3CL1 to Multiple Lung Tumors by Mesenchymal Stem Cells. *Stem Cells.* 1618–1626 (2007).

244. Loebinger, M. *et al*. TRAIL-expressing mesenchymal stem cells kill the putative cancer stem cell population. *Br. J. Cancer* **103**, 1692–1697 (2010).

245. Zhu, Y. *et al.* Human mesenchymal stem cells inhibit cancer cell proliferation by secreting DKK-1. *Leuk.* 925–933 (2009).

246. Matuskova, M. *et al.* Intrinsic properties of tumor cells have a key impact on the

bystander effect mediated by genetically engineered mesenchymal stromal cells. *The Journ. of Gene Med.* 776–787 (2012).

247. von Einem, J. C. *et al.* Treatment of advanced gastrointestinal cancer with genetically modified autologous mesenchymal stem cells: Results from the phase 1/2 TREAT-ME-1 trial. *Int. J. Cancer* 1–10 (2019).

248. Nalepa, G. & Clapp, D. W. Fanconi anaemia and cancer: an intricate relationship. *Nat. Publ. Gr.* (2018).

249. Bernardes, N. *et al.* The Bacterial Protein Azurin Impairs Invasion and FAK / Src Signalling in P-Cadherin-Overexpressing Breast Cancer Cell Models. *Int. J. Biochem. Cell Biol.* **8**, (2013).

250. Bernardes, N. Perturbing the Dynamics and Organization of Cell Membrane Components : A New Paradigm for Cancer-Targeted Therapies. *Int. J. Mol. Sci.* (2018).

251. Bernardes, N. *et al.* Azurin interaction with the lipid raft components ganglioside GM-1 and caveolin-1 increases membrane fluidity and sensitivity to anti-cancer drugs. *Cell Cycle* **17**, 1649–1666 (2018).

252. Bizzarri, A. R. *et al.* Interaction of an anti-cancer peptide fragment of azurin with p53 and its isolated domains studied by atomic force spectroscopy. *Int. Journ. of Nanom.* 3011–3019 (2011).

253. Mehta, R. R. *et al*. A cell penetrating peptide derived from azurin inhibits angiogenesis and tumor growth by inhibiting phosphorylation of VEGFR-2 , FAK and Akt. *Angiog.* 355–369 (2011).

254. Mollinedo, F. & Gajate, C. Advances in Biological Regulation Lipid rafts as major platforms for signalling regulation in cancer. *Adv. Biol. Regul.* 1–17 (2014).

255. Mollinedo, F. & Gajate, C. Lipid rafts as signalling hubs in cancer cell survival / death and invasion : implications in tumor progression and therapy. *J. Lipid Res.* **61**, 611–635 (2020).

256. Bernardes, N. *et al.* High-throughput molecular profiling of a P-cadherin overexpressing breast cancer model reveals new targets for the anti-cancer bacterial protein azurin. *Int. J. Biochem. Cell Biol.* **50**, 1–9 (2014).

257. Yamada, T. *et al.* Internalization of bacterial redox protein azurin in mammalian cells : entry domain and specificity. **7**, 1418–1431 (2005).

258. Huang, F. *et al.* Anti-cancer Actions of Azurin and Its Derived Peptide p28. *Protein J.*

(2020).

259. Bizzarri, A. R. *et al.* Interaction of an anti-cancer peptide fragment of azurin with p53 and its isolated domains studied by atomic force spectroscopy. *Int. J. Nanomed.* (2011).

260. Warso, M. A. *et al.* A first-in-class , first-in-human , phase I trial of p28 , a non-HDM2-mediated peptide inhibitor of p53 ubiquitination in patients with advanced solid tumors. *Br. J. Cancer* **108**, 1061–1070 (2013).

261. Bernardes, N. *et al.* Modulation of membrane properties of lung cancer cells by azurin enhances the sensitivity to EGFR-targeted therapy and decreased b 1 integrin-mediated adhesion. *Cell Cycle* **15**, 1415–1424 (2016).

262. Chaudhari, A. *et al.* Cupredoxin - Cancer Interrelationship : Azurin Binding with EphB2 , Interference in EphB2 Tyrosine Phosphorylation , and Inhibition of Cancer Growth. *Biochem.* 1799–1810 (2007).

263. Yamada, T. *et al.* Apoptosis or growth arrest : Modulation of tumor suppressor p53 ' s specificity by bacterial redox protein azurin. *Biochem.* **101**, 4770–4775 (2004).

264. Apiyo, D. & Wittung-Stafshede, P. Unique complex between bacterial azurin and tumor-suppressor protein p53. *Biochem. Biophys. Res. Commun.* **332**, 965–968 (2005).

265. Yamada, T. *et al.* The Bacterial Redox Protein Azurin Induces Apoptosis in J774 Macrophages through Complex Formation and Stabilization of the Tumor Suppressor Protein p53. *Infect. Immun.* **70**, 7054–7062 (2002).

266. Yamada, T. *et al.* A peptide fragment of azurin induces a p53-mediated cell cycle arrest in human breast cancer cells. *Mol. Cancer Ther.* **8**, 2947–2959 (2009).

267. Nishida, N. *et al*. Angiogenesis in cancer. *Vasc. Heal. Manag.* **2**, 213–219 (2006).

268. Choi, J. *et al.* The Bacterial Protein Azurin Enhances Sensitivity of Oral Squamous Carcinoma Cells to Anti-cancer Drugs. *Yonsei Med. J.* **52**, 773–778 (2011).

269. Mehta, R. R. *et al.* A 28-Amino-Acid Peptide Fragment of the Cupredoxin Azurin Prevents Carcinogen-Induced Mouse Mammary Lesions A 28-Amino-Acid Peptide Fragment of the Cupredoxin Azurin Prevents Carcinogen-Induced Mouse Mammary Lesions. *Cancer Prev. Res.* 1351–1360 (2010).

270. Fialho, A. *et al*. Beyond host – pathogen interactions : microbial defense strategy in the host environment. *Sci. Direct* (2007).

271. Pucci, C. *et al*. Innovative approaches for cancer treatment : current perspectives and

new challenges. *eCancer Med. Sci.* 1–26 (2019).

272. Sage, E. K. *et al*. Genetically modified mesenchymal stromal cells in cancer therapy. *Cytoth.* **18**, 1435–1445 (2016).

273. Rifai, A. *et al. In vivo*efficacy of endothelial growth medium stimulated mesenchymal stem cells derived from patients with critical limb ischemia. *J. Transl. Med.* 1–21 (2019).

274. Mathew, A. S. *et al*. Placental mesenchymal stromal cells as an alternative tool for therapeutic angiogenesis. *Cell. Mol. Life Sci.* (2019).

275. Brewster, L. *et al.* Expansion and Angiogenic Potential of Mesenchymal Stem Cells from Patients with Critical Limb Ischemia. *J. Vasc. Surg.* **65**, 826–838 (2018).

276. Kim, S. M. *et al. In vivo*near-infrared imaging for the tracking of systemically delivered mesenchymal stem cells : tropism for brain tumors and biodistribution. *Int. J. Nanomed.* 13–23 (2016).

277. Cao, M. *et al. In vivo*tracking of the tropism of mesenchymal stem cells to malignant gliomas using reporter gene-based MR imaging. *Int. J. Cancer* 1–44 (2018).

278. Yamada, T. *et al*. Chemotherapy p28-mediated Activation of p53 in G2/M Phase of the Cell Cycle Enhances the Efficacy of DNA Damaging and Antimitotic Chemotherapy. *Cancer Res.* 76(8):2354–65 (2016).

279. Lulla, R. R. *et al.* Phase 1 trial of p28 (NSC745104), a non-HDM2-mediated peptide inhibitor of p53 ubiquitination in pediatric patients with recurrent or progressive central nervous system tumors: A Pediatric Brain Tumor Consortium Study. *Neuro-Onc.* **18**, 1319–1325 (2016).

280. Madeira, C. *et al.* Gene delivery to human bone marrow mesenchymal stem cells by microporation. *J. Biotechnol.* **151**, 130–136 (2011).

281. Rahmatizadeh, F. *et al*. Bidirectional and Opposite Effects of Naïve Mesenchymal Stem Cells on Tumor Growth and Progression. *Tabriz Univ. Med. Sci.* **9**, 539–558 (2019).

282. Liang, Y. *et al.* Exosomal microRNA-144 from bone marrow-derived mesenchymal stem cells inhibits the progression of non-small cell lung cancer by targeting CCNE1 and CCNE2. *Stem Cell Res. and Ther.* **7**, 1–17 (2020).

283. Xia, C. *et al.* Mesenchymal stem cells suppress leukemia via macrophage- mediated functional restoration of bone marrow microenvironment. *Leukem.* **1**, (2020).

284. Hass, R. *et al*. Different populations and sources of human mesenchymal stem cells

(MSC): A comparison of adult and neonatal tissue-derived MSC. *Cell Commun. Signal.* **9**, 12 (2011).

285. Leong, M. F. *et al.* Electrospun Polystyrene Scaffolds as a Synthetic Substrate for Xeno-free Expansion and Differentiation of Human Induced Pluripotent Stem Cells. *Acta Biomater.* (2016).

286. Soure, A. *et al.* Integrated culture platform based on a human platelet lysate supplement for the isolation and scalable manufacturing of umbilical cord matrix-derived mesenchymal stem / stromal cells. J. Tissue Eng. Regen. Med. (2016).

287. Santos, F. *et al. Ex vivo* Expansion of Human Mesenchymal Stem Cells : A More Effective Cell Proliferation Kinetics and Metabolism Under Hypoxia. *Cell. Physio.* 27–35 (2009).

288. Qiu, J. *et al*. Enhancement of Primary and Secondary Cellular Immune Responses against Human Immunodeficiency Virus Type 1 Gag by Using DNA Expression Vectors That Target Gag Antigen to the Secretory Pathway.*J. Virol.* **74**, 5997–6005 (2000).

289. Azzoni, A. R. *et al*. The impact of polyadenylation signals on plasmid nuclease-resistance and transgene expression. *The J. of Gene Med*. **9**, 392–402 (2007).

290. Kidd, S. *et al.* Direct Evidence of Mesenchymal Stem Cell Tropism for Tumor and Wounding Microenvironments Using *In vivo*Bioluminescent Imaging. *Stem Cells* 2614–2623 (2009).

291. Vera, N. *et al.* Small Extracellular Vesicles Released from Ovarian Cancer Spheroids in Response to Cisplatin Promote the Pro-Tumorigenic Activity of Mesenchymal Stem Cells. *Mol. Sci.* **9**, 20(20) (2019).

292. Liu, B. *et al.* Stromal Cell-Derived Factor-1/CXCL12 Contributes to MMTV-Wnt1 Tumor Growth Involving Gr1+CD11b+ Cells. *PLoS ONE*. **5**, (2010).

293. Markell, L. M. *et al*. Transforming growth factor b 1 enhances tumor promotion in mouse skin carcinogenesis. *Carcinogen.* **31**, 1116–1123 (2010).

294. Elman, J. S. *et al.* Pharmacokinetics of Natural and Engineered Secreted Factors Delivered by Mesenchymal Stromal Cells. *PLoS One.* **9**, (2014).

295. Eleuteri, S. & Fierabracci, A. Insights into the Secretome of Mesenchymal Stem Cells and Its Potential Applications. *Int. J. of Mol. Sci*. **20**, 18 (2019).

296. Keshtkar, S. *et al*. Mesenchymal stem cell-derived extracellular vesicles : novel frontiers in regenerative medicine. *Stem Cell Rese. and Ther*. 1–9 (2018).

297. Devarasetty, M. *et al*. Mesenchymal stem cells support growth and organization of host-liver colorectal-tumor organoids and possibly resistance to chemotherapy. *Biofabr. 021002* (2017).

298. Nowakowski, A. *et al*. Genetic Engineering of Mesenchymal Stem Cells to Induce Their Migration and Survival. *Stem Cells Int.* **2016:49560** (2016).

299. Wang, Y. *et al.* STIM1 silencing inhibits the migration and invasion of A549 cells. 3283–3289 *Mol. Med. Rep.* (2017).

300. Oieni, J. *et al.* Nano-Ghosts: Biomimetic Membranal Vesicles, Technology and Characterization. *Methods* (2019).

301. Maskarinec, G. *et al.* Breast tumor tissue in fl ammation but not lobular involution is associated with survival among breast cancer patients in the Multiethnic Cohort. *Cancer Epidemiol.* **65**, 1877–7821 (2020).

302. Christodoulou, I. *et al*. Mesenchymal stem cells in preclinical cancer cytotherapy : a systematic review. **8**, 1–38 (2018).

303. Kalimuthu, S. *et al*. Regulated Mesenchymal Stem Cells Mediated Colon Cancer Therapy Assessed by Reporter Gene Based Optical Imaging. *Int. J. Mol. Sci.* 1–16 (2018).

304. Yaniz-Galende, E. & Hajjar, R. J. *Stem cell and gene therapy for cardiac regeneration*. *Cardiac Reg, and Rep.* **1**, (2014).

305. Nishikawa, M. & Huang, L. Nonviral Vectors in the New Millennium : Delivery Barriers in Gene Transfer. *Hum. Gene Ther.* **870**, 861–870 (2001).

306. Hall, K. M. *et al*. Decreased homing of retrovirally transduced human bone marrow CD34 D cells in the NOD / SCID mouse model. *Exp. Hematol.* **34**, 433–442 (2006).

307. Wong, T.K. & Neumann, E. Electric Field Mediated Gene Transfer. *Biochem. Biophys. Res. Commun.* **107**, (1982).

308. Lim, J. *et al.* Microporation is a valuable transfection method for efficient gene delivery into human umbilical cord blood-derived mesenchymal stem cells. *BMC Biotechnol.* **10**, 38 (2010).

309. Jinek, M. *et al.* Structures of Cas9 Endonucleases Reveal RNA-Mediated Conformational Activation. *Science.* **343**, 1–28 (2014).

310. Sun, W. & Gu, Z. Tailoring non-viral delivery vehicles for transporting genome-editing

tools. *Sci. China Mater.* **60**, 511–515 (2017).

311. Glass, Z. *et al*. Engineering the Delivery System for CRISPR-Based Genome Editing. *Trends Biotechnol.* 1–13 (2017).

312. Ran, F. A. *et al. In vivo*genome editing using *Staphylococcus aureus* Cas9. *Nature* **520**, 186–191 (2015).

313. Liang, X. *et al.* Rapid and highly efficient mammalian cell engineering via Cas9 protein transfection. *J. Biotechnol.* 1–10 (2015).

314. Tabebordbar, M. *et al. In vivo*gene editing in dystrophic mouse muscle and muscle stem cells. *Science.* **351**, 407–411 (2016).

315. Hughes, T. S. *et al.* Immunogenicity of intrathecal plasmid gene delivery: cytokine release and effects on transgene expression. *J. Gene Med.* **11**, 782–790 (2013).

316. Jiang, C. *et al.* A non-viral CRISPR / Cas9 delivery system for therapeutically targeting HBV DNA and pcsk9 in vivo. *Cell Res.* **5**, 440–443 (2017).

317. Wang, Y. *et al.* Systemic Delivery of Modified mRNA Encoding Herpes Simplex Virus 1 Thymidine Kinase for Targeted Cancer Gene Therapy. *Am. Soc. Gene Cell Ther.* **21**, 358–367 (2013).

318. Lee, K. *et al.* Nanoparticle delivery of Cas9 ribonucleoprotein and donor DNA *in vivo*induces homology-directed DNA repair. *Nat. Biomed. Eng.* 889–901 (2018).

319. Turk, R. & Prediger, E. Successful CRISPR genome editing in hard-to-transfect cells. Coralville, IA, Integrated DNA Technologies, Inc. Accessed June 2019 (2016).

320. Anders, C. & Jinek, M. *In vitro* Enzymology of Cas9. *Methods Enzymol.* 1–20 (2016).

321. Smith, J. R. *et al.* Robust , Persistent Transgene Expression in Human Embryonic Stem Cells Is Achieved with AAVS1-Targeted Integration. *Stem Cells* 496–504 (2008).

322. Hockemeyer, D. *et al.* Efficient targeting of expressed and silent genes in human ESCs and iPSCs using zinc-finger nucleases. *Nat. Biotechnol.* **27**, (2009).

323. Lombardo, A. *et al.* Site-specific integration and tailoring of cassette design for sustainable gene transfer. *Nat. Methods* **8**, (2011).

324. Qian, K. *et al.* A Simple and Efficient System for Regulating Gene Expression in Human Pluripotent Stem Cells and Derivatives. *Stem Cells* **32**, 1230–1238 (2014).

325. Zhu, Z. *et al*. The iCRISPR platform for rapid genome editing in human Pluripotent Stem

Cells. *Methods Enzym.* 1–31 (2014).

326. Haeussler, M. *et al.* Evaluation of off-target and on-target scoring algorithms and integration into the guide RNA selection tool CRISPOR. *Genome Biol.* 1–12 (2016).

327. Fei, S. & Knut, S. Optimizing the DNA Donor Template for Homology-Directed Repair of Double-Strand Breaks. *Mol. Ther. Nucleic Acid* **7**, 53–60 (2017).

328. Jingxiang, H. *et al*. The TSC1-TSC2 Complex Is Required for Proper Activation of mTOR Complex 2. *Mol. Cell. Biol.* **28**, 4104–4115 (2008).

329. Oceguera-Yanez, F. *et al.* Engineering the AAVS1 locus for consistent and scalable transgene expression in human iPSCs and their differentiated derivatives. *Methods* **101**, 43–55 (2016).

330. Castaño, J. *et al.* Generation and characterization of a human iPSC cell line expressing inducible Cas9 in the " safe harbor " AAVS1 locus. *Stem Cell Res.* **21**, 137–140 (2017).

331. Bhagwan, J. R. *et al.* Variable expression and silencing of CRISPR-Cas9 targeted transgenes identifies the AAVS1 locus as not an entirely safe harbour *F1000Research* 1–27 (2020).

332. Mizutani, T. *et al*. Biochemical and Biophysical Research Communications Transgene integration into the human AAVS1 locus enhances myosin II-dependent contractile force by reducing expression of myosin binding subunit 85. *Biochem. Biophys. Res. Commun.* **465**, 270–274 (2015).

333. Lyu, C. *et al.* Targeted genome engineering in human induced pluripotent stem cells from patients with hemophilia B using the CRISPR-Cas9 system. *Stem Cell Res. Ther.* 1–12 (2018).

334. Kurata, M. *et al.* Highly multiplexed genome engineering using CRISPR / Cas9 gRNA arrays. *PLoS One* **9**, 1–17 (2018).

335. Chen, F. & Alphonse, M. Strategies for nonviral nanoparticle-based delivery of CRISPR / Cas9 therapeutics. *WIREs Nano. and Nanob.* **9**, 1–14 (2019).

336. Kim, S. *et al*. Highly efficient RNA-guided genome editing in human cells via delivery of purified Cas9 ribonucleoproteins. *Method* 1012–1019 (2014).

337. Seki, A. & Rutz, S. Optimized RNP transfection for highly efficient CRISPR / Cas9-mediated gene knockout in primary T cells. *J. Exp. Med.* 985–997 (2018).

338. Faulkner, *et al*. CRISPR / CAS9-mediated knockout of Abi1 inhibits p185 Bcr-Abl -

induced leukemogenesis and signal transduction to ERK and PI3K / Akt pathways. *J. of Hema. and Onco.* **5**, 1–12 (2020).

339. Reinders, M. E. J. *et al.* Autologous Bone Marrow-Derived Mesenchymal Stromal Cells for the Treatment of Allograft Rejection After Renal Transplantation: Results of a Phase I Study. *Stem Cell Transl. Med.* 107–111 (2013).

340. Foss, D. *et al*. Clinical applications of CRISPR-based genome editing and diagnostics. *Transfusion* 1–11 (2019).

341. Mollanoori, H. & Teimourian, S. Therapeutic applications of CRISPR / Cas9 system in gene therapy. *Biotechnol. Lett.* (2018).

342. Baylis, F. & McLeod, M. First-in-human Phase 1 CRISPR Gene Editing Cancer Trials: Are We Ready? *Curr. Gene Ther.* 309–319 (2017).

343. Xie, C. *et al.* Genome editing with CRISPR / Cas9 in postnatal mice corrects PRKAG2 cardiac syndrome. *Nat. Publ. Gr.* 1–13 (2016).

344. Liu, Y. *et al.* One-Step Biallelic and Scarless Correction of a b-Thalassemia Mutation in Patient-Specific iPSCs without Drug Selection. *Mol. Ther. Nucleic Acid* **6**, 57–67 (2017).

345. Park, C. *et al.* Short Article Functional Correction of Large Factor VIII Gene Chromosomal Inversions in Hemophilia A Patient- Derived iPSCs Using CRISPR-Cas9. *Stem Cell* 1–8 (2015).

346. Chang, C. *et al.* Modeling Human Severe Combined Immunodeficiency and Correction by CRISPR / Cas9- Modeling Human Severe Combined Immunodeficiency and Correction by CRISPR / Cas9-Enhanced Gene Targeting. *CellReports* 1–10 (2015).

347. Pankowicz, F. P. *et al.* Reprogramming metabolic pathways *in vivo*with CRISPR/Cas9 genome editing to treat hereditary tyrosinaemia. *Nat. Commun.* **7**, 1–6 (2016).

348. Koo, T. *et al.* Selective disruption of an oncogenic mutant allele by CRISPR / Cas9 induces efficient tumor regression. *Nucleic Acids Res.* **45**, 7897–7908 (2017).

349. Li, H. L. *et al.* Precise Correction of the Dystrophin Gene in Duchenne Muscular Dystrophy Patient Induced Pluripotent Stem Cells by TALEN and CRISPR-Cas9. *Stem Cell Reports* **4**, 143–154 (2015).

350. Wang, L. *et al.* R ESEARCH ARTICLE CRISPR / Cas9-mediated targeted gene correction in amyotrophic lateral sclerosis patient iPSCs. *Protein Cell* **8**, 365–378 (2017).

351. Firth, A. L. *et al.* Functional Gene Correction for Cystic Fibrosis in Lung Epithelial Cells Generated From Patient iPSCs. *Cell Rep.* **12**, 1385–1390 (2015).

352. Hainzl, S. *et al.* COL7A1 editing via CRISPR/Cas9 in recessive dystrophic epidermolysis bullosa. *Mol. Ther.* 39 (2017).

353. Bartholomew, A. *et al.* Mesenchymal stem cells suppress lymphocyte proliferation *in vitro* and prolong skin graft survival in vivo. *Exp. Hematol.* **30**, 42–48 (2002).

354. Ding, Q. *et al.* Enhanced efficiency of human pluripotent stem cell genome editing through replacing TALENs with CRISPRs. *Science.* **12**, 393–394 (2014).

355. Barrangou, R. *et al.* CRISPR provides acquired resistence against viruses in prokaryotes. *Cell Stem Cell* **1709**, (2012).

356. Chen, Q. *et al.* Fate decision of mesenchymal stem cells : adipocytes or osteoblasts ? *Cell Death Differ.* 1128–1139 (2016).

357. Lesueur, L. *et al*. Overcoming the Specific Toxicity of Large Plasmids Electrotransfer in Primary Cells *In vitro*. *Mol. Ther. - Nucleic acids* 1–10 (2016).

358. Yin, H. *et al.* Structure-guided chemical modification of guide RNA enables potent non-viral *in vivo*genome editing. *Nat. Biotechnol.* **35**, 1179–1187 (2018).

359. Brinkman, E. K. *et al*. Easy quantitative assessment of genome editing by sequence trace decomposition. *Nucleic Acids Res.* **42**, (2014).

360. Germini, D. *et al.* A One-Step PCR-Based Assay to Evaluate the Efficiency and Precision of Genomic DNA-Editing Tools. *Methods Clin. Dev.* **5**, 43–50 (2017).

361. Kang, H. *et al.* CCR5 Disruption in Induced Pluripotent Stem Cells Using CRISPR / Cas9 Provides Selective Resistance of Immune Cells to CCR5-tropic HIV-1 Virus. *Mol. Ther. - Nucleic acids* (2015).

362. Agarwala, V. *et al*. DNA targeting specificity of RNA-guided Cas9 nucleases. *Nat. Biotechnol.* **31**, 827–832 (2014).

363. Chakrabarti, A. M. *et al*. Target - specific precision of CRISPR - mediated genome editing. *BioRxiv* (2018).

364. Galipeau, J. & Sensébé, L. Mesenchymal stromal cells: clinical challenges and therapeutic opportunities. *Cell Stem Cell* **22**, 824–833 (2018).

365. Mendicino, M. *et al*. Forum MSC-Based Product Characterization for Clinical Trials : An FDA Perspective. *Stem Cell* **14**, 141–145 (2014).

366. Lin, P. *et al*. Polybrene inhibits human mesenchymal stem cell proliferation during lentiviral transduction. *PLoS One* **6**, (2011).

367. Zhang, F. *et al.* CRISPR / Cas9 for genome editing : progress , implications and challenges. *Hum. Mol. Genet.* **15**, 1–21 (2014).

368. Galland, S. & Stamenkovic, I. Mesenchymal stromal cells in cancer : a review of their immunomodulatory functions and dual effects on tumor progression S Galland and I Stamenkovic. *J. Pathol.* **2020**, 555–572 (2019).

369. Silva, M. *et al*. Conditioned Medium From Azurin-Expressing Human Mesenchymal Stromal Cells Demonstrates Antitumor Activity Against Breast and Lung Cancer Cell Lines. *Front. Cell Dev. Biol.* **8**, 1–13 (2020).

370. Kosicki, M. *et al. Dynamics of Indel Profiles Induced by Various CRISPR / Cas9 Delivery Methods*. *Progress in Molecular Biology and Translational Science* **152**, (2017).

371. Li, H. *et al*. Design and specificity of long ssDNA donors for CRISPR-based knock-in. *BioRxiv* (2019).

372. Roth, T. L. *et al.* Reprogramming human T cell function and specificity with non-viral genome targeting. *Nature* (2018).

373. Bollen, Y. *et al*. How to create state-of-the-art genetic model systems : strategies for optimal CRISPR-mediated genome editing. *Nucleic Acids Res.* **46**, 6435–6454 (2018).

374. Sasaki, A. & Kinjo, M. Monitoring intracellular degradation of exogenous DNA using diffusion properties. *J. Control. Release* **143**, 104–111 (2010).

375. Hsu, P. D. *et al*. Review Development and Applications of CRISPR-Cas9 for Genome Engineering. *Cell* **157**, 1262–1278 (2014).

376. Richardson, C. D. *et al.* CRISPR–Cas9 genome editing in human cells occurs via the Fanconi anemia pathway. *Nat. Genet.* (2018).

377. Li, Z. *et al.* Establishment of a HEK293 cell line by CRISPR / Cas9- mediated luciferase knock-in to study transcriptional regulation of the human SREBP1 gene. *Biotechnol. Lett.* **2**, (2018).

378. Soto-velasquez, M. *et al*. A Novel CRISPR / Cas9-Based Cellular Model to Explore Adenylyl Cyclase and cAMP Signalling s. *Mol. Pharmacol.* 963–972 (2018).

379. Paquet, D. *et al.* Efficient introduction of specific homozygous and heterozygous mutations using CRISPR/Cas9. *Nature* 1–18 (2016).

380. Richardson, C. D., Ray, G. J., Dewitt, M. A., Curie, G. L. & Corn, J. E. Enhancing homology-directed genome editing by catalytically active and inactive CRISPR-Cas9 using asymmetric donor DNA. *Nat. Publ. Gr.* 1–7 (2016).

381. Zhu, Z. *et al*. Resource An iCRISPR Platform for Rapid , Multiplexable , and Inducible Genome Editing in Human Pluripotent Stem Cells. *Cell Stem Cell* 1–12 (2014).

382. Wang, G. *et al.* Efficient , footprint-free human iPSC genome editing by consolidation of Cas9 / CRISPR and piggyBac technologies. *Nat. Protoc.* **12**, 88–103 (2016).

383. Cells, E. *et al.* Efficient Ablation of Genes in Human Hematopoietic Short Article Efficient Ablation of Genes in Human Hematopoietic Stem and Effector Cells using CRISPR / Cas9. *Stem Cell* **15**, 643–652 (2014).

384. Miyaoka, Y. *et al.* Isolation of single-base iPS cells without antibiotic selection. *Nat. Methods* 1–7 (2014).

385. Malhotra, V. & Perry, M. C. Classical Chemotherapy: Mechanisms, Toxicities and the Therapeutic Window. *Cancer Biol. Ther.* 4–6 (2003).

386. Zhang, Y. *et al.* Escherichia coli Nissle 1917 Targets and Restrains Mouse B16 Melanoma and 4T1 Breast Tumors through Expression of Azurin. *Appl. Environ. Microbiol.* **78**, 7603–7610 (2012).

387. Boura, J. S. *et al*. Direct Head-To-Head Comparison of Cationic Liposome-Mediated Gene Delivery to Mesenchymal. *Hum. Gene Ther. Methods* **48**, 38–48 (2013).

388. Ezquer, F. E. *et al*. Two complementary strategies to improve cell engraftment in mesenchymal stem cell-based therapy : Increasing transplanted cell resistance and increasing tissue receptivity. *Cell Adh. Migr.* **11**, 110–119 (2017).

389. Herranz, N. & Gil, J. Mechanisms and functions of cellular senescence. *J. Clin. Invest.* **128**, (2018).

390. Piñeiro-Ramil, M. *et al.* Immortalizing Mesenchymal Stromal Cells from Aged Donors While Keeping Their Essential Features. *Stem Cells Int.* **2020**, (2020).

391. Liu, T. M. *et al.* Molecular Basis of Immortalization of Human Mesenchymal Stem Cells by Combination of p53 Knockdown and Human Telomerase. **22**, 268–278 (2013).

392. Torre, A. G. *et al.* An immortalised mesenchymal stem cell line maintains mechano-responsive behaviour and can be used as a reporter of substrate stiffness. *Sci. Rep.* 1–13 (2018).

393. Ullah, M. *et al*. Mesenchymal Stromal Cell Homing : Mechanisms and Strategies for Improvement. *IScience* **15**, 421–438 (2019).

394. Tan, X. *et al*. Mesenchymal Stem Cell-Derived Microparticles : A Promising Therapeutic Strategy. *Int. J. Mol. Sci.* 14348–14363 (2014).

395. Su-Yan, B. & Hua, C. Mesenchymal stem cells release membrane microvesicles in the process of apoptosis. *Heart* **98**, 302920 (2012).

396. Masterson, C. H. *et al*. Modulating the distribution and fate of exogenously delivered MSC to enhance therapeutic potential : knowns and unknowns. *Intensive Care Med. Exp.* **7**, 1–21 (2019).

397. Chinnadurai, R. *et al.* Actin Cytoskeletal Disruption following Cryopreservation Alters the Biodistribution of Human Mesenchymal Stromal Cells In Vivo. *Stem Cell Reports* **3**, 60–72 (2014).

398. Nobre, A. R. *et al.* NG2+ /Nestin+ mesenchymal stem cells dictate DTC dormancy in the bone marrow through TGFβ2. *BioRxiv* (2020).

399. Jossen, V. *et al*. Manufacturing human mesenchymal stem cells at clinical scale : process and regulatory challenges. *Appl. Microbiol. Biotechnol.* 3981–3994 (2018).

400. Heathman, T. R. J. *et al.* Scalability and process transfer of mesenchymal stromal cell production from monolayer to microcarrier culture using human platelet lysate. *Cytotherapy* **18**, 523–535 (2016).

401. Lipsitz, Y. Y. *et al*. Quality cell therapy manufacturing by design. *Nat. Publ. Gr.* **34**, 393–400 (2016).

402. Liu, S. *et al.* Manufacturing Differences Affect Human Bone Marrow Stromal Cell Characteristics and Function : Comparison of Production Methods and Products from Multiple Centers. *Sci. Rep.* 1–11 (2017).

403. Becherucci, V. *et al.* Human platelet lysate in mesenchymal stromal cell expansion according to a GMP grade protocol : a cell factory experience. *Stem Cell Res. Ther.* 1–10 (2018).

404. Fernandez-Rebollo, E. *et al.* Human Platelet Lysate versus Fetal Calf Serum : These Supplements Do Not Select for Different Mesenchymal Stromal Cells. *Sci. Rep.* 1–8 (2017).

405. Crespo-Diaz, R. *et al.* Platelet Lysate Consisting of a Natural Repair Proteome Supports Human Mesenchymal Stem Cell Proliferation and Chromosomal Stability. *Cell*

Transplant. **20**, 797–811 (2011).

406. Blázquez-Prunera, A. *et al*. Human mesenchymal stem cells maintain their phenotype , multipotentiality , and genetic stability when cultured using a defined xeno-free human plasma fraction. *Stem Cell Res. Ther.* 1–11 (2017).

407. Maskarinec, G. *et al.* Breast Tumor Tissue Inflammation but not Lobular Involution is Associated with Survival among Breast Cancer Patients in the Multiethnic Cohort. *Cancer Epidemiol.* 1–17 (2021).

408. Spiro, R. G. Protein glycosylation : nature , distribution , enzymatic formation , and disease implications of glycopeptide bonds. *Glycob.* **12**, (2002).

409. Luca, A. *et al.* RNA-seq analysis reveals significant effects of EGFR signalling on the secretome of mesenchymal stem cells. *Oncotar.* **5**, (2014).

410. Wu, C. *et al.* Combinatorial Control of Suicide Gene Expression by Tissue-specific Promoter and microRNA Regulation for Cancer Therapy. *Mol. Ther.* **17**, 2058–2066 (2009).

411. Chao, C. *et al*. Gene Therapy for Human Lung Adenocarcinoma Using a Suicide Gene Driven by a Lung-Specific Promoter Delivered by JC Virus-Like Particles. *PLoS One* 1–12 (2016).

412. Shibata, T. *et al*. Enhancement Of Gene Expression Under Hypoxic Conditions Growth Factor And The Erythropoietin Genes. *Hypoxic Stress Proteins Gene Regul.* **42**, 913–916 (1998).

413. Shibata, T. *et al*. Development of a hypoxia-responsive vector for tumor- specific gene therapy. *Nonviral Transf. Technol.* 493–498 (2000).

414. Hernandez-Alcoceba, R., Pihalja, M., Nunez, G. & Clarke, M. F. Evaluation of a new dual-specificity promoter for selective induction of apoptosis in breast cancer cells. *Nat. Publ. Gr.* **8**, 298–307 (2001).

415. Yang, L. *et al.* Tumor-specific gene expression using the survivin promoter is further increased by hypoxia. *Gene Ther.* 1215–1223 (2004).

416. Ah, H. *et al.* S. Hypoxia / hepatoma dual speci fi c suicide gene expression plasmid delivery using bio-reducible polymer for hepatocellular carcinoma therapy. *J. Control. Release* **171**, 1–10 (2013).

417. Yin, X. *et al.* Pgas, a Low-pH-Induced Promoter, as a Tool for Dynamic Control of Gene Expression for Metabolic Engineering of Aspergillus niger. *Appl. Environ. Microbiol.* **83**,

1–14 (2017).

418. Li, C. *et al.* Intelligent microbial cell factory with genetic pH shooting (GPS) for cell self - responsive base / acid regulation. *Microb. Cell Fact.* 1–13 (2020).

419. Torres, R. *et al*. Induction of the acid inducible lipF promoter is reversibly inhibited in pH ranges of pH 4 . 2 - 4 . 0. *BMC Res. Notes* 1–6 (2018).

420. Das, A. T. *et al*. Tet-On Systems For Doxycycline-inducible Gene Expression. *Curr. Gene Ther.* 156–167 (2016).

421. Hockemeyer, D. *et al.* Genetic engineering of human pluripotent cells using TALE nucleases. *Br. Commun.* **29**, 731–734 (2011).

422. Zhu, Z. *et al*. A CRISPR/Cas-Mediated Selection-free Knockin Strategy in Human Embryonic Stem Cells. *Stem Cell Reports* **4**, 1103–1111 (2015).

423. Chu, V. T. *et al.* Increasing the efficiency of homology-directed repair for CRISPR-Cas9-induced precise gene editing in mammalian cells. *Nat. Biotechnol.* (2015).

424. Shy, B. R. *et al*. Co-incident insertion enables high efficiency genome engineering in mouse embryonic stem cells. *Nucleic Acids Res.* **44**, 7997–8010 (2016).

425. Maruyama, T. *et al.* Inhibition of non-homologous end joining increases the efficiency of CRISPR/Cas9-mediated precise genome editing. *Nat. Biotechnol.* **33**, 538–542 (2015).

426. Vartak, S. V & Raghavan, S. C. Inhibition of nonhomologous end joining to increase the specificity of CRISPR / Cas9 genome editing. *FEBS* **282**, 4289–4294 (2015).

427. Lin, S. *et al*. Enhanced homology-directed human genome engineering by controlled timing of CRISPR / Cas9 delivery. *Elife* 1–13 (2014).

428. Zhang, J. *et al.* Efficient precise knockin with a double cut HDR donor after CRISPR / Cas9-mediated double-stranded DNA cleavage. *Genome Biol.* 1–18 (2017).

429. Yin, J. Q. *et al*. Manufacturing of primed mesenchymal stromal cells for therapy. *Nat. Biomed. Eng.* 29–31 (2018).

430. Zhang, J. *et al.* The challenges and promises of allogeneic mesenchymal stem cells for use as a cell-based therapy. *Stem Cell Res. Ther.* 1–7 (2015).

VIII. APPENDIX

VIII.1. THE CONDITIONED MEDIUM OF TRANSIENT AZURIN-EXPRESSING HUMAN MESENCHYMAL STROMAL CELLS DEMONSTRATES ANTI-TUMOR ACTIVITY AGAINST BREAST AND LUNG CANCER CELL LINES

(Supplementary information of Chapter II)

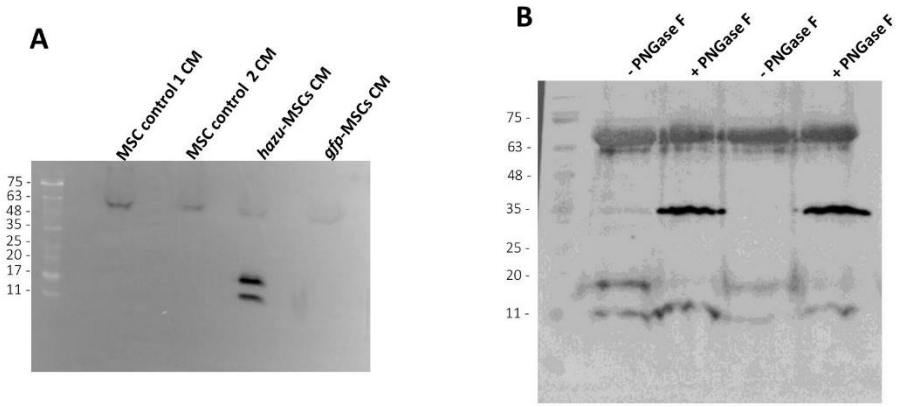

Figure VIII.1.1 - (A) Azurin is secreted by MSC to the conditioned media (CM) at 96h after microporation. A representative image of Western blotting for one donor is depicted (complete membrane). B) Ten micrograms of total protein from CM were incubated with PNGase F to remove N-linked oligosaccharides from glycoproteins. Western blotting image of MSC-CM from two independent donors is depicted (complete membrane).

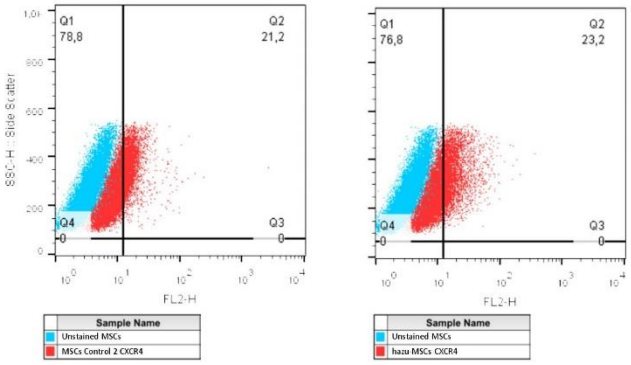

Figure VIII.1.2 - Characterization of CXCR4 expression by flow cytometry of naïve (control 2) MSC and engineered MSC (*hazu*-MSC), as a readout of the migratory potential of these cells.

VIII.2. XENO-FREE PROTOCOL FOR THE PRECISE GENE EDITING OF HUMAN MESENCHYMAL STROMAL CELLS USING THE CRISPR/CAS9 TECHNOLOGY

(Supplementary information of Chapter III)

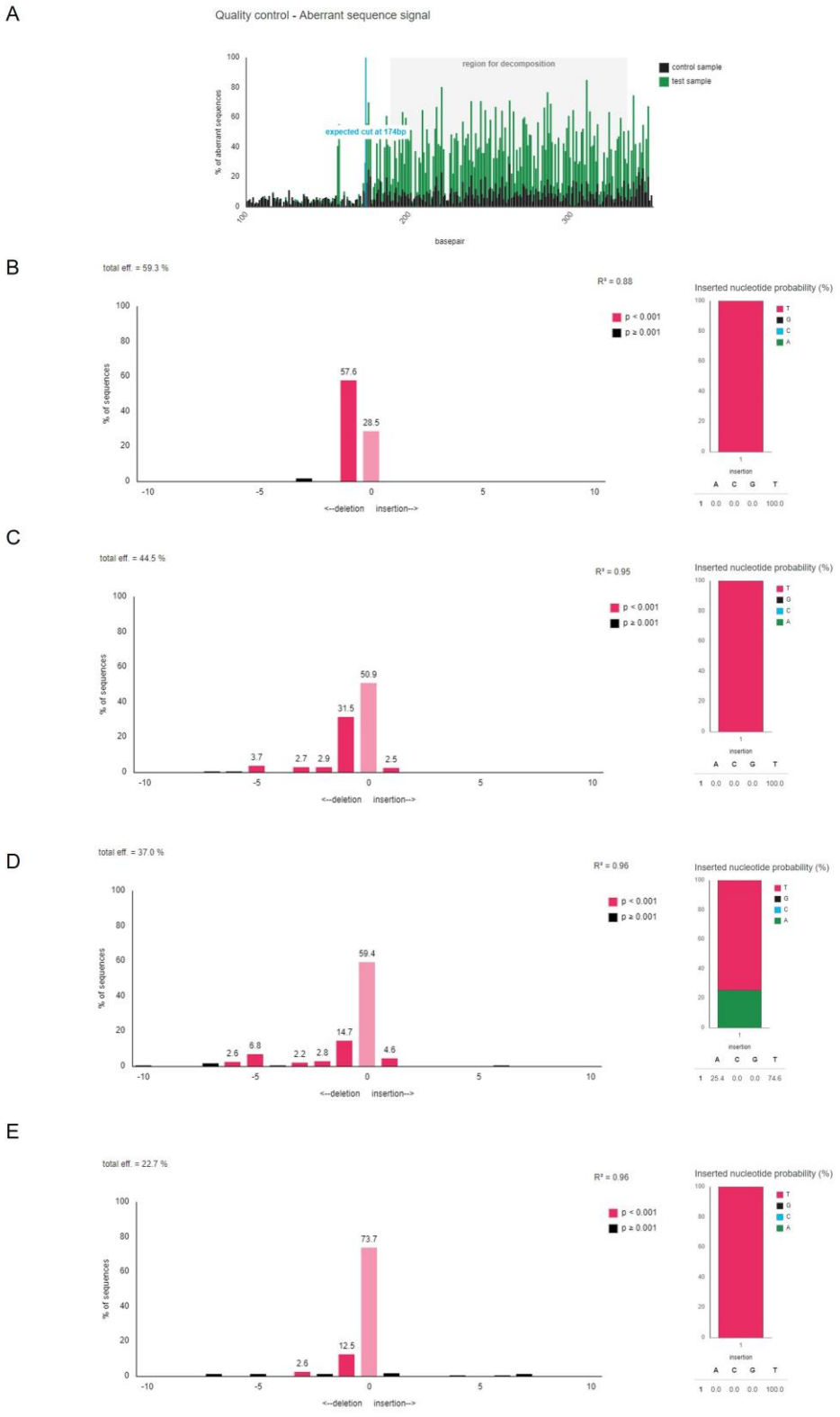

Figure VIII.2.1 (Caption in the next page)

Figure VIII.2.1 - Output graph obtained with TIDE software depicting the calculated percentage of sequences with no genomic alterations and indels, the Cas9 cleavage efficiency (total efficiency, %) and inserted nucleotide (%) probability. A) Representative output graph with aberrant sequence signal identification; B) Output graph for BM donor 1; C) Output graph for BM donor 2; D) Output graph for UCM donor 1; D) Output graph for UCM donor 2. A – adenine; T- thymine; G – guanine; C- cytosine.

VIII.3. ESTABLISHMENT OF STABLE CAS9-ENGINEERED HUMAN BONE MARROW-DERIVED MESENCHYMAL STROMAL CELLS EXPRESSING AZURIN IN SERUM/XENO-FREE CONDITIONS

(Supplementary information of Chapter IV)

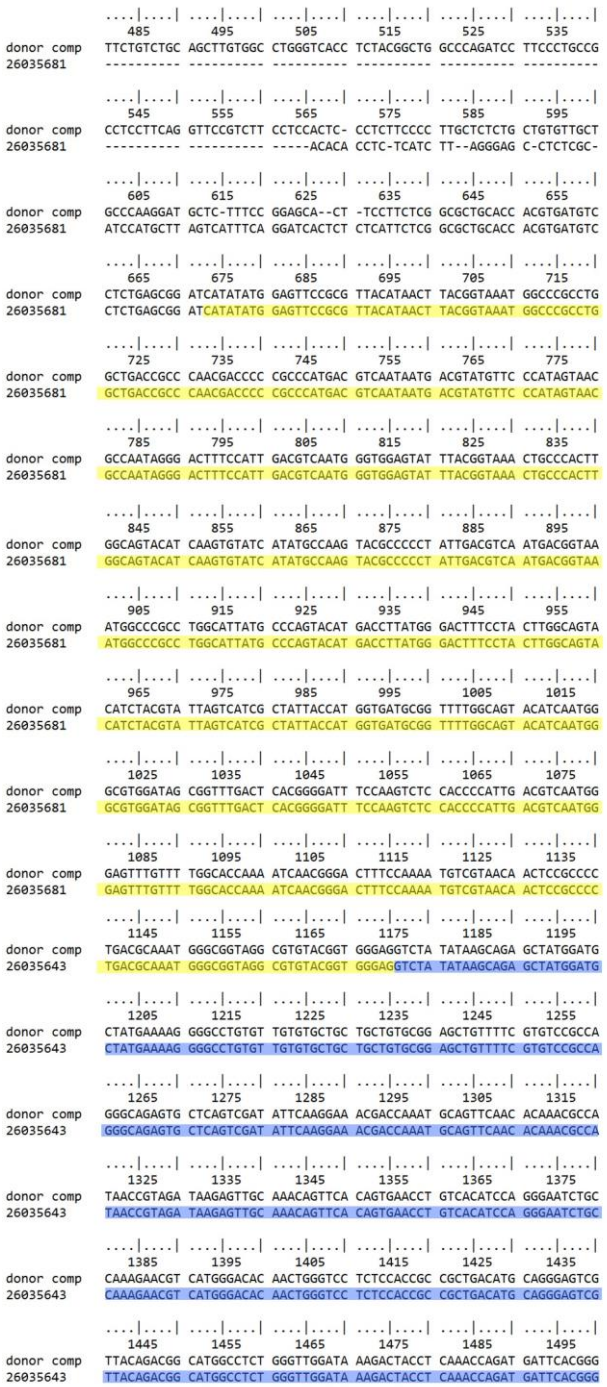

Figure VIII.3.1 - Portion of the alignment between the DNA sequencing results of HDR Donor 2 and the reference sequence of Donor 2 inserted in the AAVS1 locus of *PPP1R12C* gene in MSC genome. Sequence highlighted in yellow represents the CMV promotor sequence and in blue represents the *hazu* gene sequence.

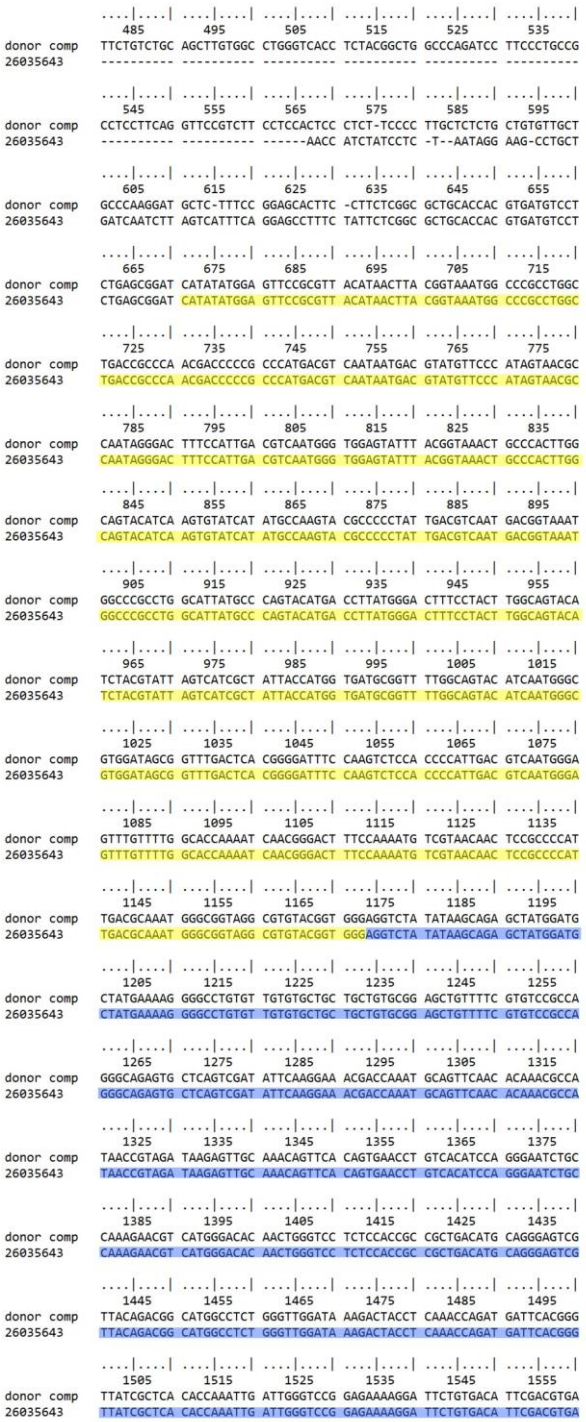

Figure VIII.3.2 - Portion of the alignment between the DNA sequencing results of HDR Donor 3 and the reference sequence of Donor 2 inserted in the AAVS1 locus of *PPP1R12C* gene in MSC genome. Sequence highlighted in yellow represents the CMV promotor sequence and in blue represents the *hazu* gene sequence.

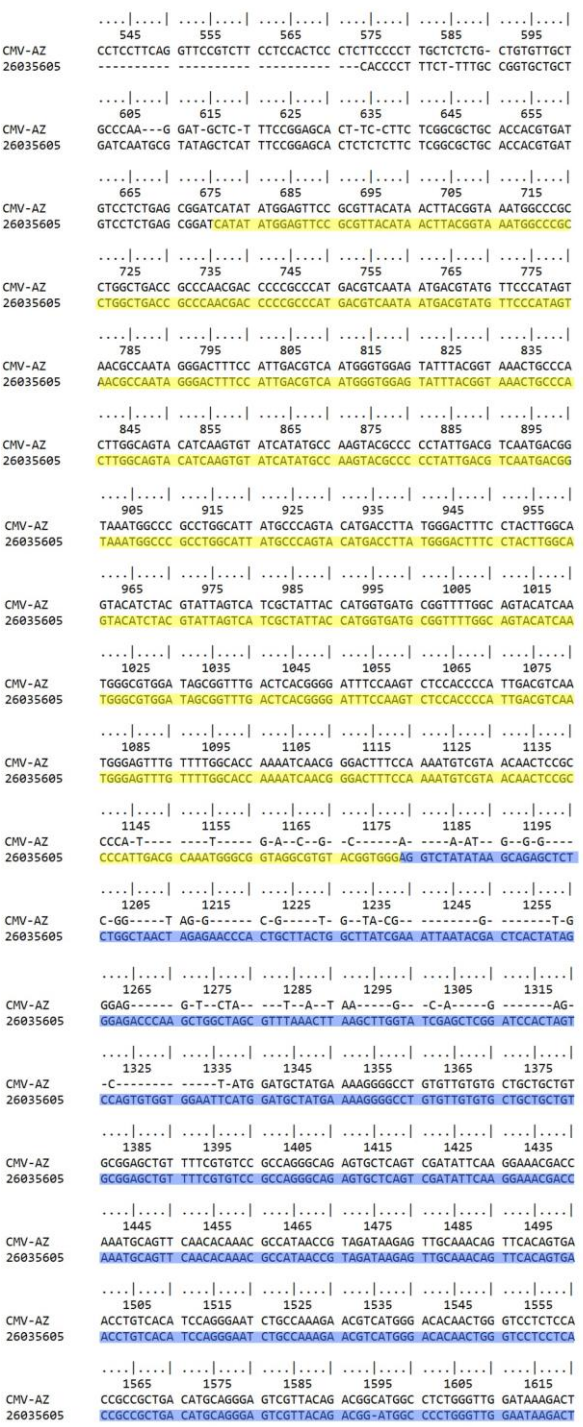

Figure VIII.3.3 - Portion of the alignment between the DNA sequencing results of HDR Donor 4 and the reference sequence of Donor 2 inserted in the AAVS1 locus of *PPP1R12C* gene in MSC genome. Sequence highlighted in yellow represents the CMV promotor sequence and in blue represents the *hazu* gene sequence.

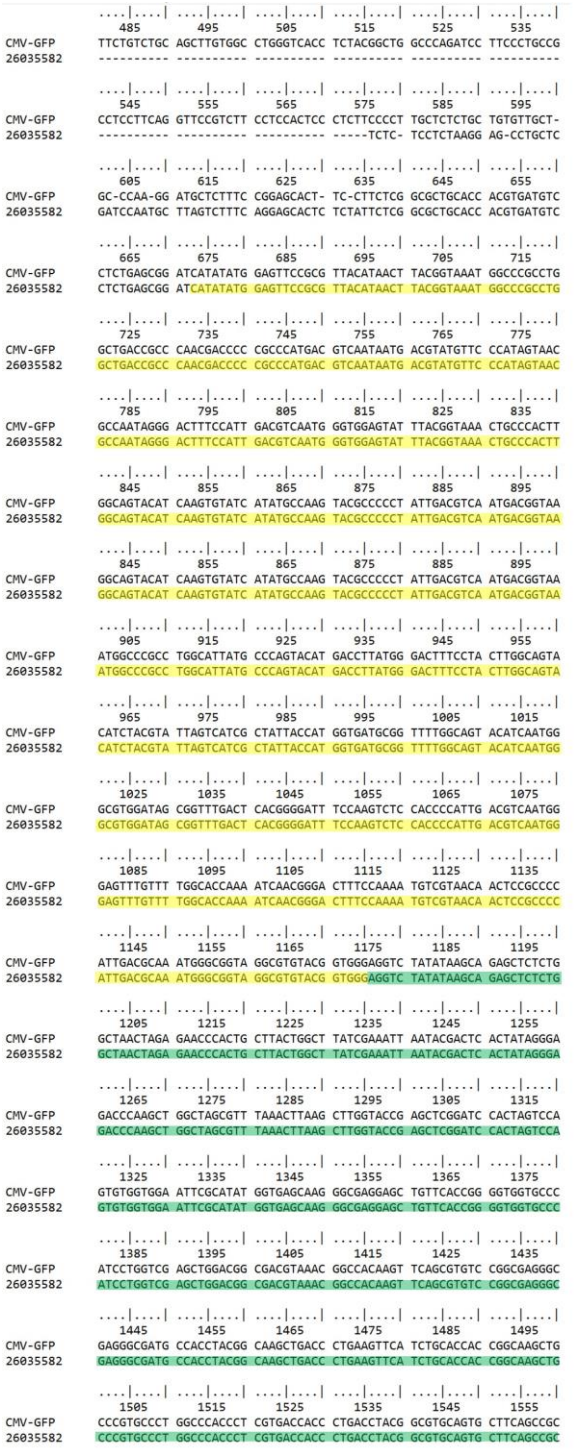

Figure VIII.3.4 - Portion of the alignment between the DNA sequencing results of HDR Donor 5 and the reference sequence of Donor 2 inserted in the AAVS1 locus of PPP1R12C gene in MSC genome. Sequence highlighted in yellow represents the CMV promotor sequence and in green represents the GFP gene sequence.